Morphological analysis and morphometry of the occipital condyle and its relation to surrounding structures: implication in craniovertebral junction surgery

Mr. Pakpoom Thintharua

A Thesis Submitted in Partial Fulfillment of the Requirements
for the Degree of Master of Science in Medical Sciences
Common Course
FACULTY OF MEDICINE
Chulalongkorn University
Academic Year 2021

การวิเคราะห์และการวัดเชิงสัณฐานวิทยาของปุ่มกระดูกท้ายทอยและความสัมพันธ์กับโครงสร้างกระดูกที่อยู่โดยรอบ: นัยทางศัลยกรรมบริเวณรอยต่อกะโหลกศีรษะส่วนท้ายทอยกับกระดูกสันหลัง

นายภาคภูมิ ถิ่นท่าเรือ

วิทยานิพนธ์นี้เป็นส่วนหนึ่งของการศึกษาตามหลักสูตรปริญญาวิทยาศาสตรมหาบัณฑิต
สาขาวิชาวิทยาศาสตร์การแพทย์ ไม่สังกัดภาควิชา/เทียบเท่า
คณะแพทยศาสตร์ จุฬาลงกรณ์มหาวิทยาลัย
ปีการศึกษา 2564

Thesis Title	Morphological analysis and morphometry of the occipital condyle and its relation to surrounding structures: implication in craniovertebral junction surgery
By	Mr. Pakpoom Thintharua
Field of Study	Medical Sciences
Thesis Advisor	Professor VILAI CHENTANEZ, Ph.D.

Accepted by the FACULTY OF MEDICINE, Chulalongkorn University in Partial Fulfillment of the Requirement for the Master of Science

-- Dean of the FACULTY OF MEDICINE

(Associate Professor CHANCHAI SITTIPUNT, M.D.)

THESIS COMMITTEE

-- Chairman

(Professor SITHIPORN AGTHONG, Ph.D.)

-- Thesis Advisor

(Professor VILAI CHENTANEZ, Ph.D.)

-- Examiner

(Assistant Professor DEPICHA JINDATIP, Ph.D.)

-- Examiner

(KRITSADA LEUNGCHAVAPHONGSE, Ph.D.)

-- External Examiner

(Assistant Professor Suwadee Chaunchaiyakul, Ph.D.)

ภาคภูมิ ถิ่นท่าเรือ : การวิเคราะห์และการวัดเชิงสัณฐานวิทยาของปุ่มกระดูกท้ายทอยและความสัมพันธ์กับโครงสร้างกระดูกที่อยู่โดยรอบ: นัยทางศัลยกรรมบริเวณรอยต่อกะโหลกศีรษะส่วนท้ายทอยกับกระดูกสันหลัง. (Morphological analysis and morphometry of the occipital condyle and its relation to surrounding structures: implication in craniovertebral junction surgery) อ.ที่ปรึกษาหลัก : ศ. ดร.วิไล ชินธเนศ

ความรู้ทางกายวิภาคของปุ่มกระดูกท้ายทอย (OC) และความสัมพันธ์กับโครงสร้างโดยรอบมีความสำคัญต่อการหลีกเลี่ยงการบาดเจ็บระหว่างการผ่าตัดบริเวณรอยต่อกะโหลกศีรษะส่วนท้ายทอยกับกระดูกสันหลัง (CVJ) อาทิเช่น Far lateral approach (FLA) ดังนั้นการศึกษานี้มีวัตถุประสงค์เพื่อประเมินสัณฐานวิทยาของปุ่มกระดูกท้ายทอย และความสัมพันธ์กับจุดไดกัสตริก (DP), ฟอราเมนแม็กนั่ม (FM), จูกูลาร์ ฟอราเมน (JF) และ ช่องไฮโพกลอสซัล (HC) การศึกษานี้ใช้กะโหลกศีรษะจำนวน 100 กะโหลก จากการสังเกตุส่วนใหญ่ OC มีลักษณะเป็นวงรีคิดเป็น 33.0% ของตัวอย่างทั้งหมด และพบว่า 31.5% ของ OC ยื่นเข้าสู่ FM ในขณะที่ความยาว ความกว้าง และความสูงเฉลี่ยของ OC คือ 21.32 ± 2.44, 10.51 ± 1.41 และ 7.39 ± 1.14 มม. ตามลำดับ รูเปิดนอกกะโหลก (eHC) และรูเปิดภายในกะโหลก (iHC) ของ HC โดยส่วนใหญ่ 74.0% พบที่ 1/3 ด้านหน้าของ OC และ 45.0% พบที่ 1/3 ตรงกลางของ OC ตามลำดับ ระยะทางเฉลี่ยจากขอบหลังสุดของ OC (OCPE) ไปยัง eHC, iHC และ JF คือ 13.70 ± 2.23 , 9.00 ± 1.59, และ 16.15 ± 2.35 มม. ตามลำดับ รูปร่างของ FM พบมากที่สุดคือหกเหลี่ยมคิดเป็น 27.0% ค่าเฉลี่ยของเส้นผ่านศูนย์กลางตามยาวของ FM (APD) คือ 34.19 ± 2.46 มม. เส้นผ่านศูนย์กลางตามขวางของ FM (TD) เท่ากับ 29.17 ± 2.14 มม. และดัชนีของ FM (FMI) เท่ากับ 1.18 ระยะห่างเฉลี่ยระหว่าง DP และจุดสังเกตของกระดูกได้แก่ค่า Op-DP, OCPT-DP และ JF-DP คือ 54.54 ± 3.50, 36.72 ± 4.07 และ 34.18 ± 4.15 มม. ตามลำดับ ความชุกของช่องคอนไดลาร์ส่วนหลัง 57.0% พบทั้งสองข้าง ในขณะที่ 34.0% พบเพียงข้างเดียว การวิเคราะห์และข้อมูลทางสัณฐานวิทยาของ OC และความสัมพันธ์กับโครงสร้างโดยรอบ สามารถช่วยให้ศัลยแพทย์ตระหนักถึงการบาดเจ็บของระบบหลอดเลือดและประสาทและความไม่สเถียรของ CVJ จากการผ่าตัด

สาขาวิชา	วิทยาศาสตร์การแพทย์	ลายมือชื่อนิสิต	
ปีการศึกษา	2564	ลายมือชื่อ อ.ที่ปรึกษาหลัก	

6370040430 : MAJOR MEDICAL SCIENCES

KEYWORD: Craniovertebral junction, Digastric point, Far lateral approach, Foramen magnum, Occipital condyle

Pakpoom Thintharua : Morphological analysis and morphometry of the occipital condyle and its relation to surrounding structures: implication in craniovertebral junction surgery. Advisor: Prof. VILAI CHENTANEZ, Ph.D.

Anatomical knowledge of the occipital condyle (OC) and its relationships to surrounding structures is important for avoiding injury during craniovertebral junction (CVJ) surgeries such as the far lateral approach (FLA). Therefore, this study was conducted to evaluate the morphology and morphometry of OC and its relationship to digastric point (DP), foramen magnum (FM), jugular foramen (JF), and hypoglossal canal (HC). The study was performed on 100 dry skulls. Oval-like condyle was the most common OC shape, representing for 33.0% of all samples. The OC protruded into FM in 31.5 %. The average length, width and height of the OC were 21.32 ± 2.44, 10.51 ± 1.41, and 7.39 ± 1.14 mm, respectively. Extracranial orifice of HC (eHC) and intracranial orifice of HC (iHC) were commonly found 74.0% in anterior 1/3 of OC, and 45.0% in middle 1/3 of OC, respectively. The mean distance from posterior edge of the OC (OCPE) to eHC, iHC and JF were 13.70 ± 2.23 mm, 9.00 ± 1.59 mm, and 16.15 ± 2.35 mm, respectively. The most common shape of FM was hexagonal in 27.0%. The mean of anteroposterior diameter (APD) was 34.19 ± 2.46 mm, transverse diameter (TD) was 29.17 ± 2.14 mm and foramen magnum index (FMI) was 1.18. The mean distance between DP and bony landmarks, including Op-DP, OCPT-DP, and JF-DP values, were 54.54 ± 3.50, 36.72 ± 4.07, and 34.18 ± 4.15 mm, respectively. The prevalence of bilateral and unilateral posterior condylar canal (PCC) was 57.0% and 34.0%, respectively. The morphological analysis and morphometry data of OC and its relation to surrounding structures can help surgeons be aware of neurovascular injury and CVJ instability by surgery.

Field of Study:	Medical Sciences	Student's Signature	
Academic Year:	2021	Advisor's Signature	

ACKNOWLEDGEMENTS

First and foremost, I'd like to thank my thesis advisor, Prof. Vilai Chentanez, for her invaluable help, patience, motivation, and encouragement throughout my thesis. Her guidance was helpful during the research and writing of this thesis. I would not have achieved this far, and this thesis would not be completed without all the support that I always received from her.

I would like to thank Prof. Sithiporn Agthong who was the chairman of the thesis defense for his kindness, teaching and suggestions. In addition, I would like to thank the rest of my thesis committee: Assist. Prof. Dr. Depicha Jindatip, Dr. Kritsada Leungchavaphongse, and Assist. Prof. Dr. Suwadee Chaunchaiyakul serving as my committee and for their advice.

Finally, I most gratefully acknowledge my beloved parents and my friends for all of their supporting, encouragement and care me spiritually throughout my entire life.

Pakpoom Thintharua

TABLE OF CONTENTS

List of Tables

Page

LIST OF FIGURES

Page

List of definitions of abbreviations

Abbreviation	Definition
a1/3	Anterior one third of occipital condyle
a2/3	Anterior two third of occipital condyle
AID	Anterior intercondylar distance of occipital condyle
APD	Anteroposterior diameter of foramen magnum
Bas	Basion
C1	Atlas
C1-C2	Atlantoaxial joint
C2	Axis
CF	Condylar fossa
CN IX	Glossopharyngeal nerve
CN VII	Facial nerve
CN X	Vagus nerve
CN XI	Accessory nerve
CN XII	Hypoglossal nerve
CSF	Cerebrospinal fluid
CT	Computerized tomography
CVJ	Craniovertebral junction
DG	Digastric groove
DM	Digastric muscle
DP	Digastric point
eHC	Extracranial orifice of hypoglossal canal
FLA	Far lateral approach
FM	Foramen magnum
FMI	Foramen magnum index
HC	Hypoglossal canal
iHC	Intracranial orifice of hypoglossal canal
JB	Jugular bulb

JF	Jugular foramen
JF-DP	Distance between the posterior most end of jugular foramen to digastric point
JP	Jugular process
JT	Jugular tubercle
LC	Lower clivus
m1/3	Middle one third of occipital condyle
MRI	Magnetic resonance imaging
MT	Mastoid process
OC	Occipital condyles
O-C1	Atlantooccipital joint
OCAT-Bas	Distance from the anterior tip of occipital condyle to basion
OCAT-Op	Distance from the anterior tip of occipital condyle to opisthion
OC-H	Occipital condyle height
OC-L	Occipital condyle length
OCPT-eHC	Distance from the posterior tip of occipital condyle to extracranial orifice of hypoglossal canal
OCPT-iHC	Distance from the posterior tip of occipital condyle to intracranial orifice of hypoglossal canal
OCPT-JF	Distance from the posterior tip of occipital condyle to the posterior-most end of jugular foramen
OCPT-Bas	Distance from the posterior tip of occipital condyle to basion
OCPT-DP	Distance between the posterior tip of occipital condyle and digastric point
OCPT-Op	Distance from the posterior tip of occipital condyle to opisthion
OC-W	Occipital condyle width
Op	Opisthion
Op-DP	Distance between the end of the posterior border of foramen magnum (opisthion) to digastric point
Op-JF	Distance between opisthion and posterior-most end of jugular foramen

p1/3	Posterior one third of occipital condyle
p2/3	Posterior two third of occipital condyle
PCC	Posterior condylar canal
PID	Posterior intercondylar distance of occipital condyle
SS	Sigmoid sinus
TD	Transverse diameter of foramen magnum
TS	Transverse sinus
VA	Vertebral artery

Chapter I Backgrounds and rationales

The craniovertebral junction (CVJ) is an area that connects the cranium to the upper cervical spine, it consists of atlas (C1), axis (C2), foramen magnum (FM), and the lower clivus (LC) that supports the brainstem. It is bounded laterally by the jugular foramen (JF), the hypoglossal canals (HC), and the occipital condyles (OC) (1-3). OC, HC, and posterior margin of the JF are the condylar part of FM. OC is the only part of occipital bone articulated with C1. Neurovascular structures associate with CVJ are the medulla oblongata, the upper spinal and lower cranial nerves (CN IX, X, XI, and XII), vertebral arteries (VA) with their branches, and vertebral veins (4). CVJ is a common site for various lesions including neoplasms (intra- and extradural tumors), vascular lesions such as a VA aneurysm, rheumatic diseases, malformations, and degenerative pathologies. (1, 2, 4-6). Lesions at CVJ are difficult to manage because of their location and complex anatomic relations (7).

Far lateral approach (FLA) is used to access the ventrolateral part of CVJ and LC by drilling the lateral edge of the FM rim for tumor removal and the treatment of vascular lesions (8, 9). There are several types of FLA including transcondylar, supracondylar, and paracondylar approaches (10, 11). The complications of this approach are the development of cerebrospinal fluid (CSF) leak, damage to the VA and neural structures (1, 8, 9). The main steps of FLA include patient positioning, incision markings, antisepsis and scalp incision, muscle exposure, VA exposition, craniotomy, opening of the dura mater, tumor resection and dural closure, respectively (5, 12, 13). Craniotomy of FLA includes lateral part of the occipital squama to the inferior rim of the FM (13). It was performed by resection of the posterior arch of C1, drilling the inferior portion of OC near the posterior margin of the JF, and lateral to the condyle. This process increases the angle of exposure, greater visualization, and enhances access to the ventrolateral and ventral aspects of the CVJ (5, 12, 14).

The stability of CVJ depends mainly on the length of the OC, drilling the OC in FLA can increase the risk of developing CVJ instability. Only the posteromedial part of OC must be removed to provide direct access to the ventral FM and LC areas. Previous studies reported that resection approximately 43 % of the long axis the OC would provide good access to the ventral area of the FM (1). Bejjani et al. (2000) (15), stated that resection of the posterior OC less than 70% would not show evidence of CVJ instability.

HC has been used as a landmark for OC resection. It was claimed to locate in the middle part of OC. Therefore, OC resection could not extend beyond the HC to prevent hypoglossal nerve (CN XII) injury and CVJ instability (7, 9, 16, 17). However, previous study showed that the HC was not always located at the middle part of OC. HC was related to anterior one-third of OC in 85% of cases and middle one-third of OC in 15% of cases (18) . Therefore, OC resection extends to the HC in patients with an anterior located HC may increase the risk of CVJ instability (17, 19).

Research questions

Primary Research Question

1. What are the shapes and dimension of occipital condyle in dry skulls?

2. What are the distances between the occipital condyle and surrounding structures including the hypoglossal canal, jugular foramen, foramen magnum and digastric point?

Secondary Research Question

3. Are there any variations of the location of hypoglossal canal related to occipital condyle?

4. Are there any differences between sides and sex?

Research Objectives

1. To determine the shapes and dimension of occipital condyle in dry skulls.
2. To investigate the occipital condyle protrusion related to foramen magnum.
3. To measure the intercondylar distance of occipital condyle.
4. To measure the distances from posterior tip of the occipital condyle to the hypoglossal orifices.
5. To measure the distance between occipital condyle and jugular foramen.
6. To determine the shapes and dimension of foramen magnum in dry skulls.
7. To investigate the location of hypoglossal canal, jugular foramen related to occipital condyle.
8. To investigate the posterior condylar canal in the condylar fossa.
9. To measure the distance from the digastric point to jugular foramen, posterior tip of occipital condyle and opisthion.
10. To determine the difference between sides and sex.

Conceptual framework

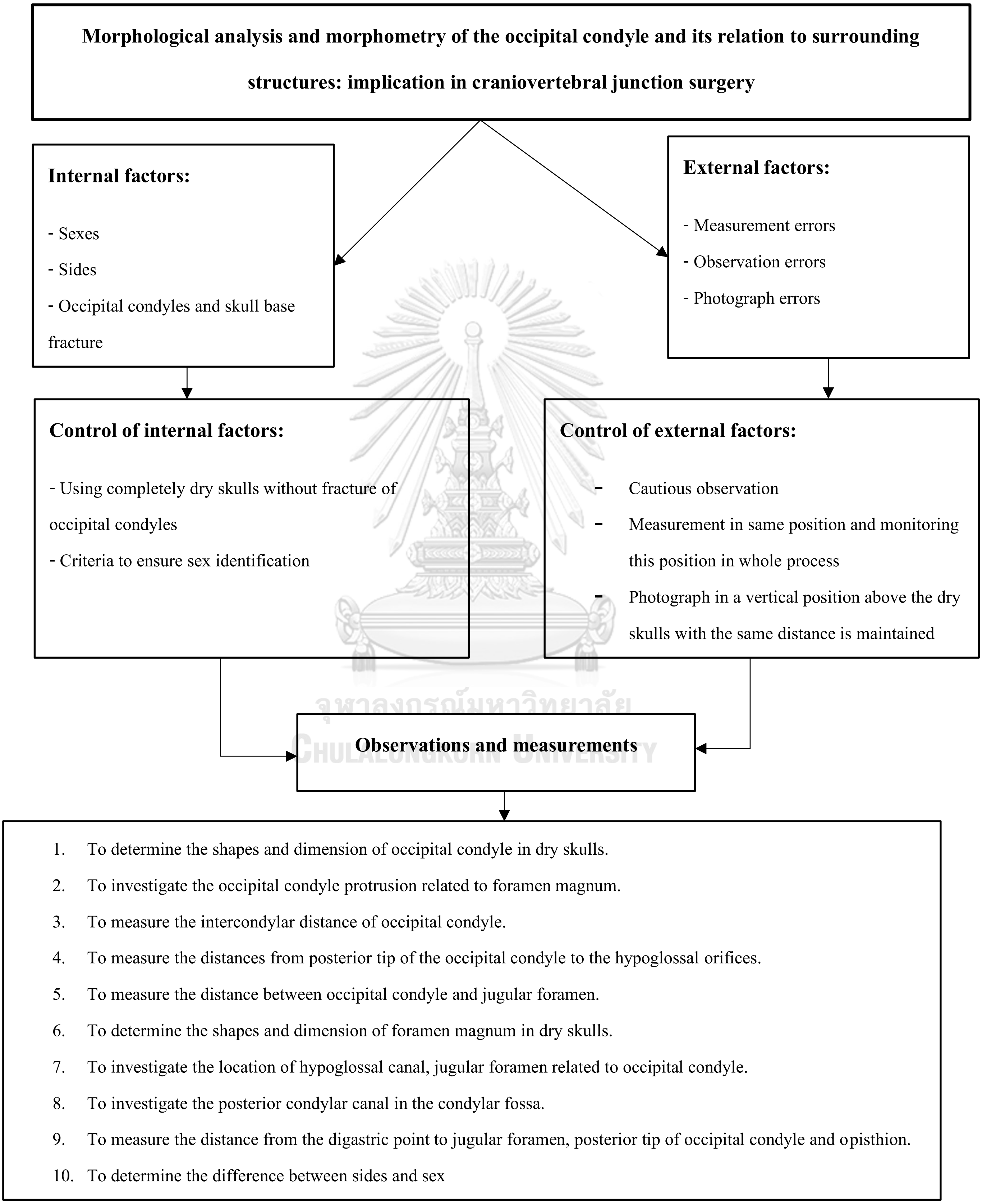

Keywords: Craniovertebral junction, Digastric point, Far lateral approach, Foramen magnum, Occipital condyle

Research design: Descriptive study

Expected benefits and applications:

This current study will explain more anatomical knowledge in detail of the morphometric study of the occipital condyles and surrounding structures related to the craniotomy step of the far lateral approach procedure. Detailed of anatomical knowledge of the occipital condyles and their surrounding structures may have the potential to improve surgical outcomes and decrease craniovertebral junction instability and neurovascular injury.

Chapter II Literature review

1. The anatomical structure of occipital condyle and its location

OCs are the two bony structures presented in the inferior surface of the occipital bone and located laterally to the FM. Usually, it is described as an ovoid structure, with a projection convex downward and lateral, and its long axis directs anteriorly and medially. Most of the anatomical and biomechanical studies of the CVJ have involved the morphological or morphometric analysis of OC (1, 20-22) (**Fig. 1**).

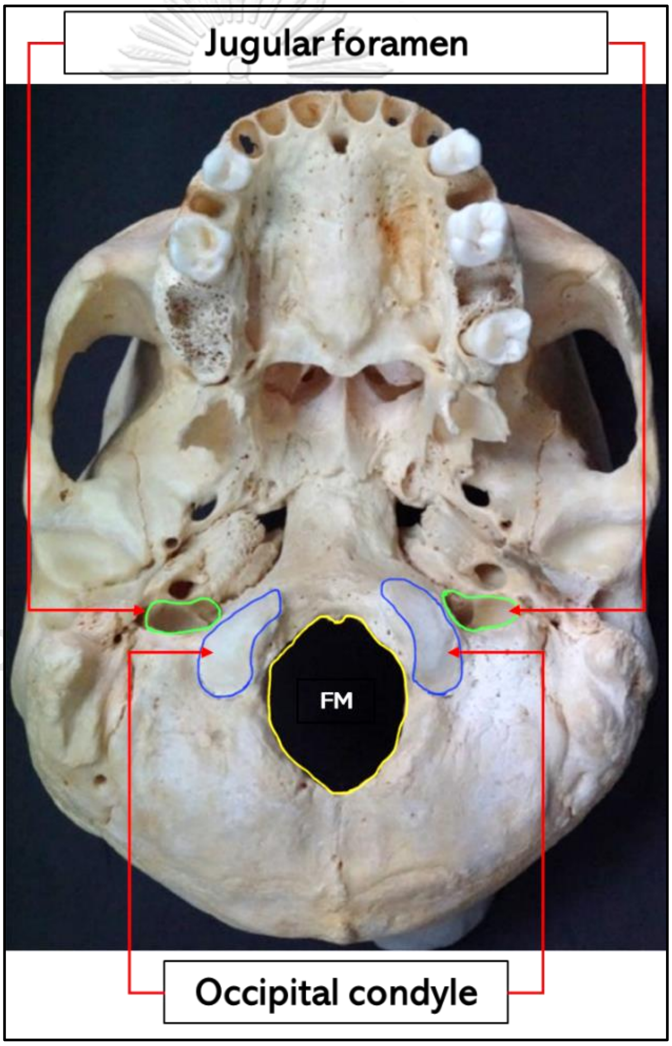

Figure 1. The inferior view of the skull showing the foramen magnum (yellow line), both sides of jugular foramen (green line), and both sides of occipital condyle (blue line). FM = foramen magnum.

The dimensions of OC are defined as the maximum anteroposterior distance between anterior and posterior tips of OC (OC-L), the maximum transverse distance between the medial and lateral border of OC (OC-W), and the maximum vertical distance between the upper and lower boundary of the medial margin of OC (OC-H), respectively (1, 4, 7, 23) (**Fig. 2**).

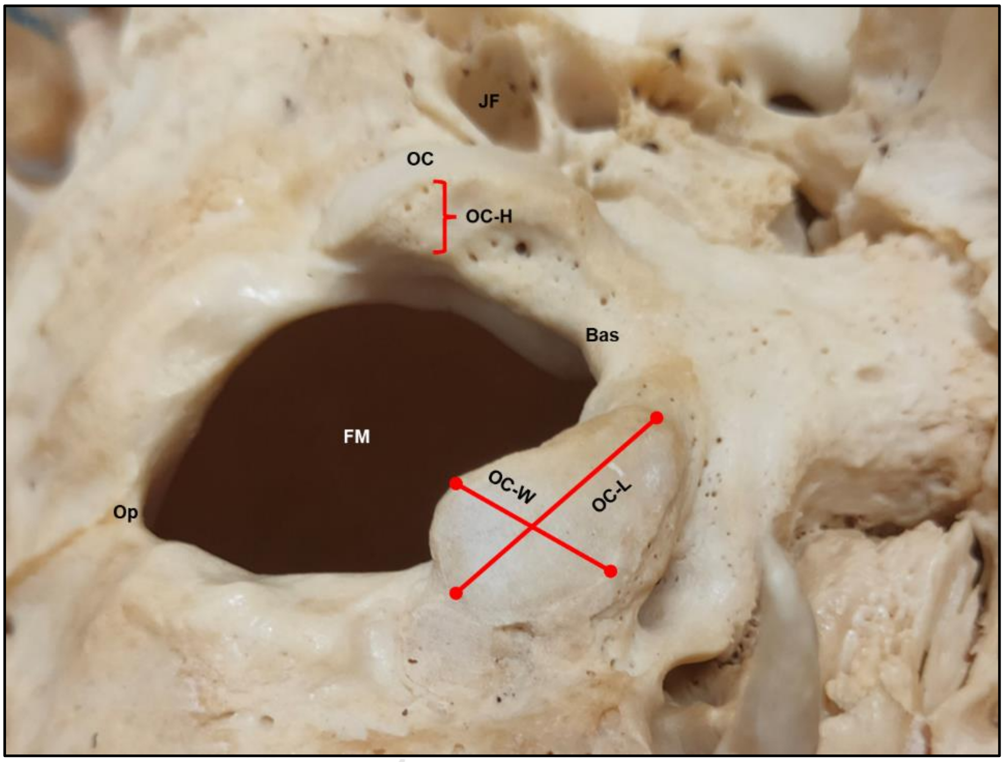

Figure 2. Inferior view of occipital bone showing the measurement of the left of OC-L, OC-W, and the right OC-H. Bas = basion, FM = foramen magnum, JF = jugular foramen, OC = occipital condyle, OC-H = occipital condyle height, OC-L = occipital condyle length, and OC-W = occipital condyle width, Op = opisthion.

The dimension of OC was significantly larger in male than female (17, 24) . The OC-L, OC-W, and OC-H of male skull were reported to be larger than female significantly (25, 26) . The dimensions of OC in previous studies are shown in **Table 1**.

Table 1. Comparison of the OC dimensions in previous studies

Parameters	**Sides**	**Sex**	**Measurements**	**Kumar and Nagar (2014) (26)**	**Saluja et al. (2016) (23)**	**Lyrtzis et al. (2017) (17)**	**Di et al. (2019) (1)**	**Anjum et al. (2021) (21)**
				(N= 100) India	**(N= 228) India**	**(N = 282) Greece**	**(N = 100) China**	**(N = 200) India**
OC-L (mm)	Rt	Male	Mean ± SD	23.88 ± 1.50	-	24.33 ± 2.57	-	23.50 ± 2.71
			Range	21.50-26. 80	-	18.45-29.59	-	-
		Female	Mean ± SD	22.60 ± 1.30	-	22.95 ± 2.96	-	22.44 ± 2.01
			Range	20.30-24.90	-	13.34-29.92	-	-
		Total	Mean ± SD	-	22.90 ± 3.11	-	23.73 ± 2.03	-
			Range	-	16.61-27.88	-	-	-
	Lt	Male	Mean ± SD	24.99 ± 1.82	-	24.07 ± 2.59	-	23.34 ± 3.06
			Range	21.80-27. 50	-	15.15-29.47	-	-
		Female	Mean ± SD	24.20 ± 1.62	-	23.23 ± 2.71	-	22.62 ± 2.41
			Range	21.10-27.30	-	16.79-28.54	-	-
		Total	Mean ± SD	-	22.60 ± 2.72	-	23.43 ± 1.90	-
			Range	-	17.89-29.27	-	-	-
OC-W (mm)	Rt	Male	Mean ± SD	12.97 ± 1.43	-	12.10 ± 1.50	-	12.19 ± 1.53
			Range	10.20-16.40	-	9.45-16.38	-	-
		Female	Mean ± SD	12.65 ± 1.33	-	11.43 ± 1.47	-	11.46 ± 1.56
			Range	10.10-15.20	-	7.77-15.05	-	-
		Total	Mean ± SD	-	12.98 ± 1.62	-	12.99 ± 1.19	-
			Range	-	10.89-16.39	-	-	-
	Lt	Male	Mean ± SD	12.97 ± 1.43	-	12.21 ± 1.66	-	12.29 ± 1.47
			Range	10.20-16.40	-	9.01-16.59	-	-
		Female	Mean ± SD	13.85 ± 1.01	-	11.46 ± 1.51	-	11.87 ± 1.45
			Range	10.90-16.80	-	8.40-15.01	-	-
		Total	Mean ± SD	-	12.97 ± 1.46	-	13.23 ± 1.14	-
			Range	-	10.51-15.88	-	-	-
OC-H	Rt	Male	Mean ± SD	8.64 ± 0.74	-	10.13 ± 1.53	-	8.89 ± 1.02
			Range	6.70-7.30	-	-	-	-

(mm)		Female	Mean ± SD	6.92 ± 0.72	-	10.09 ± 1.66	-	8.70 ± 1.12
			Range	6.65-7.20	-	-	-	-
		Total	Mean ± SD	-	9.32 ± 1.23	-	9.34 ± 0.97	-
			Range	-	6.02-11.85	-	-	-
	Lt	Male	Mean ± SD	9.32 ± 0.78	-	10.17 ± 1.38	-	8.85 ± 1.13
			Range	-	-	-	-	-
		Female	Mean ± SD	9.21 ± 0.76	-	9.88 ± 1.51	-	8.62 ± 1.10
			Range	8.22-10.21	-	-	-	-
		Total	Mean ± SD	-	9.12 ± 1.23	-	9.36 ± 0.91	-
			Range	-	6.35-11.16	-	-	-

OC-H = occipital condyle height, OC-L = occipital condyle length, and OC-W = occipital condyle

According to Naderi et al. (2005) (19), OC was classified based on its length into three types as the following: type I (OC-L was shorter than 20 mm), type II (OC-L was 20 - 26 mm), and type III (OC-L was longer than 26 mm), respectively. However, the range of type II and type III length was different in the other two studies (18, 27). Knowledge in OC-L is necessary for OC resection process during transcondylar approach because the length of posterior one-third (p1/3) can be calculated from the total length of OC (27). Females had a significant shorter OC-L than males ($p < 0.001$) (26), and had a significant larger proportion of OC Type I (32.6%) than males (5.8%) ($p = 0.001$) (28). The prevalence of OC types in previous studies are shown in **Table 2**.

Table 2. Prevalence of OC types based on its length

Types of OC	Sex	*Naderi et al. (2005) (19)	**Kalthur et al. (2014) (27)	**Verma et al. (2016) (18)	*Cheruiyot et al. (2018) (28)
		(N=404) Turkey	(N=142) India	(N=100) India	(N=104) Kenya
Type I (short)	Male	-	5.50%	-	5.80%
	Female	-	21.90%	-	32.60%
	Total	8.60%	-	13.00%	38.40%
Type II (Moderate)	Male	-	83.60%	-	45.20%
	Female	-	71.90%	-	15.40%
	Total	77.20%	-	62.00%	60.60%
Type III (long)	Male	-	10.90%	-	1.00%
	Female	-	6.30%	-	0.00%
	Total	14.10%	-	25.00%	1.00%

* Type I OC-L: <20 mm, type II OC-L: 20-26 mm, type III OC-L: >26 mm)

** Type I OC-L: <20 mm, type II OC-L: 20-24 mm, type III OC-L: >24 mm)

OC articulates with the superior articular facets of C1, forming the atlantooccipital (O-C1) joint. The stability of this joint is maintained by the compatibility of the articular surfaces together with capsule and ligament factors. In addition, male brain is heavier than female, and a higher load causes an increase in mechanical forces transmitted through the O-C1 joint (17, 28) (**Fig. 3**). Therefore, the OC dimension of males is usually larger than females.

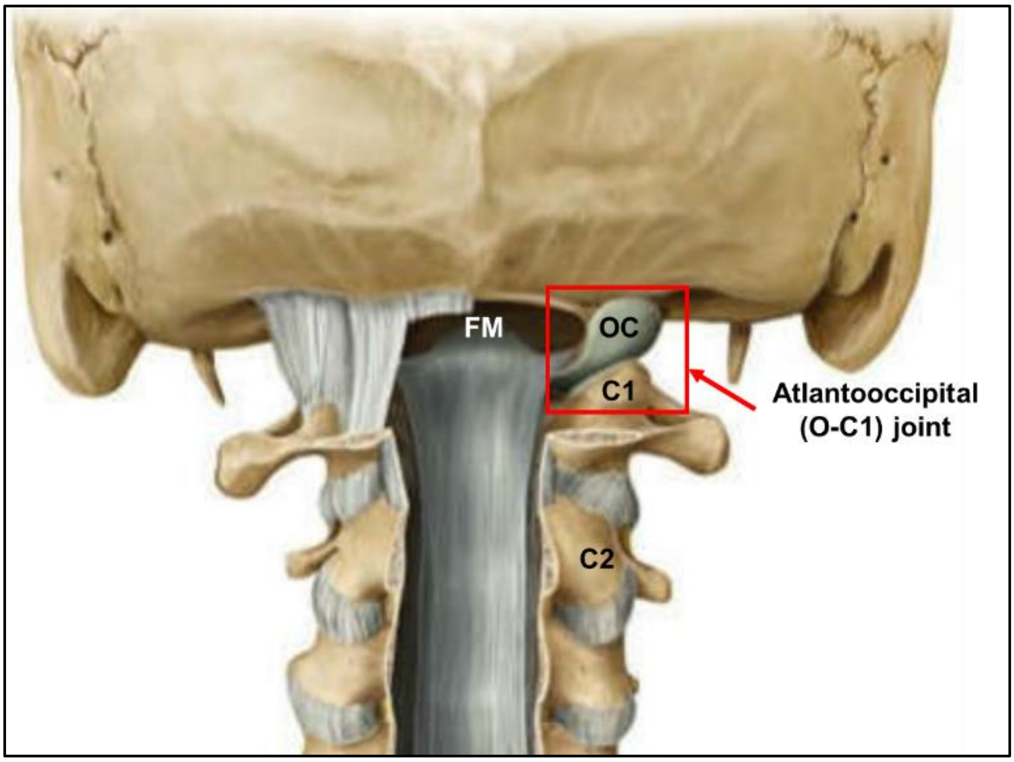

Figure 3. Posterior view of skull and cervical spine showing the articulation of OC and C1 forming the O-C1 joint (modified from Gilroy et al. (2008)) (29). C1 = atlas, C2 = axis, FM = foramen magnum, OC = occipital condyle, and O-C1 = atlantooccipital joint.

The results of partial excision of a condyle at O-C1 joint (condylectomy) in the short type are different from the results obtained in the long type of OC. Therefore, removing the same amount of bone stock results in greater O-C1 joint instability in shorter condyles compared to longer ones, whereas a longer condyle may necessitate more widespread resection for optimum visualization (23, 27, 28). In addition, the thickness of OC also matters during condylectomy as one should know how deep of the OC must be drilled (21) . The greater thickness of OC may facilitate the successful screw placement during occipitocervical fixation (23). The OC-W is also of surgical importance as one should know how much the condyle could be resected medially (27) .

Di et al. (2019) (1) found that by resecting approximately 43% of OC length (23.58 ± 1.96 mm), the HC border could be reached. However, Bejjani et al. (2000) (15), suggested that resection less than 70% of OC would not show any evidences of CVJ instability. Other researchers reported the safe approximately amount of the posterior OC resection as shown in **Table 3**.

Table 3. Comparison of the approximate amount of the posterior OC resection

Authors	**Vishteh et al. (1999) (30)**	**Shin et al. (2006) (31)**	**Barut et al. (2009) (32)**	**Karasu et al. (2009) (33)**	**Lyrtzis et al. (2017) (17)**	**Mazur et al. (2017) (16)**	**Di et al. (2019) (1)**	**MEHDI et al. (2020) (5)**
	(N=6)	**(N=51)**	**(N=56)**	**(N=20)**	**(N=141)**	**(N=9)**	**(N=50)**	**(N=6)**
Populations	**America**	**America**	**Turkey**	**India**	**Greeks**	**America**	**China**	**Pakistan**
Samples	Cadaveric head	Patients	Dry skulls	Dry skulls	Dry skulls	Cadaveric head	Dry skulls	Patients
Posterior OC resection (safe zone)	less than 50%	Less than 50%	54.30%	41.90%	34.5% (males) 34.6% (females)	15.4 - 63.7%	43.00%	30 - 40%

OC = occipital condyle

Kumar and Nagar (2014) (26) found that the anterior intercondylar distance of OC (AID) was 17.63 mm, and the posterior intercondylar distance of OC (PID) was 42.02 mm (**Fig. 4**). The PID was significantly longer in males than females (p = 0.002), this might be implied that female had narrow sagittal intercondylar angle when compared to males. In contrast, the AID was not significantly different between sex (p = 0.864) (28) . Furthermore, Farid and Fattah (2018) (34) revealed that the AID was 18.97 mm, while the PID was 38.39 mm.

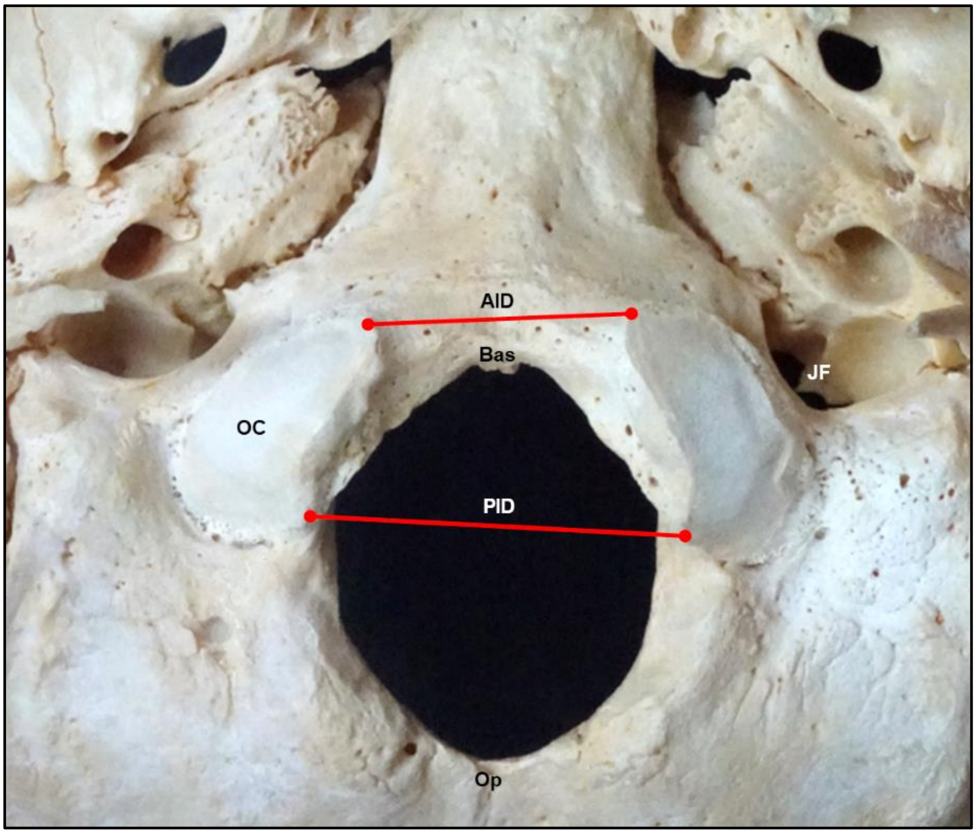

Figure 4. Inferior view of occipital bone showing AID and PID of OC. AID = anterior intercondylar distance of occipital condyle, Bas = basion, JF = jugular foramen, OC = occipital condyle, Op = opisthion, and PID = posterior intercondylar distance of occipital condyle.

Hence, the anterior and posterior intercondylar distances show how the OC is oriented and converging, which is necessary for screw insertion during occipitocervical fixation. In addition, shorter AID and PID may offer challenges during condylectomy by lateral approach (23). Ozer et al. (2017) (35) reported that the sagittal intercondylar angle was 68.7 ± 10.6 and the sagittal condylar angle was 32.9 ± 7.6 and 38.2 ± 7.3 degrees on the right and left sides, respectively (**Fig. 5**). As a result, OC converges ventrally. This causes OC to have different anterior and posterior angles. A wider sagittal condylar angle appears to be more beneficial for reaching the ventral FM. The asymmetry in the anterior and posterior intercondylar distances, length, and shape of OC may affect the lateral approach. These data are beneficial preoperative information before determining the amount of bone that must be removed during resection of the p1/3 of OC (4, 27, 34, 35) .

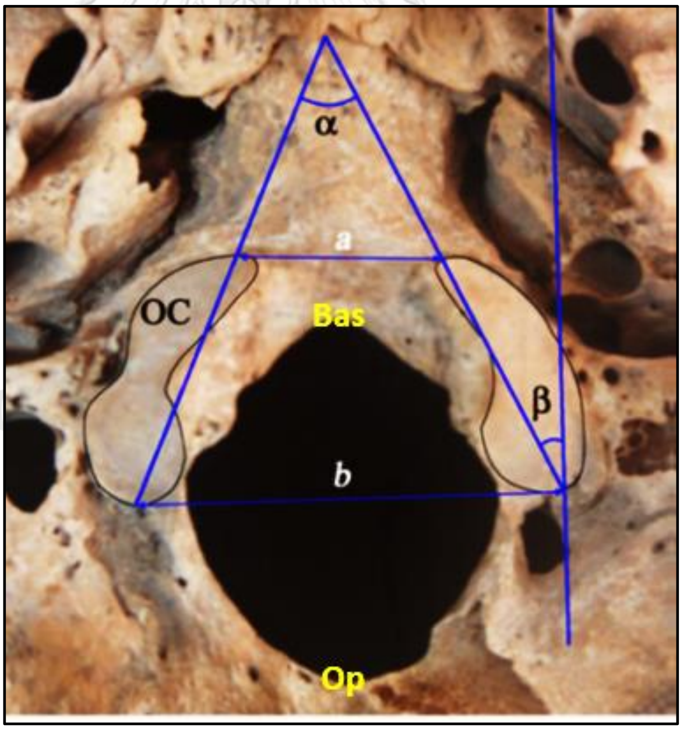

Figure 5. Inferior view of occipital bone showing sagittal intercondylar angle (α) and the left sagittal condylar angle (ß) (35). a = anterior intercondylar distance of occipital condyle, b = posterior intercondylar distance of occipital condyle, Bas = basion, OC = occipital condyle, and Op = opisthion.

Naderi et al. (2005) (19) classified the shapes of OC into eight types as follows: oval-like condyle, kidney-like condyle, S-like condyle, eight-like condyle, triangle-like condyle, ring-like condyle, two-portioned condyle, and deformed condyle, respectively. The most common shape was oval-like condyle (50%), whereas the most unusual shape was two-portioned condyle (0.8%) described in Turkish population (**Fig. 6**).

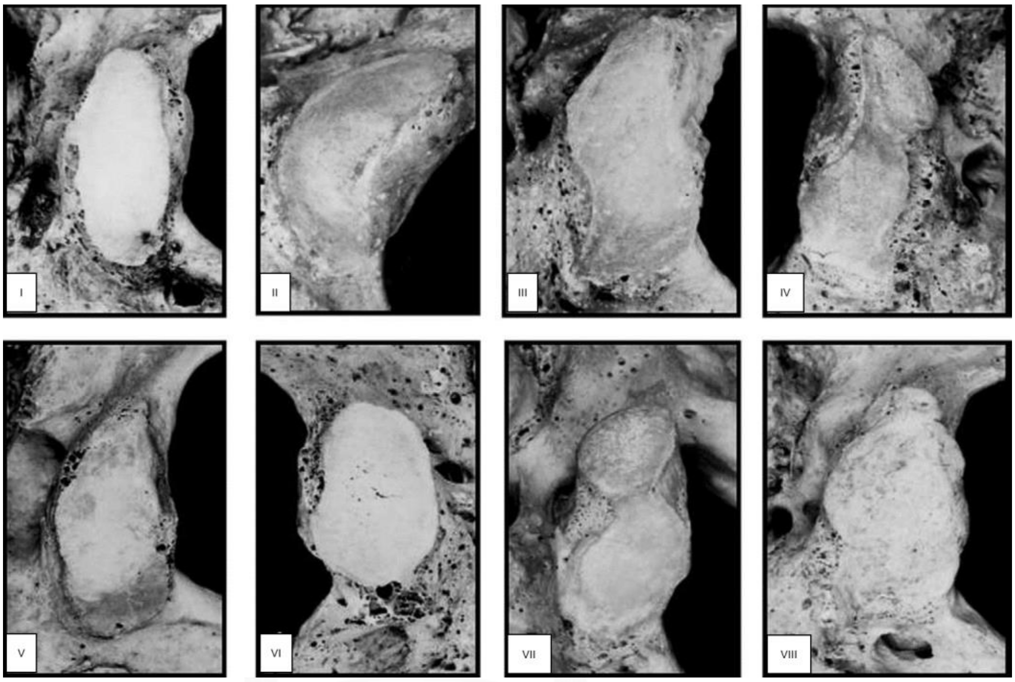

Figure 6. Eight types of occipital condyle—type I: oval-like condyle; type II: kidney-like condyle; type III: S-like condyle; type IV: eight-like condyle; type V: triangle condyle; type VI: ring-like condyle; type VII: two-portioned condyle, and type VIII: deformed condyle (19) .

In addition, Anjum et al. (2021) (21) classified the shapes of OC into ten types as follows: eight-like, elongated-like, irregular-like, kidney-like, oval-like, round-like, s-like, triangular-like, rectangular-like, and two portioned -like condyles. The oval-like condyle was the most common in both males (40%) and females (42.4%). In contrast, the kidney-like was the most common shape in Iran population with a prevalence of 34.4%, whereas deformed or irregular (2.2%) was the most unusual shape (36).

Verma et al. (2016) (18) concluded that the shape of OC was also important during condylectomy, as kidney-like, triangles, and deformed types required wider condylectomy to reach ventral lesions. The nail insertion was easier and more convenient to fix in an oval-like because of its large surface area, while it is difficult in a triangle, ring-like, and two-portioned type of OC. Naderi et al. (2005) (19) suggested that the shape of OC may affect the amount of condylectomy. The different types of OC, such as the triangle, the deformed, and kidney-like type may require a more extensive condylectomy to reach the ventral lesions.

Chethan et al. (2012) (37) reported a protrusion of OC into FM with a prevalence of 20.7%. These can lead to compression of structures passing through the FM. Muthukumar et al (2005) (38) found 20% of the skulls with OC protruded into the FM. Therefore, more bone resection during the transcondylar approach was need in the presence of OC protrusion (32) . In consequence, the knowledge of the OC-L, OC-W, and OC-H, shape of the OC, and its articular facet will help the surgeons to decide the extent of bone that can be removed (18) .

2. The morphology and morphometric study of foramen magnum, hypoglossal canal, jugular foramen, and posterior condylar canal

FM is in the center of the skull base giving a passage for various essential structures such as the medulla oblongata, meninges, and vertebral arteries (34) . There are three parts of FM. These are the dorsal (squamosal) part, the ventral (clival), and the condylar part of FM. The condylar part includes the OC, posterior margin of the JF and HC (4).

Shape of FM was classified as round (22.6%), oval (15.1%), egg (18.9%), tetragonal (18.9%), pentagonal (3.8%), hexagonal (5.6%) and irregular (15.1%) shapes (37) . However, Aragão et al. (2014) (39) classified the shapes of FM into nine types as pear-shaped (37.3%), rounded (15.5%), tetragonal (10.9%), biconvex (10.9%), hexagonal (9.1%), oval (5.5%), pentagonal (2.7%), heptagonal (1.8%) and irregular (6.4%), respectively (**Fig. 7**).

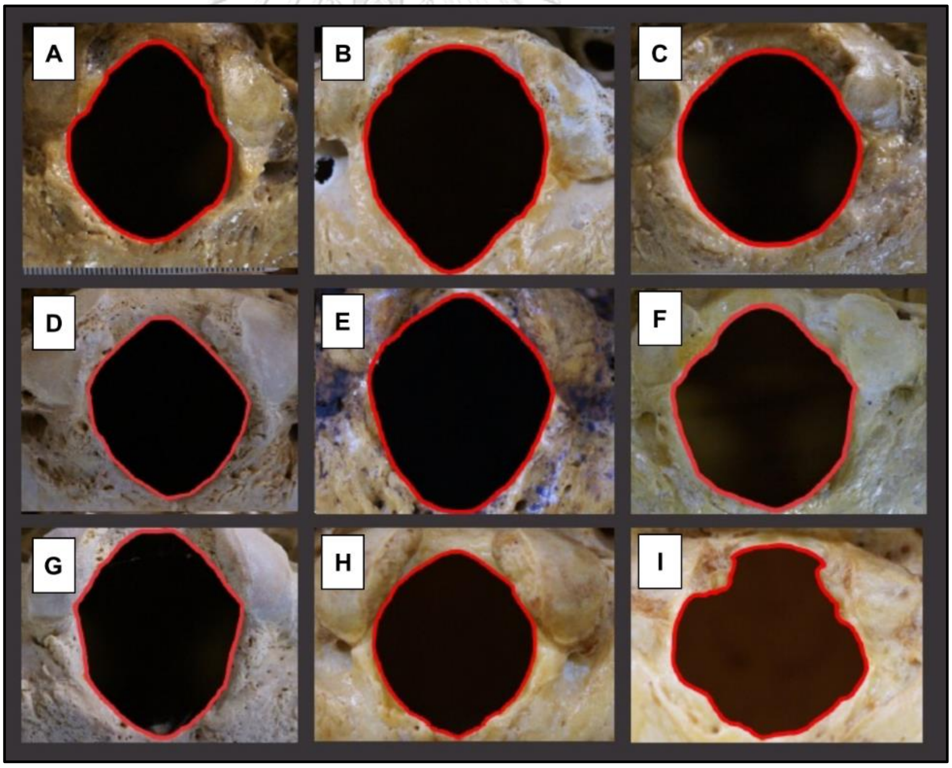

Figure 7. Different shapes of foramen magnum (inferior view). A: Pear, B: Oval, C: Rounded, D: Tetragonal, E: Pentagonal, F: Hexagonal, G: Heptagonal, H: Biconvex, and I: Irregular shapes, respectively (39) .

The shape of FM is necessary for determining the amount of bone to be removed. The transcondylar approach is appropriate for patients who have a small FM, a short distance between the FM and the brainstem, and a large OC (4, 40). Moreover, the FM shape can affect the surgical field. A round shape provides a wider operative angle than an oval shape (41).

The anteroposterior diameter (APD) of FM was measured from the end of the anterior border (basion) to the end of the posterior border (opisthion). The transverse diameter (TD) of FM was measured from the point of maximum concavity on the right margin to the maximum concavity on the left margin of FM (**Fig. 8**). The mean of APD and TD from previous study were 33.79±2.60 mm and 28.25±1.83 mm, respectively (42) . If the APD of FM is wide, it provides a better surgical exposure and more suitable for condylar resection. Additionally, the diameters of FM should be well documented for a safe OC resection (4).

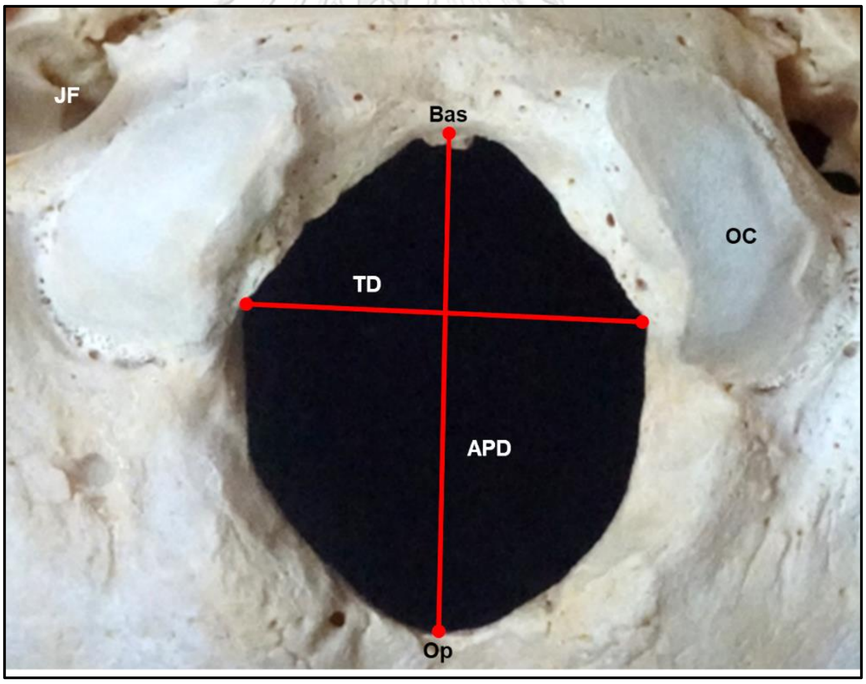

Figure 8. The measurement of APD and TD of the foramen magnum. APD = anteroposterior diameter of foramen magnum, Bas = basion, JF = jugular foramen, OC = occipital condyle, Op = opisthion, and TD = transverse diameter of foramen magnum.

Muthukumar et al. (2005) (38) calculated the FM index (FMI) by dividing the APD by TD. When the FMI was equal to or more than 1.2, the FM was considered as oval shape. Knowledge of the FMI is necessary for determining the appropriate surgical technique. Especially, in the transcondylar approach, the diameters of FM should be known for a safe OC resection (4, 43). In case with lesion located anterior to the brain stem, if the FM was an oval shape, a wider resection would be needed when compared to the rounded one (32) .

The HC or anterior condylar canal passes in a mediolateral direction through the base of OC. HC transverses superiorly to OC at the junction of anterior one-third (a1/3) and posterior two-third (p2/3) of OC. HC lies a little bit above and anterolateral to FM (**Fig. 9**). HC contains a hypoglossal nerve (CN XII), an emissary vein from the basilar plexus, meningeal branch of ascending pharyngeal artery, and the venous plexus (1, 7, 44, 45) . Verma et al. (2016) (18) defined the extent of HC in relation to OC into a1/3, m1/3, and p1/3 of the OC, respectively. They found that the HC was related to a1/3 of OC in 85.0% of cases and m1/3 of OC in 15.0% of cases. HC has been used as a middle landmark of OC. It was recommended to do not drill beyond the HC during OC resection. OC drilling can cause complications with CN XII nerve injuries or O-C1 joint instabilities. The accurate knowledge of the position of HC is essential to avoid unintentional injury to the CN XII (16, 28). Venous bleeding may occur when trying to avoid compressing the CN XII. This is often difficult as the venous plexus is usually the initial structure encountered when entering the HC. Therefore, understanding the possible positions of the HC when drilling into the occipital bone is extremely important during surgical (43) .

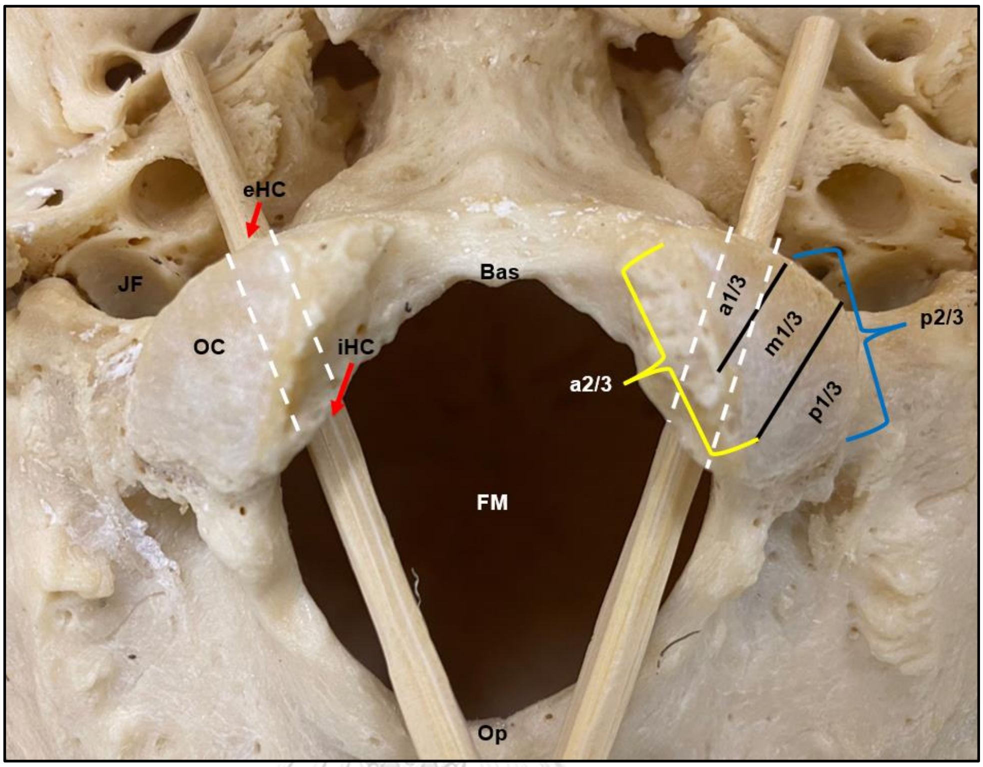

Figure 9. Inferior view of the skull base shows hypoglossal canal (dotted line) and its orifices (red arrows); eHC and iHC. a1/3 = anterior one third of OC, a2/3 = anterior two third of OC, Bas = basion, m1/3 = middle one third of OC, p1/3 = posterior one third of OC, p2/3 = posterior two third of OC, eHC = extracranial orifice of hypoglossal canal, FM = foramen magnum, iHC = intracranial orifice of hypoglossal canal, JF = jugular foramen, OC = occipital condyle, and Op = opisthion.

Moreover, Kalthur et al. (2014) (27) revealed that the locations of intracranial orifices of HC (iHC) were present in m1/3 in 100% of OC in male and female. The extracranial orifice of HC (eHC) was found in a1/3 in 98.0% and 93.7% for males and females. Only 1-2% was present in m1/3 (**Fig. 10 - 11**). If resection extends superior and inferior to HC, most of the jugular tubercle (JT) and all condyles will be removed. Therefore, the locations of the iHC and eHC, JF, and JT are important as they may get affected during the transcondylar approach. The location of the iHC and eHC may affect the lateral approaches to the CVJ. To avoid CN XII injury the location of HC should be determined in the preoperative imaging stage (19) .

JF is formed by the jugular notches of the temporal and occipital bones. The structures that traverse JF are the glossopharyngeal (CN IX), vagus (CN X), accessory nerves (CN XI) with their ganglia, the sigmoid sinus (SS) and jugular bulb (JB), the inferior petrosal sinus, the meningeal branches of the ascending pharyngeal and occipital arteries (46-48) (**Fig. 9 - 10**).

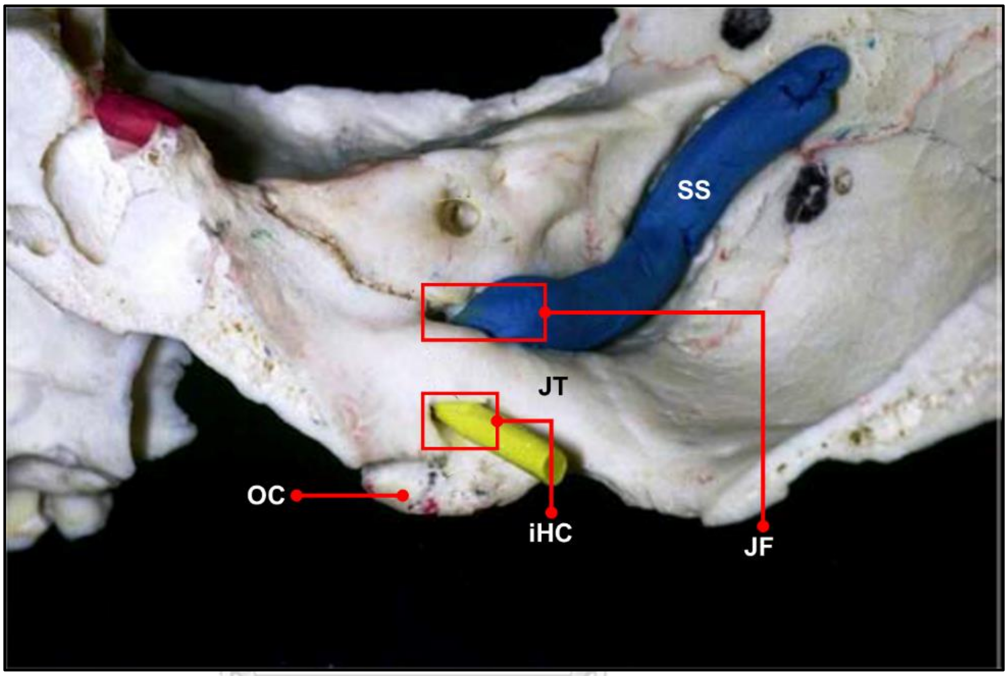

Figure 10. The left midsagittal view of the human skull base showing iHC, JF, JT, and OC (Modified from Karasu et al. (2009)) (33) . iHC = intracranial orifice of hypoglossal canal, JF = jugular foramen, JT = jugular tubercle, OC = occipital condyle, and SS = sigmoid sinus.

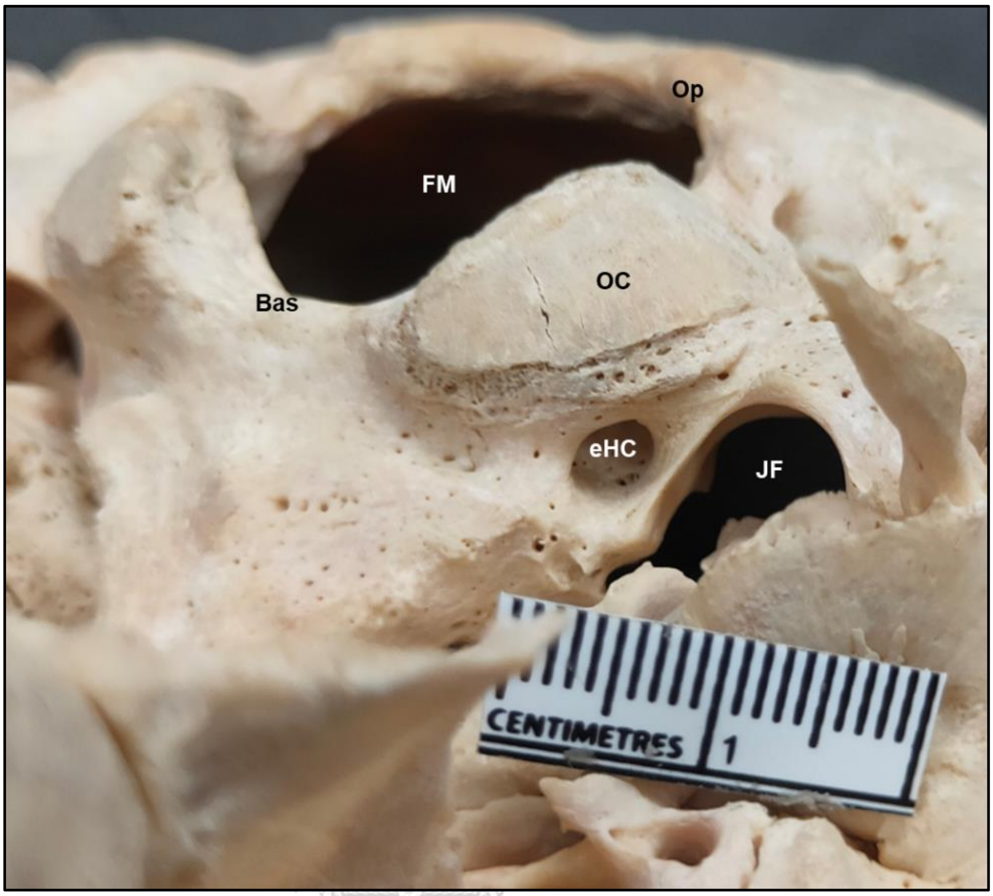

Figure 11. The right anterolateral view of human skull base showing the right side of extracranial orifice of hypoglossal canal (eHC), jugular foramen (JF), and occipital condyle (OC). Bas = basion, FM = foramen magnum, and Op = opisthion.

A condylar emissary vein is usually found in the condylar fossa (CF), and it should be identified on preoperative CT and MR images before surgery because it can be large, and its perforation can cause massive venous bleeding (9). The CF is located posterior to OC where the posterior condylar emissary vein often passes through the posterior condylar canal (PCC) or condylar foramen (36) . This canal connects the JF and the CF (32) (**Fig. 12**).

Bayat et al. (2014) (36) report that CF was presented in 60.0% of dry skull (24.0% in right side and 36.0% in left side) and PCC was found in 60.0%. Muthukumar et al. (2005) (38) reported the occurrence of PCC in 60.0% of specimens and more frequently found on the right side. In addition, Vanitha et al. (2015) (49) found that the PCC presented in 88.1%, in which 49.0% were bilateral and 37.0% were unilateral. Moreover, double and triple PCC were found in 1.1% both. The bony relations of the occipital condylar region on the external cranial base are shown in **Fig. 12**.

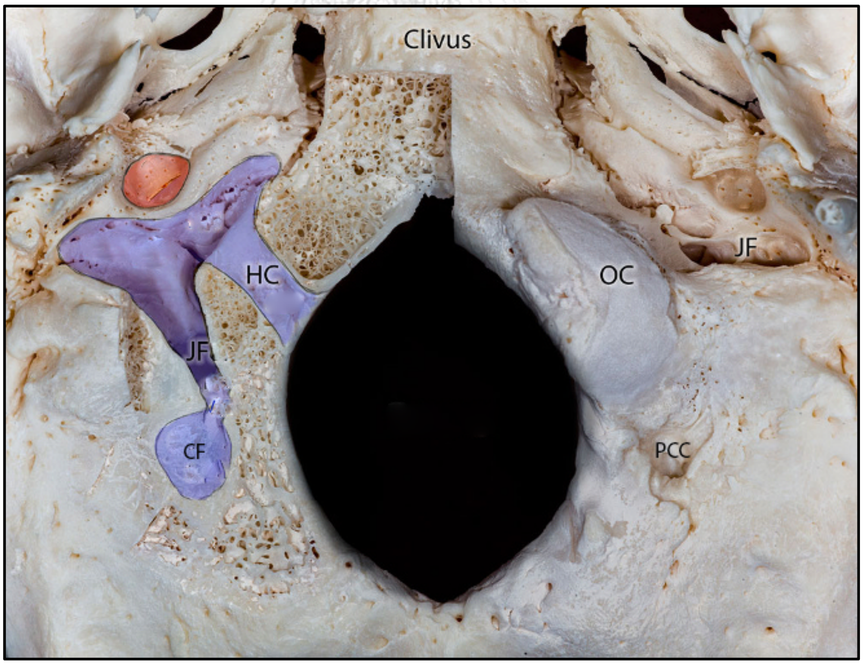

Figure 12. Inferior view of occipital bone showing the entire length of HC in the partial removed OC (right), JF, CF, and PCC. (Modified from Hellstern et al. (2019)) (50) . CF = condylar fossa, HC = hypoglossal canal, JF = jugular foramen, OC = occipital condyle, and PCC = the posterior condylar canal.

3. The distance between occipital condyles, foramen magnum, hypoglossal canal, and jugular foramen

The distance between OC, FM, HC, and JF has been widely studied. Ilhan et al. (2017) (4) measured the distances between OC and opisthion (Op), OC and basion (Bas). The distance from the anterior tip of OC to opisthion (OCAT-Op), and basion (OCAT-Bas) were measured as 39.43 ± 3.34 and 12.09 ± 1.76 mm, respectively. The distance from the posterior tip of OC to opisthion (OCPT-Op) and bsaion (OCPT-Bas) were 27.52 ± 2.59 and 27.93 ± 2.67 mm, respectively (**Fig. 13**). The longer distance of OCPT-Op is important since it represents the width of surgical exposure in suboccipital craniotomy and provides a free corridor for posterolateral approach and a longer corridor provides a wider space for a FLA (4, 27) . The tip of OC is closed to the median plane that should be considered during the application of screws into OC. This knowledge is essential for preventing adjacent neurovascular structures injury (23) .

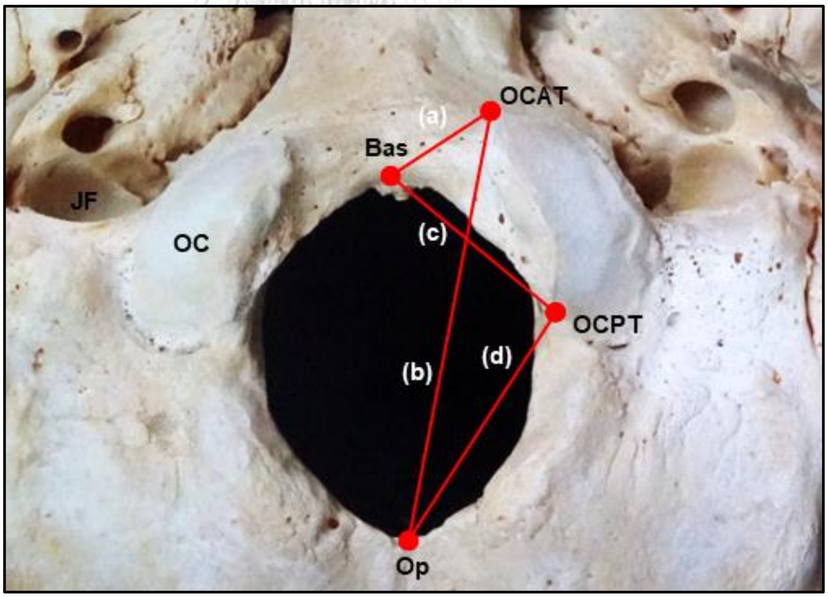

Figure 13. The left side of the inferior view of the skull showing (a) = OCAT-Bas, (b) = OCAT-Op, (c) = OCPT-Bas, and (d) = OCPT-Op. JF = jugular foramen, OC = occipital condyle, OCAT-Bas = distance between the anterior tip of occipital condyle and basion, OCAT-Op = distance between the anterior tip of occipital condyle and opisthion, OCPT-Bas = distance between the posterior tip of occipital condyle and basion, and OCPT-Op = distance between the posterior tip of occipital condyle and opisthion.

Karasu et al. (2009) (33) revealed the distances from posterior tip of OC to intracranial orifice of HC (OCPT-iHC) and extracranial orifice of HC (OCPT-eHC) were 8.4 ± 1.15 and 13.22 ± 2.24 mm, respectively (**Fig. 14**). Moreover, Di et al. (2019) (1) reported the right and left OCPT-iHC in Chinese skulls were 10.18 ± 1.44 mm, and 10.23 ± 1.14 mm. The right and left OCPT-eHC were 14.68 ± 1.69 mm, and 14.54 ± 1.55, respectively. OCPT-iHC and OCPT-eHC represents the HC depth and is of great significance during transcondylar approach, as it indicates the maximum amount of OC resection without entering the HC and damaging the structures present in HC (17, 18) .

Verma et al. (2016) (18) revealed the distance from the posterior tip of OC to the posterior-most end of JF (OCPT-JF), was 15.73 ± 3 mm on the right side and 16.77 ± 2.9 mm on the left side (**Fig. 14**). In addition, the JF was related to the a2/3 of OC in 90.0%, a1/3 of OC in 7.0%, and to the whole extent of OC in 3.0% cases in the North Indian population. Various neurovascular structures exit from the JF may be at risk during CVJ surgeries (18) .

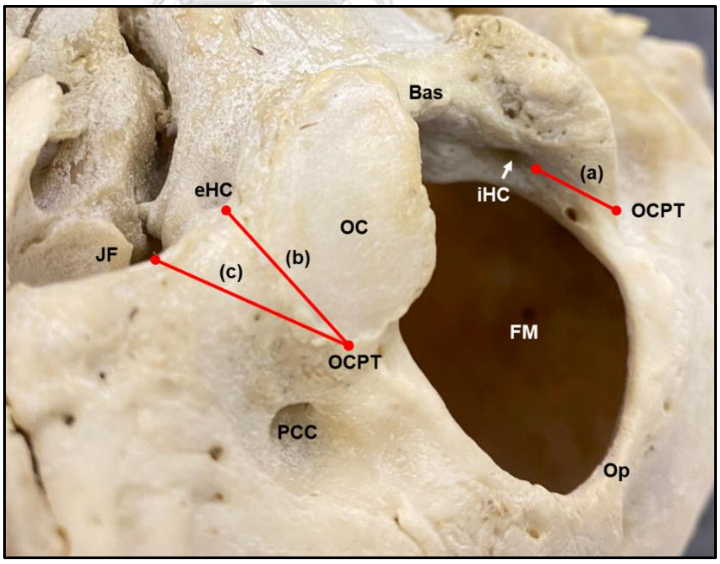

Figure 14. In the right inferolateral view, measurements of the left OCPT-iHC (a), the right OCPT-eHC (b), and OCPT-JF (c). Bas = basion, FM = foramen magnum, JF = jugular foramen, OC = occipital condyle, OCPT-eHC = distances from the posterior tip of occipital condyle to extracranial orifice of hypoglossal canal, OCPT-iHC = distances from the posterior tip of occipital condyle to intracranial orifice of hypoglossal canal, OCPT-JF = distance from the posterior tip of occipital condyle to the posterior-most end of jugular foramen, Op = opisthion, and PCC = posterior condylar canal.

4. The surface landmark for predicting the sigmoid sinus (SS) during bone resection

SS is a continuation of the transverse sinus (TS) and becomes the SS where the tentorium cerebelli ends (**Fig. 15**). It begins inferior to the temporal bone, posteromedial to the mastoid cells, and runs to the JF, extending through an S-shaped groove, where it meets the superior JB (51). The extracranial estimation of the intracranial venous sinuses is important for neurosurgeons to avoid venous sinus injury and resultant of blood loss or sinus occlusion with possible risk of venous infarction (52).

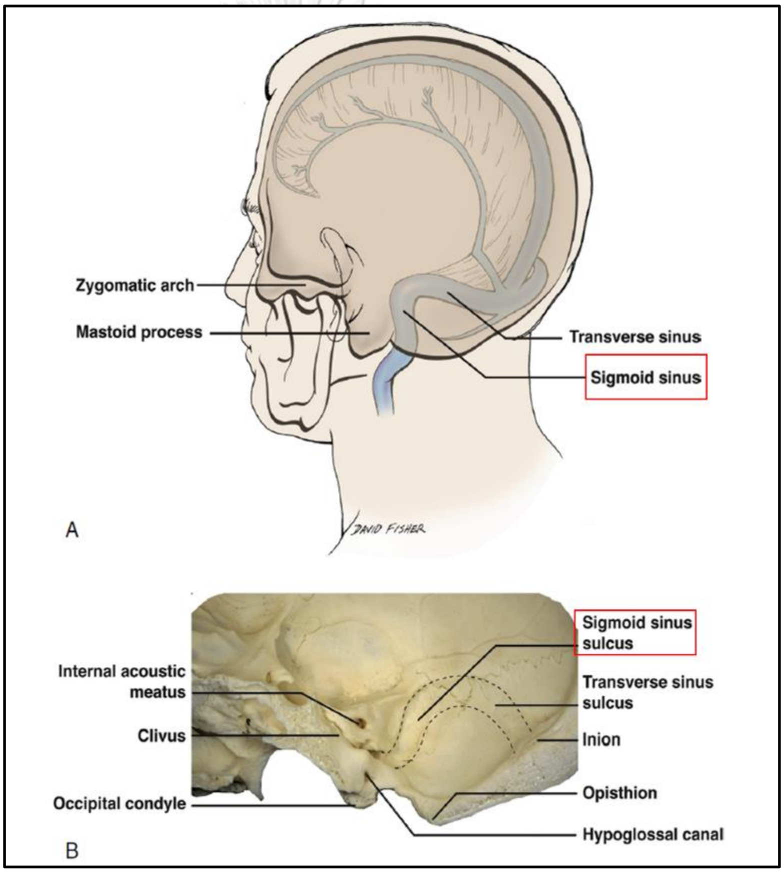

Figure 15. The left lateral view showing A: course of sigmoid sinus within the cranium, B: the sagittal section through a dry skull specimen showing the right sigmoid sinus sulcus (Modified from Aly and Tubbs (2020)) (51) .

The digastric point (DP) is located at the top of the digastric groove (DG). This DP is easily identifiable in dry skulls and during surgical procedures because the DG is covered by the posterior belly of the digastric muscle (DM). The relationship of the DP with the SS can be used as a lateral limit on the suboccipital access (53) (**Fig. 16**). Preoperative identification of the positions of the SS plays an important role in determining the success of craniotomy (54) .

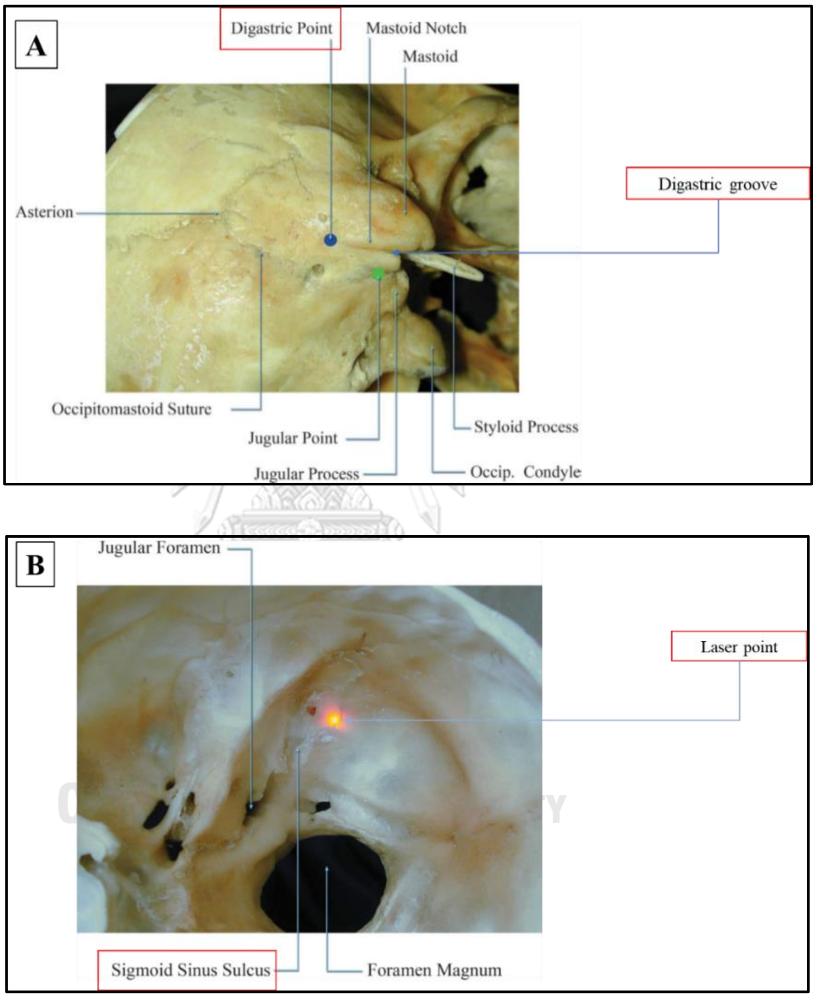

Figure 16. A: The right superolateral view shows digastric point, which is defined as the point at the top of the digastric groove (blue circle), B: Superior view of the internal skull using a laser pointer transillumination to detect the correspondence of the right digastric point in the inner surface of the skull (Modified from Raso et al (2011)) (53).

Raso et al. (2011) (53) studied the DP in 127 skulls (254 sides), They found the DP projected over the SS in 49.6% of cases on the right and in 29.9% on the left. When the DP did not project over the SS, the mean distance between this point and the SS was 3.10 mm. The surface landmarks are widely used for surgical planning. The DP is a visible landmark in lateral approaches to the posterior cranial fossa (54).

Information of distance, Op-DP, OCPT-DP, and JF-DP may help the surgeons in performing a craniotomy.

5. The craniovertebral junction and its lesions

The CVJ is an area that connects the cranium to the upper cervical spine, it consists of the first two cervical vertebrae (C1, and C2), FM, and LC that supports the brainstem. It is bounded laterally by JF, HC, and OC (1-3) (**Fig. 17**). The neurovascular structures associate with CVJ are the medulla oblongata, the upper spinal and low cranial nerves (CN IX, X, XI, and XII), vertebral arteries (VA) with their branches, and vertebral veins (4) .

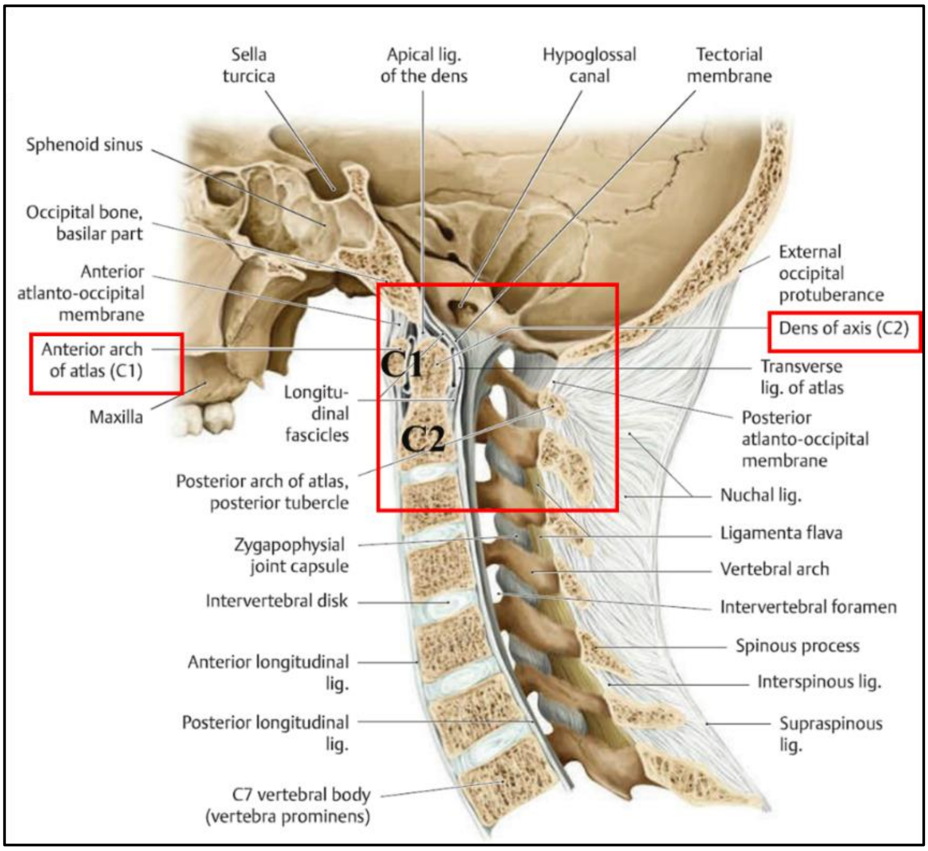

Figure 17. The midsagittal section (left lateral view) of craniovertebral junction area that connects cranium to the upper cervical spine (Modified from Gilroy et al. (2008) (29) . C1 = atlas and C2 = axis.

The CVJ is an area of transition between brainstem and spinal cord. It consists of O-C1 and atlantoaxial (C1-C2) joint. O-C1 joint acts as flexion and extension of the cranium. C1-C2 joint acts as mobility in flexion, extension, axial rotation, and to less lateral flexion because of the biconvex shape. The transverse and alar ligaments stabilize this joint complex. The major concern of CVJ instability is the stenotic injury to spinal cord and its derivatives (55, 56).

The CVJ is a common site for various lesions including neoplasms (intra- and extradural tumors), vascular lesions such as a vertebral artery aneurysm, rheumatic diseases, malformations of the CVJ, and degenerative pathologies (1, 2, 4-6) . The lesions at CVJ are difficult to treat because of their location and complex anatomic relations (7).

6. The far lateral approach (FLA) and its applications

FLA is used to access the ventrolateral part of CVJ and LC by drilling the lateral edge of the FM rim for tumor removal and the treatment of vascular lesions (8, 9) (**Fig. 18**). There are several types of FLA including transcondylar, supracondylar, and paracondylar approaches (10, 11) (**Fig. 19**).

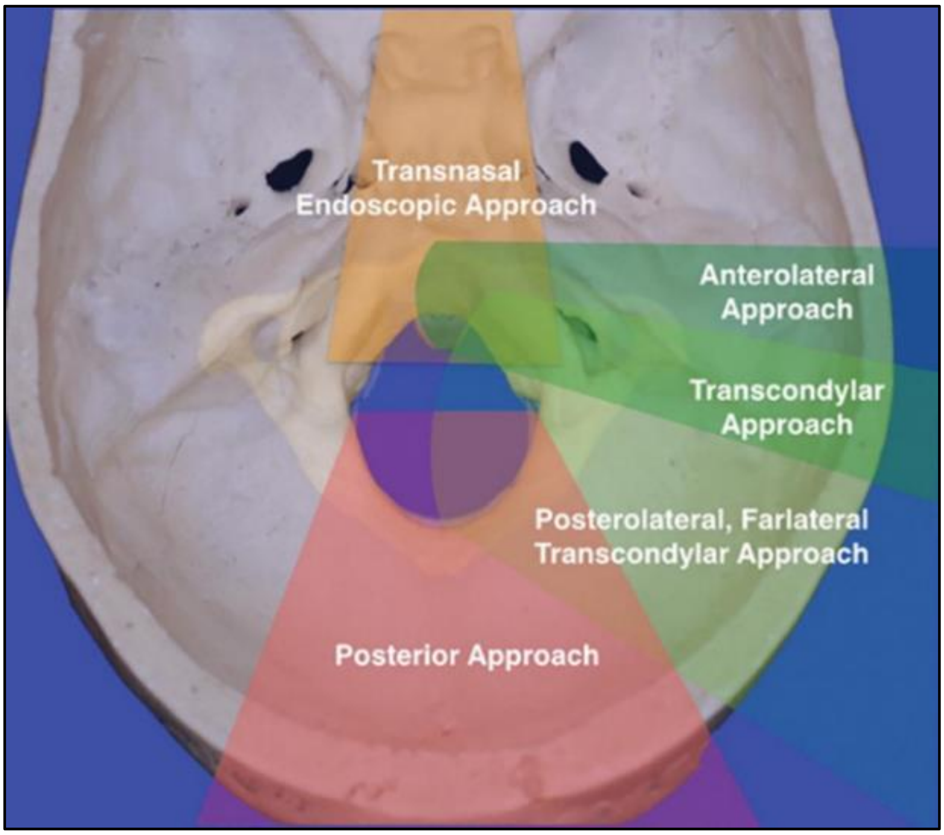

Figure 18. Superior view of the internal skull showing surgical corridors to craniovertebral junction (CVJ) includes the anterolateral, far lateral transcondylar, posterior, posterolateral, transcondylar, and transnasal endoscopic approaches. (Available from: https://link.springer.com/chapter/10.1007/978-3-030-18700-2_16)

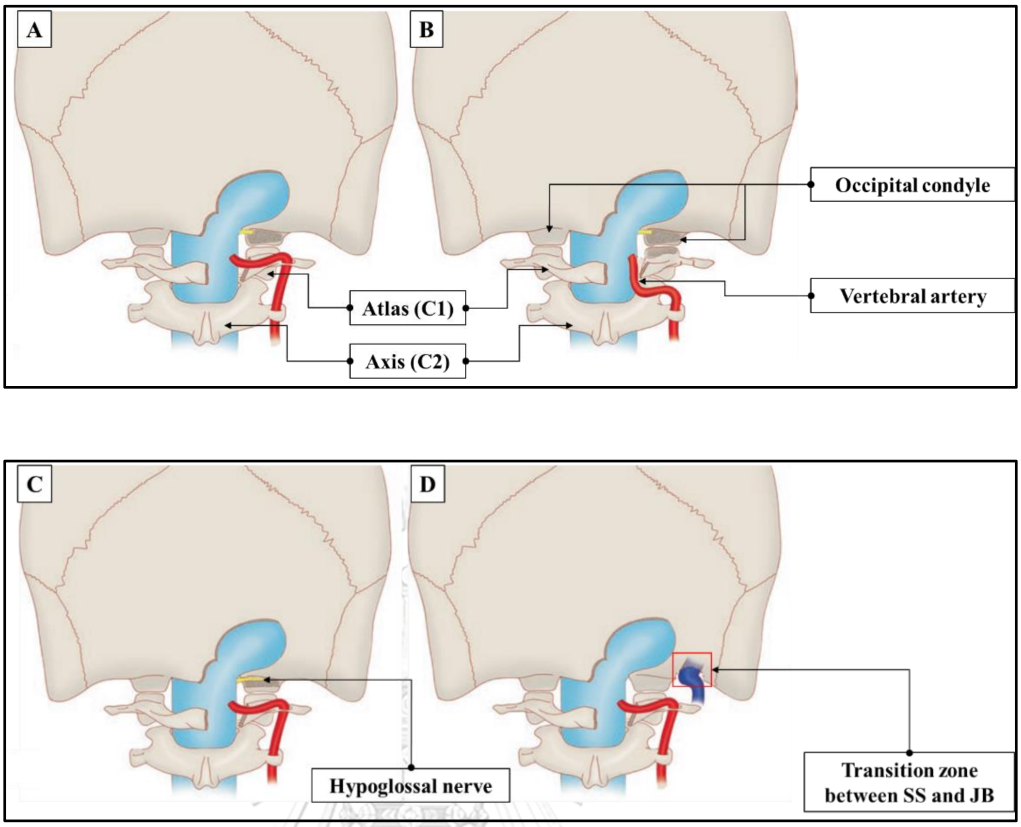

Figure 19. The posterior view of skull showing A: The transcondylar variants, incorporates removal of posterior third of OC to HC. The shaded area denotes exposed cancellous bone, deep to articular surface of OC and caudal HC. B: The complete transcondylar variant requires removal of posterior aspect of C1 lateral mass to open transverse foramen. This allows for inferomedial displacement of VA. OC and C1 lateral mass are then both drilled to the depth of medial HC. C: The supracondylar variant increases rostral exposure while preserving articular surface of OC. The shaded region denotes exposed cancellous bone below HC. D: The paracondylar variants, removal of JP lateral to OC, exposes transition between SS and JB (red box) (Modified from Au et al. (2018)) (10). C1 = atlas, HC = hypoglossal canal, JB = jugular bulb, JP = jugular process, OC = occipital condyle, SS = sigmoid sinus, and VA = vertebral artery.

Transcondylar approach is directed through the OC or the O-C1 joint and adjacent parts of the condyle by drilling the condyles to allow a more lateral approach and provide the assessment to LC and pre-medullary area. Supracondylar approach is directed through the area above OC, provides access to the region of and medial to the HC and JT. The paracondylar exposure directed through the area lateral to the OC which includes drilling of the jugular process of the occipital bone in the area lateral to the OC and accesses the posterior part of the JF and the posterior aspect of the facial nerve (CN VII) and mastoid on the lateral side of the JF (57) . The complications of FLA are the development of cerebrospinal fluid (CSF) leak, damage to the VA, and damage of neural structures (1, 8, 9). However, a variant of FLA can be used according to the nature of the location of a lesion in the CVJ and the relation with the surrounding neurovascular tissues (32).

Mazur et al. (2017) (16) found that removed 29% of OC caused alterations in cadaveric biomechanics. Furthermore, they reported in 2019 that two of five patients whose OC resection extended beyond the HC had a delayed presentation of severe CVJ deformity after surgery. (**Fig. 20**), changes in CVJ biomechanics may occur when even p1/3 of the OC was resected. Therefore, less bone removal may be required during surgery than was performed in the cadaveric model (58) .

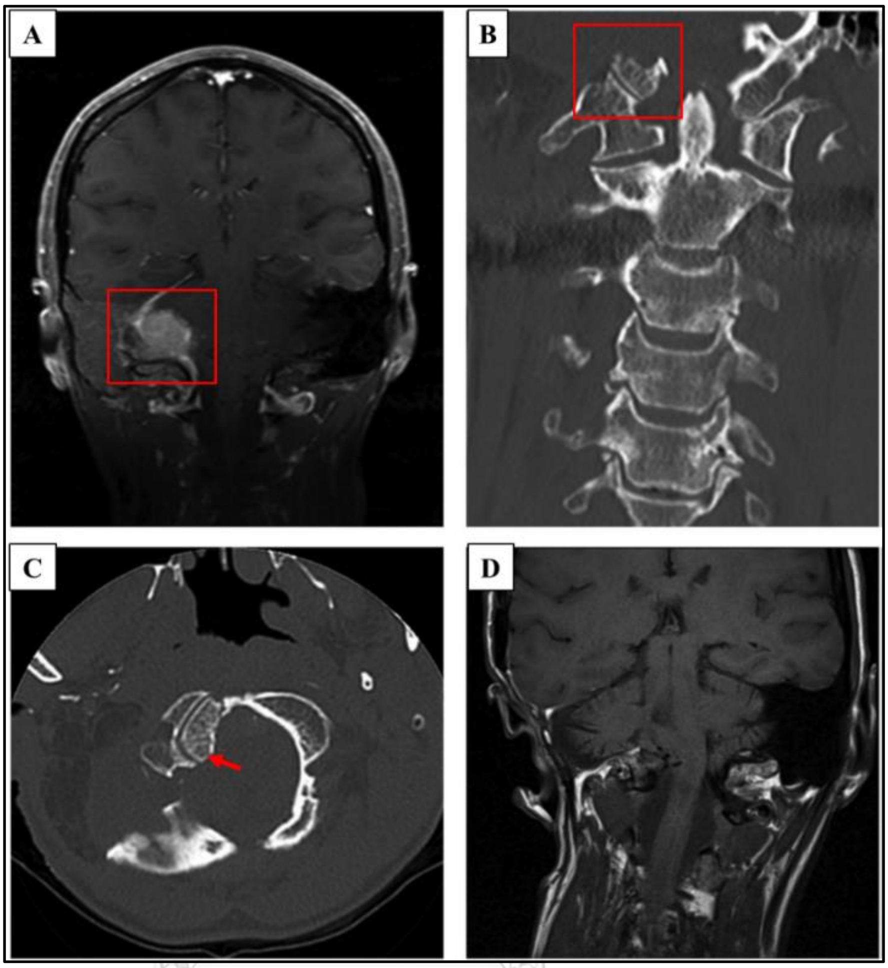

Figure 20. A: Contrast-enhanced MRI demonstrating a jugular foramen meningioma with extension inferiorly into FM and invasion into OC and supracondylar region (red box). B: The coronal view of postoperative CT image demonstrating the remnant of the right OC after extensive drilling of bone during tumor resection (red box). C: The axial view of postoperative CT image demonstrating the remnant of the right OC. D: At 3 years, coronal MRI demonstrated persistent coronal deformity (From Mazur et al. (2019)) (58) . CT = computerized tomography scan, FM = foramen magnum, MRI = magnetic resonance imaging, and OC = occipital condyle.

Chapter III Material and methods

Target population and sample population

This current study used the adult human dry skulls with unknown age and cause of death. The samples for this study were taken from the department of anatomy, faculty of medicine, Chulalongkorn University, Thailand.

Inclusion criteria

1. Adult human dry skulls with intact occipital condyle.

Exclusion criteria

2. Adult human dry skulls reveal the occipital condyle fracture.
3. Skulls that with broken at the cranial base.

Sample size determination

From the pilot study of 20 skulls (10 males and 10 females), the standard deviation (SD) of occipital condyle length (OC-L) was 3.22 millimeter. This current study used the sample size equation from the descriptive study and confidence interval (CI) set as 95%.

$$n = \frac{z^2\alpha/_2\sigma^2}{d^2}$$

When $z^2\alpha/_2$ = 1.96 (two-tailed)

SD = standard deviation = 3.22

σ^2 = variance = sd^2 = $\mathbf{3.22}^2$ = 10.37

d = acceptable error = 0.5 mm

Therefore $$n = \frac{(1.96)^2(3.22)^2}{(0.5)^2}$$

n = 159.32

The calculated sample size was at least 160 occipital condyles (80 dry skulls). In this study, 100 dry skulls (50 male and 50 female skulls) were determined.

Research Framework

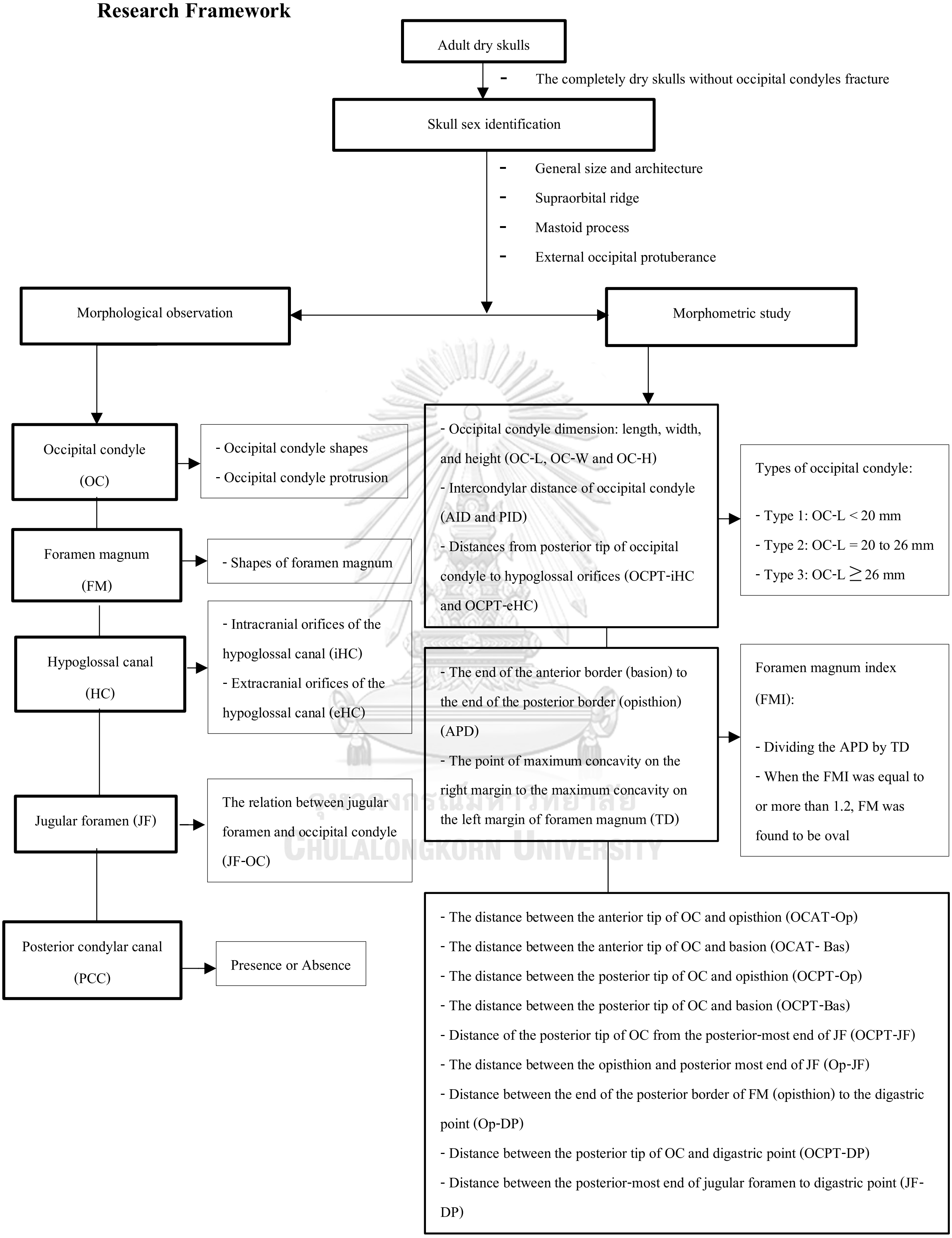

Materials and Methods

Equipment

1. ABSOLUTE Digimatic Caliper (Mitutoyo ® 0-150 mm)
2. Permanent marker
3. Pencil
4. Digital camera

Methods

1. Sex determination of the skull

Our first step was to randomly select the samples (**Fig. 21**). Then, we determined the sex of skulls. We used nonmetric traits for determining the sex of skulls. There are differences in the skull pattern and skull traits between sexes, for example, mastoid process, supraorbital ridge, size and architecture of skull, zygomatic extensions, nasal aperture, and mandible gonial angle. The Determination of sex by using only these six traits shows an accuracy of 94.0% (59) . The mandible gonial angle will not be considered because not all the included skulls have a mandible. According to modified Krogman's cranioscopy traits by grading, males had larger and rougher external occipital protuberance than females (60) . In this study, we used general size and architecture, supraorbital ridges, mastoid process, and external occipital protuberance for sex determination of skulls (**Fig. 22**). **Table 4** shows four criteria used to differentiate between male and female skulls. The sex determination was done by two investigators separately. If there was any conflict, the consensus was done.

Figure 21. All dry skulls were stored in plastic boxes, two of them contain in each box.

Table 4. Showing the five criteria to identifies the sex difference between male and female

Criteria	Male	Female
General size and architecture	Large/Rugged	Small/Smooth
Supraorbital ridge	Round and dull	Sharper
Mastoid process	Medium to Large	Small to medium
External occipital protuberance	Large/ Rough	Small/Smooth

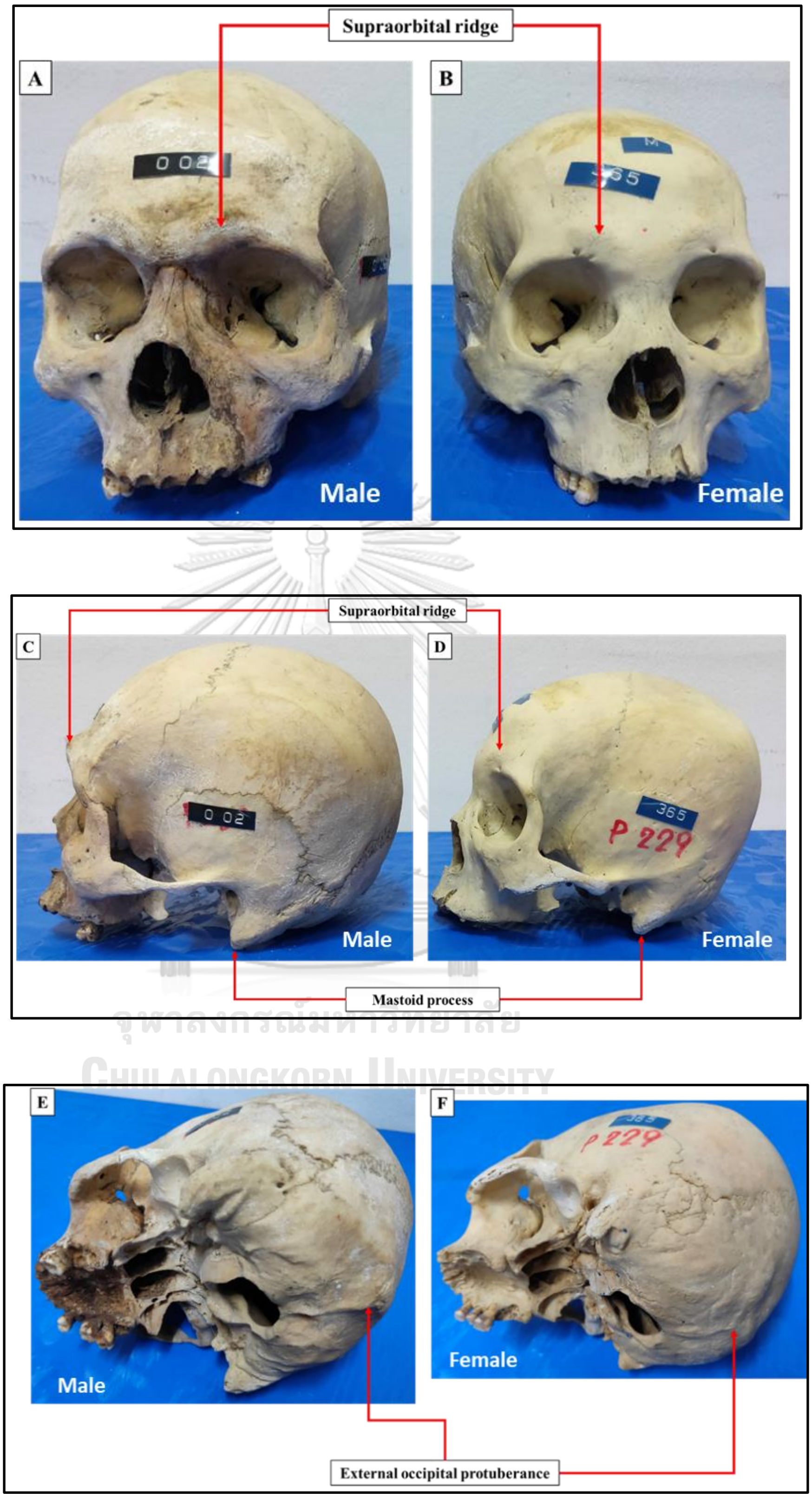

Figure 22. A: Anterior view of a male skull with large size and round supraorbital ridge. B: Anterior view of a female skull with a smaller size and a sharp supraorbital ridge. C: The left lateral view of male skull with a

large volume of a mastoid process, and thick and rounded supraorbital ridge. D: The left lateral view of female skull with a small volume of a mastoid process, thin supraorbital ridge. E: The left posterolateral view of male skull with a prominent occipital protuberance. F: The left posterolateral view of male skull with a less marked occipital protuberance.

2. Identify the anatomical structure on the base of the skulls

There are many bony structures, foramina, and canals for blood vessels and cranial nerves on the skull base. Fourteen structures on the skull base were identified by using an Atlas of Anatomy textbook (29) , and Ilhan et al. (2017) (4) (**Fig. 23**).

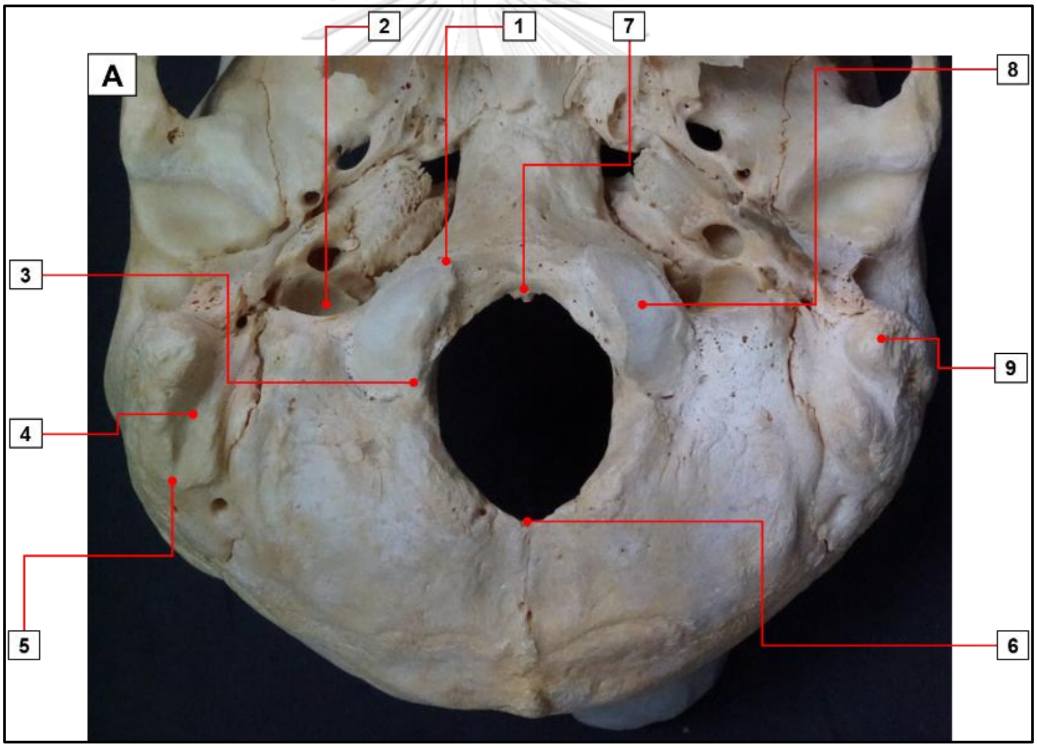

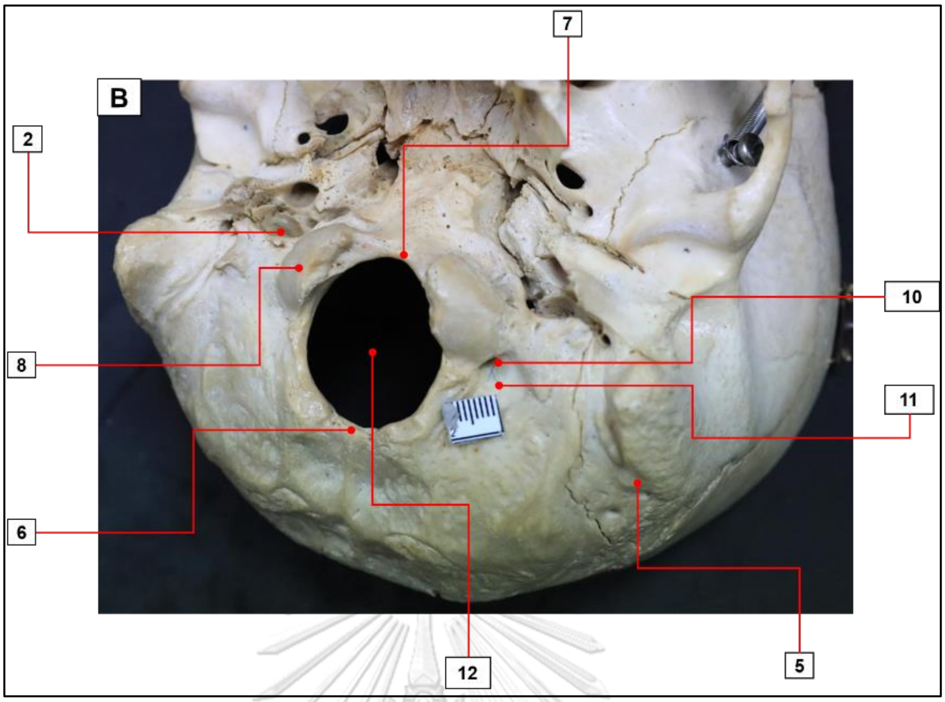
B
7
2
8
10
11
6
12
5

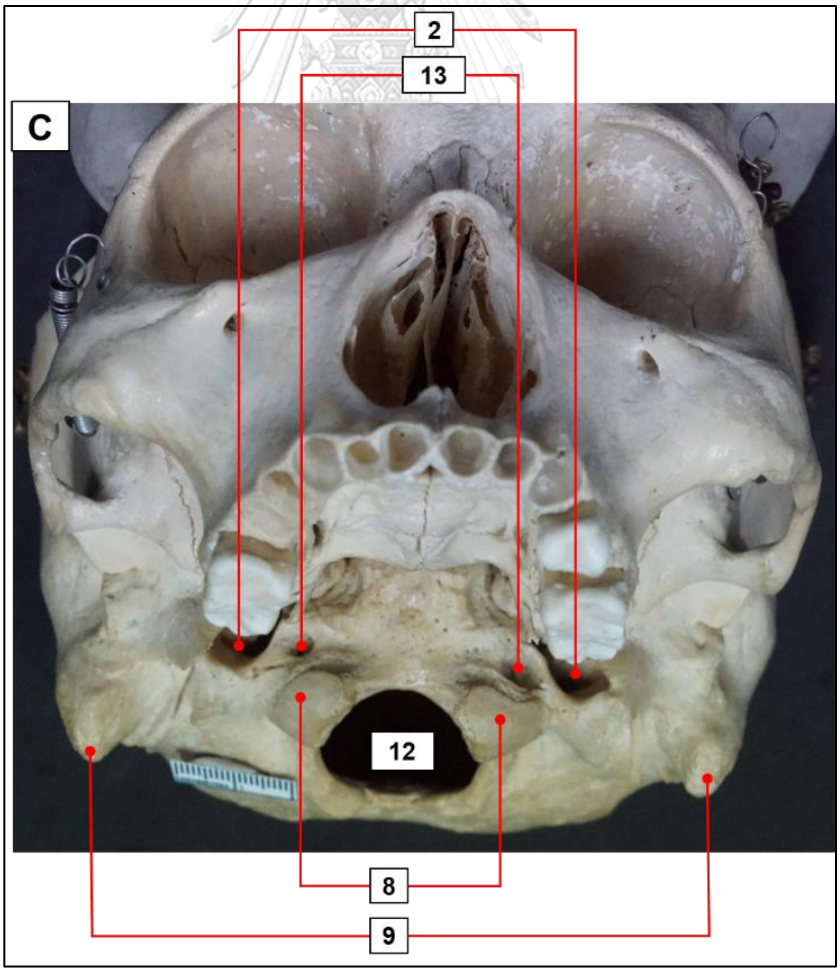
2
13
C
12
8
9

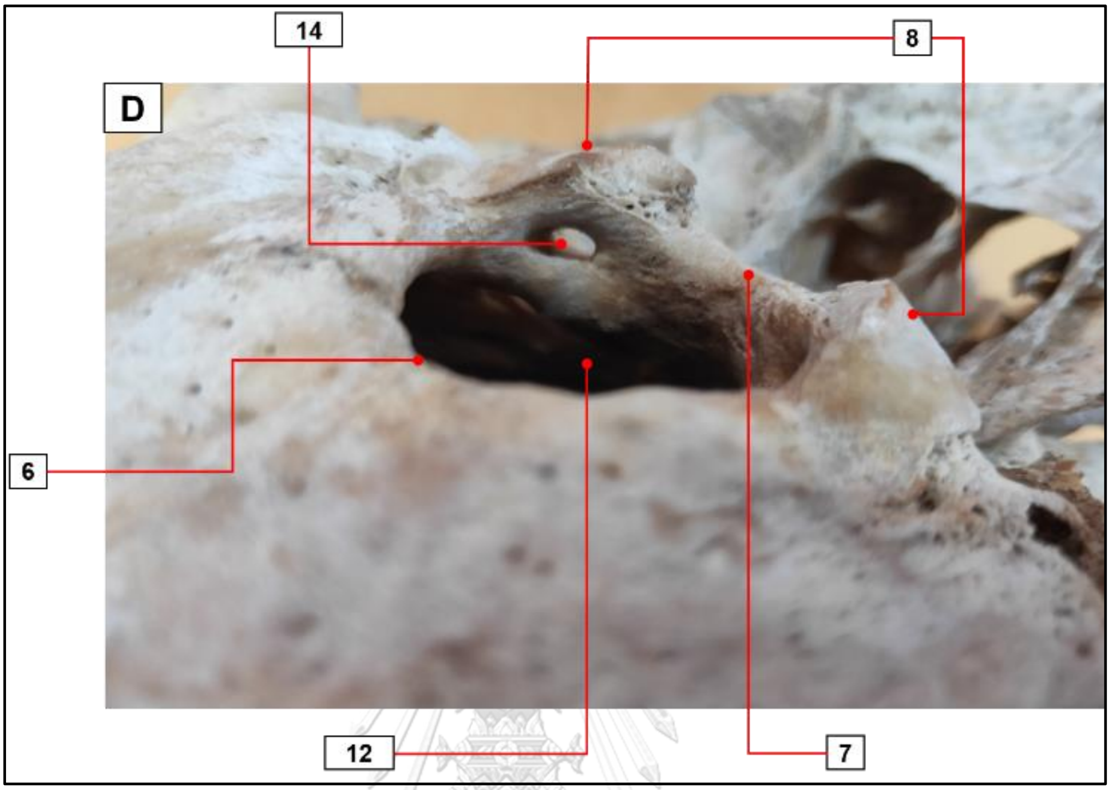

Figure 23. A: Inferior view, B: Left - inferolateral view, C: Inferoanterior view and D: Left posterolateral views of occipital bone. 1 - Anterior tip of the occipital condyle (OCAT), 2 – Jugular foramen (JF), 3 – Posterior tip of the occipital condyle (OCPT), 4 – Digastric groove (DG), 5 – Digastric point (DP), 6 – Opisthion (Op), 7 – Basion (Bas), 8 – Occipital condyle (OC), 9 – Mastoid process (MT), 10 – Posterior condylar canal (PCC), 11 – Condylar fossa (CF), 12 – Foramen magnum (FM), 13 – Extracranial orifice of hypoglossal canal (eHC), 14 – intracranial orifice of hypoglossal canal (iHC).

3. Marking the specific points on the skull base with a permanent marker. There were fourteen points of eight bony landmarks to be marked for measuring the parameters (**Table 5 and Fig. 24**).

Table 5. List of landmarks on the skull base

No	**Marking point**	**Number**
1	Anterior tips of OC (Lt/Rt)	2
2	Posterior tips of OC (Lt/Rt)	2
3	Most medial point on the medial border of OC (Lt/Rt)	2
4	Most lateral point on the lateral border of OC (Lt/Rt)	2
5	Posterior- most end of JF (Lt/Rt)	2
6	Middle point of the anterior margin of FM (basion)	1
7	Middle point of the posterior margin of FM (opisthion)	1
8	Digastric point (Lt/Rt)	2

FM = foramen magnum, JF = jugular foramen, and OC = occipital condyle

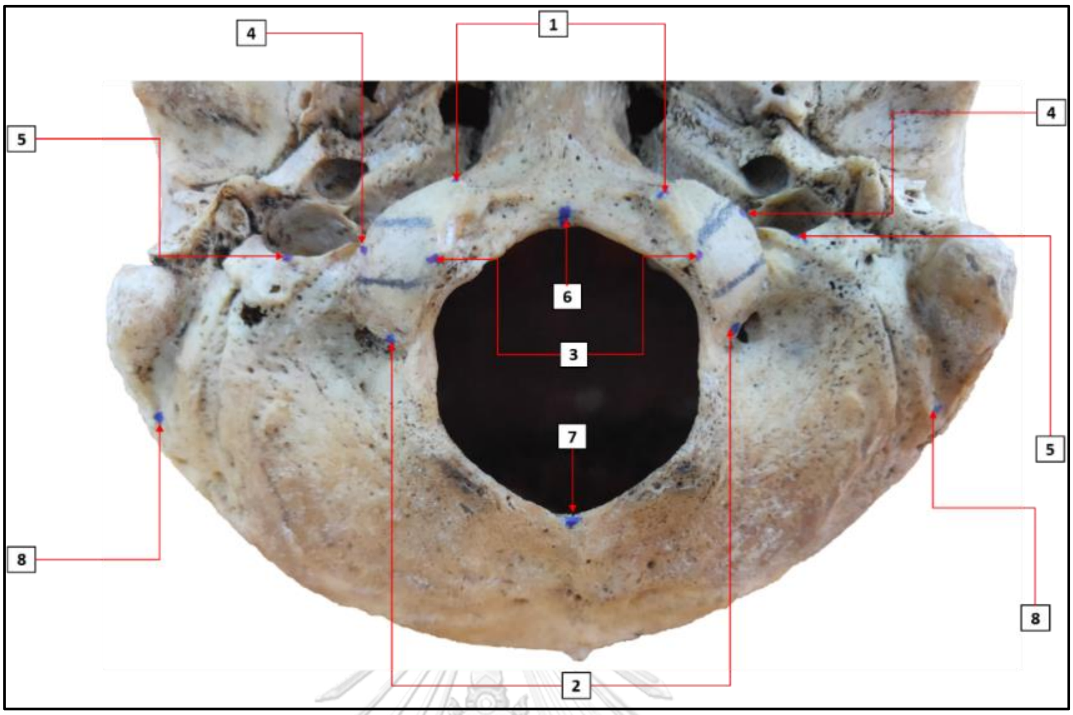

Figure 24. Inferior view of the occipital bone. 1; anterior tips occipital condyle (left), 2; posterior tips of the occipital condyle (left), 3; most medial point on the medial border of occipital condyle (right), 4; most lateral point on the lateral border of occipital condyle (left), 5; posterior most end of jugular foramen (right), 6; middle point of the anterior margin of foramen magnum, 7; middle point of the posterior margin of foramen magnum, and 8 - digastric point (right).

4. Observations and Measurements

Seven morphological studies were observed (**Table 6**). Eighteen proposed measurements were recorded to two decimal places by using ABSOLUTE Digimatic Caliper (Mitutoyo ® 0-150 mm) accurate to 0.02 mm (**Table 7**).

Table 6. Morphological observation

Morphological observation	Recording
OC shape	Type I; oval-like condyle, type II; kidney-like condyle, type III; S-like condyle, type IV; eight-like condyle, type V; triangle condyle, type VI; ring-like condyle, type VII; two-portioned condyle, and type VIII; deformed condyle
OC protrusion (p-OC)	Yes No
Location of iHC (L-iHC)	Location 1; Anterior 1/3 of OC length Location 2; Junction between anterior and middle 1/3 of OC length Location 3; Middle 1/3 of OC length Location 4; Junction between middle and posterior 1/3 of OC length Location 5; Posterior 1/3 of OC length
Location of eHC (L-eHC)	Location 1; Anterior 1/3 of OC length Location 2; Junction between anterior and middle 1/3 of OC length Location 3; Middle 1/3 of OC length Location 4; Junction between middle and posterior 1/3 of OC length Location 5; Posterior 1/3 of OC length
JF relation to OC (JF - OC)	Anterior 1/3 of OC length Anterior 2/3 of OC length Entire OC length
FM shape	Type I; Pear - shaped, type II; Oval, type III; Rounded, type IV; Tetragonal, type V; Pentagonal, type VI; Hexagonal, type VII; Heptagonal, type VIII; Biconvex, and type IX; Irregular shapes
PCC	Presence Absence

eHC = extracranial orifice of hypoglossal canal, FM = foramen magnum, iHC = intracranial orifice of hypoglossal canal, JF = jugular foramen, OC = occipital condyle, and PCC = posterior condylar canal.

Table 7. Definition of eighteen measurements proposed in this study

Abbreviation	Definition
OC-L	The maximum anteroposterior distance between anterior and posterior tips of OC (facet)
OC-W	The maximum transverse distance between most medial point on the medial border and most lateral point on the lateral border of OC
OC-H	The maximum vertical distance between upper and lower boundary of medial margin of OC
OCPT-iHC	The distances from posterior tip of the OC to intracranial orifice of HC
OCPT-eHC	The distances from posterior tip of the OC to extracranial orifice of HC
AID	The distance between anterior tips of right and left OC
PID	The distance between posterior tips of right and left OC
OCAT-Op	The distance between the anterior tip of OC and opisthion
OCAT- Bas	The distance between the anterior tip of OC and basion
OCPT-Op	The distance between the posterior tip of OC and opisthion
OCPT-Bas	The distance between the posterior tip of OC and basion
OCPT-JF	The distance from the posterior tip of OC to the posterior-most end of JF (midpoint of posterior edge)
Op-JF	The distance between the opisthion and posterior most end of JF (midpoint of posterior edge)
APD	Measured from the end of the anterior border (basion) to the end of the posterior border (opisthion) of FM
TD	Measured from the point of maximum concavity on the right margin to the maximum concavity on the left margin of FM
Op-DP	The distance between the end of the posterior border of FM (opisthion) to DP
OCPT-DP	The distance between the posterior tip of OC and DP
JF-DP	The distance between the posterior most end of JF to DP

AID = anterior intercondylar distance of occipital condyle, APD = anteroposterior diameter of foramen magnum, Bas = basion, DP = digastric point, eHC = extracranial orifice of hypoglossal canal, FM = foramen magnum, iHC = intracranial orifice of hypoglossal canal, JF = jugular foramen, OC = occipital condyle, OCAT = anterior tip of occipital condyle, OC-H = occipital condyle height, OC-L = occipital condyle length, OCPT = posterior tip of occipital condyle, OCPT = posterior tip of occipital condyle, Op = opisthion, OC-W = occipital width, PID = posterior intercondylar distance of occipital condyle, and TD = transverse diameter of foramen magnum.

4.1 OC shapes were classified into eight types based on the facet shape (19) (**Fig. 25**). The protrusion of OC into the FM was observed.

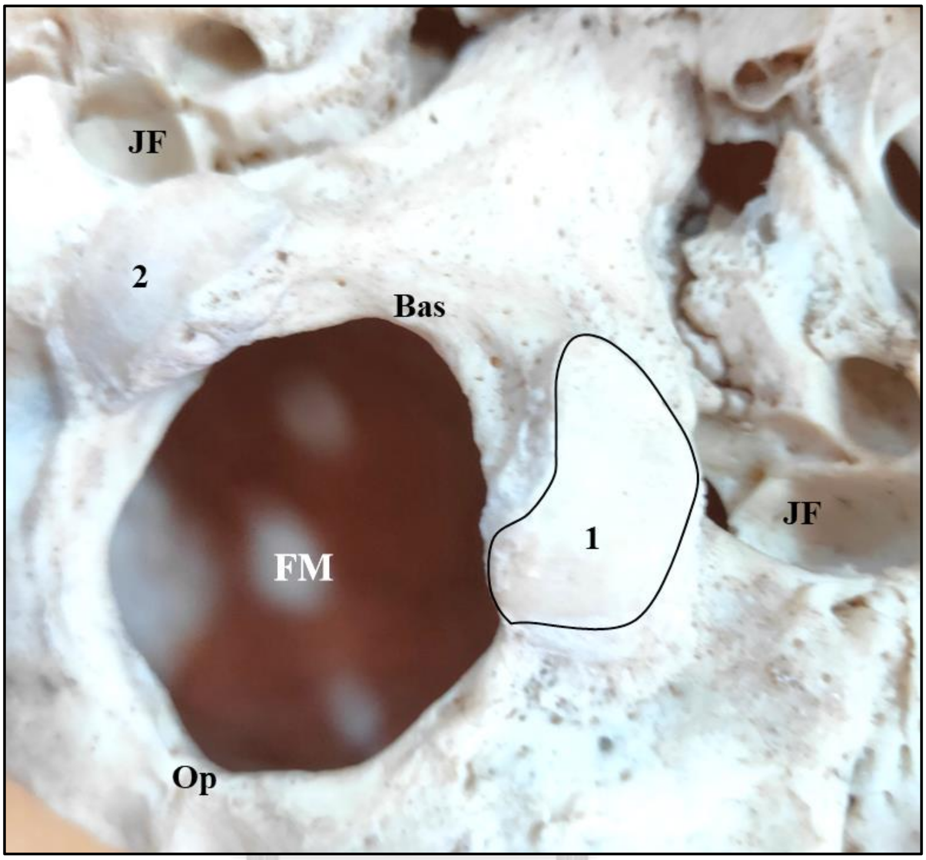

Figure 25. Inferior view of the skull represents occipital condyle. 1; left occipital condyle, and 2; right occipital condyle. The shape of articular facets of the occipital condyle were considered in the classification of shapes. Bas = basion, FM = foramen magnum, JF = jugular foramen, and Op = opisthion.

4.2 Dimension of OC: length, width, and height were measured by a digital vernier calipers (**Fig. 2**). Then, the length of OC was divided into three equal parts: anterior one-third (a1/3), middle one-third (m1/3), and posterior one-third (p1/3), respectively (27) (**Fig. 9**).

4.3 The locations of iHC, eHC, and JF in relation to each part of OC-L were determined (**Fig. 26**). Distances from the posterior tip of OC to iHC, eHC and the posterior-most end of JF were measured (**Fig. 14 and 15**).

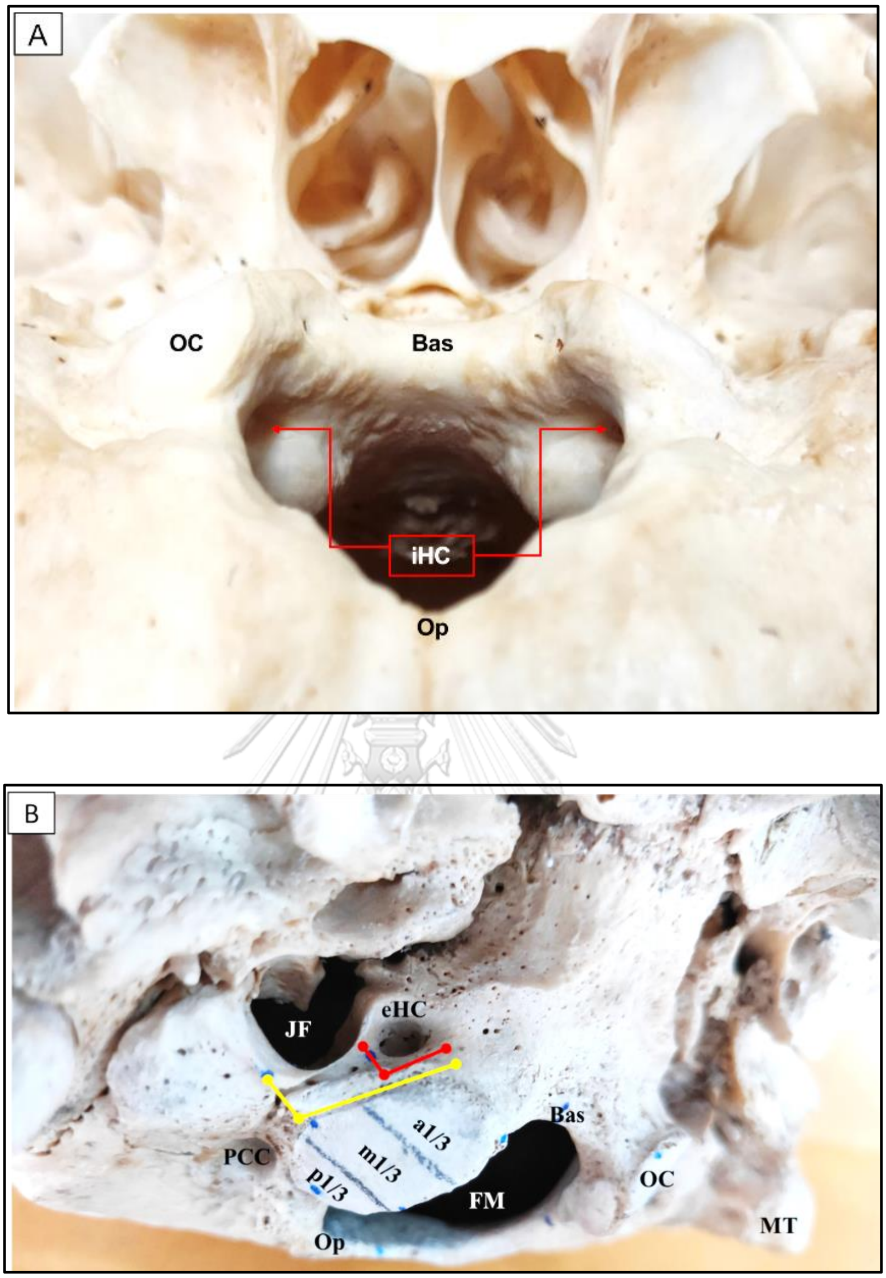

Figure 26. A: Posteroanterior view of occipital bone showing the right and left intracranial orifice of hypoglossal canal. B: Right inferolateral view showing extracranial orifice of hypoglossal canal related to anterior 1/3 of occipital condyle length (red line). jugular foramen related to anterior 2/3 of occipital condyle length (yellow line) Bas = basion, eHC = extracranial orifice of hypoglossal canal, FM = foramen magnum, iHC = intracranial orifice of hypoglossal canal, JF = jugular foramen, MT = mastoid process, OC = occipital condyle, OC-L = occipital condyle length, Op = opisthion, and PCC = posterior condylar canal.

4.4 Distance between the anterior and posterior tips of both OC was measured (**Fig. 4**).

4.5 Distances of the anterior and posterior tips of OC to Bas and Op of FM were measured (**Fig. 13**). Measuring of the distance between Op and the posterior-most end of JF was performed (**Fig. 27**).

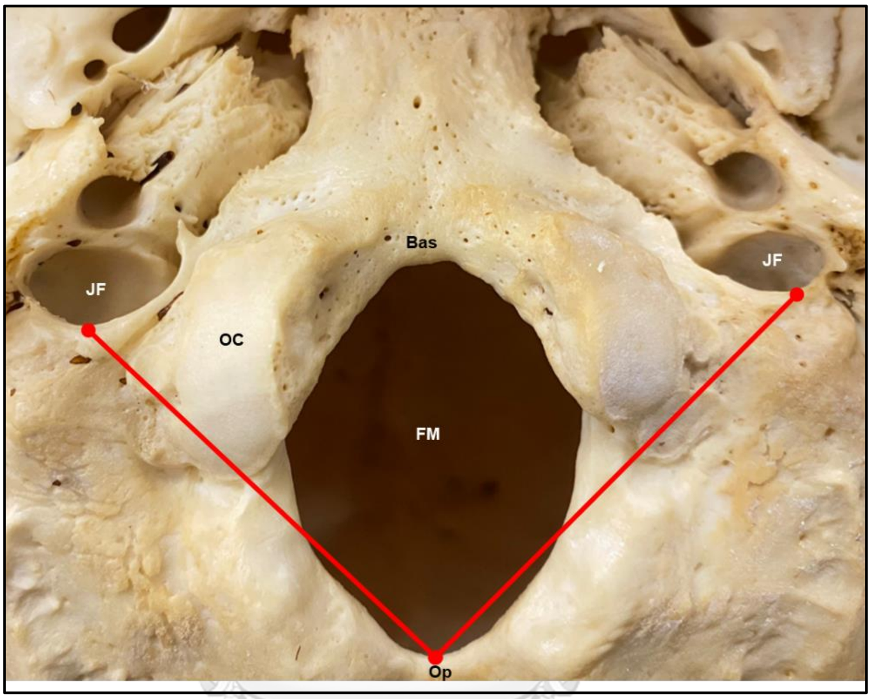

Figure 27. Inferior view of the skull base showing the distance between the opisthion and the posterior-most end of jugular foramen (Op-JF). Bas = basion, FM = foramen magnum, JF = jugular foramen, OC = occipital condyle, and Op = opisthion.

4.6 FM shapes were classified into nine types as shown in **Table 7** and **Fig. 7** (39). APD and TD were measured from the end of the Bas to the Op and from the point of maximum concavity on the right margin to the maximum concavity on the left margin of FM, respectively (**Fig. 8**). FMI was calculated APD divided by TD.

4.7 The existence of the PCC was observed. It could be bilateral, unilateral, or absent (**Fig. 28**).

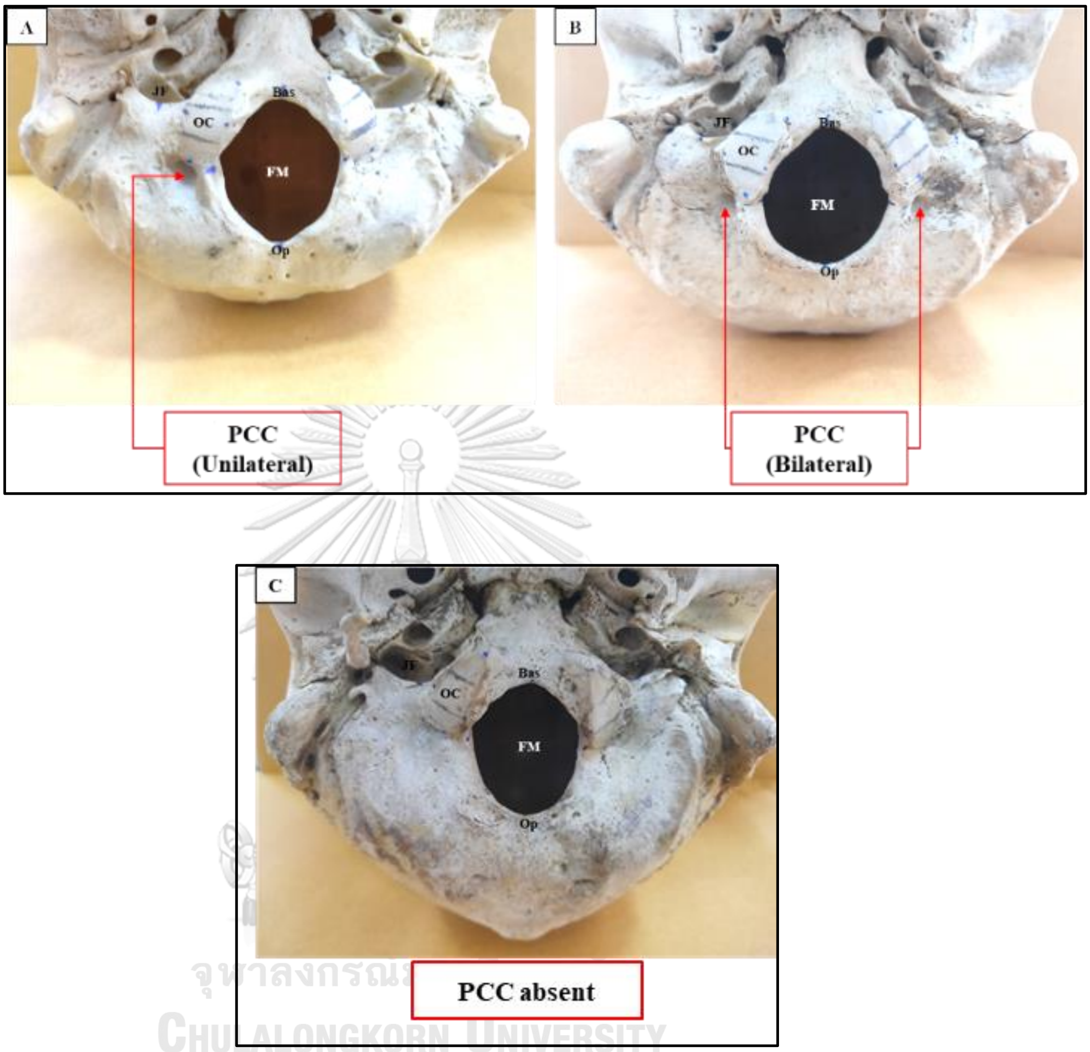

Figure 28. Inferior view of occipital bone shows A: PCC is only present on the right side (unilateral), B: PCC is present on both sides (bilateral), and C: PCC is absent on both sides. Bas = basion, FM – foramen magnum, JF = jugular foramen, OC = occipital condyle, Op = opisthion, and PCC = posterior condylar canal.

4.8 The distance of DP to Op (Op-DP), JF (JF-DP), and posterior tip of OC (OCPT-DP) were measured (**Fig. 29**).

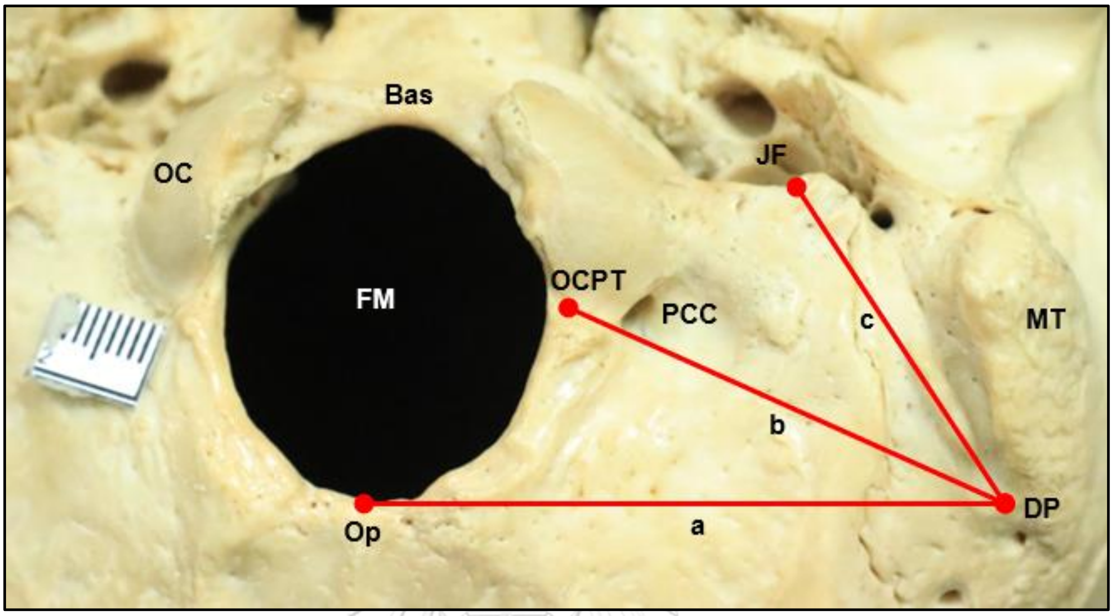

Figure 29. Inferior view of skull showing the left distances of a = distance between opisthion to digastric point (Op - DP), b = distance between the posterior tip of occipital condyle and digastric point (OCPT - DP), and c = distance between the posterior most end of jugular foramen to digastric point (JF - DP). Bas = basion, DP = digastric point, FM = foramen magnum, JF = jugular foramen, MT = mastoid process, OC = occipital condyle, OCPT = posterior tip of occipital condyle, Op = opisthion, and PCC = posterior condylar canal.

All measurements were measured twice by a single investigator to minimize intraobserver error.

Data Analysis and Statistics

The statistical analysis was performed by IBM SPSS Statistics, Version 22.0. To calculate Mean with SD of each parameter, paired t-test analysis to assess the mean difference in sides, independent t-test analysis to assess the mean difference in male and female skulls. The Chi-square test was used to investigate a possible correlation between the descriptive variables. The result was considered statistically significant when $p < 0.05$. Intraobserver reliability was determined for accuracy of measurement.

Ethical Consideration

Specimens used in this study were donated for anatomical study with respected to the right of the donors in their skulls.

An approval from the human research ethics committee and the director of King Chulalongkorn Memorial hospital was required for this current study (IRB No. 0988/64).

Chapter IV Results

The results are presented in six subsections including (1) morphological analysis and morphometry of the occipital condyle, (2) morphological analysis and morphometry of the foramen magnum, (3) the location of hypoglossal orifice and its relation to occipital condyle, (4) the relation between jugular foramen and occipital condyle, (5) the prevalence of posterior condylar canal, and (6) the distance between digastric point and surrounding structures. **Tables 8 - 9** show all morphometric measurements data.

Table 8. Morphometric measurement data based on sex and side

Parameters	Total Mean ± SD (Min – max)	*p* value	Male Mean ± SD (Min – max)				Female Mean ± SD (Min – max)			
			Left	Right	Total	*p* value	Left	Right	Total	*p* value
	(N =200)		(N =50)	(N =50)	(N =100)		(N =50)	(N =50)	(N =100)	
OC-L	21.32 ± 2.44 (16.02 - 28.80)	0.000*	22.08 ± 2.46 (18.16 - 28.80)	22.19 ± 2.58 (18.18 - 28.34)	22.13 ± 2.51 (18.16 - 28.80)	0.745	20.32 ± 2.02 (16.02 - 24.82)	20.68 ± 2.15 (16.38 - 25.97)	20.50 ± 2.08 (16.02 - 25.97)	0.220
OC-W	10.51 ± 1.41 (7.38 - 15.07)	0.294	10.31 ± 1.36 (7.38 - 15.07)	10.51 ± 1.59 (7.67 - 14.64)	10.41 ± 1.48 (7.38 - 15.07)	0.394	10.58 ± 1.21 (7.43 - 13.62)	10.65 ± 1.48 (8.21 - 13.70)	10.62 ± 1.34 (7.43 - 13.70)	0.766
OC-H	7.39 ± 1.14 (4.54 - 10.81)	0.484	7.31 ± 1.09 (5.24 - 10.28)	7.59 ± 1.19 (5.48 - 10.81)	7.45 ± 1.14 (5.24 - 10.81)	0.024*	7.14 ± 1.18 (4.54 - 9.51)	7.53 ± 1.06 (5.29 - 9.71)	7.34 ± 1.13 (4.54 - 9.71)	0.003*
OCAT- Bas	11.49 ± 1.43 (8.27 - 15.85)	0.961	11.69 ± 1.60 (8.27 - 15.85)	11.29 ± 1.39 (8.58 - 14.75)	11.49 ± 1.50 (8.27 - 15.85)	0.137	11.60 ± 1.28 (8.83 - 14.34)	11.36 ± 1.44 (8.57 - 14.33)	11.48 ± 1.36 (8.57 - 14.34)	0.271
OCAT- Op	39.11 ± 3.25 (24.47 - 47.52)	0.000*	40.27 ± 2.92 (34.68 - 47.52)	39.91 ± 2.77 (33.82 - 46.27)	40.09 ± 2.84 (33.82 - 47.52)	0.091	38.18 ± 3.47 (24.47 - 44.07)	38.08 ± 3.26 (28.11 - 44.29)	38.13 ± 3.35 (24.47 - 44.29)	0.658
OCPT- Bas	25.19 ± 2.18 (19.86 - 32.34)	0.047*	25.28 ± 2.32 (20.37 - 31.17)	25.71 ± 2.17 (21.72 - 31.59)	25.50 ± 2.25 (20.37 - 31.59)	0.09	24.55 ± 2.06 (19.86 - 29.46)	25.22 ± 2.06 (20.23 - 32.34)	24.88 ± 2.08 (19.86 - 32.34)	0.029*
OCPT- Op	27.38 ± 2.68 (21.16 - 35.47)	0.680	27.45 ± 2.98 (21.46 - 35.47)	27.46 ± 2.76 (21.53 - 34.37)	27.46 ± 2.86 (21.46 - 35.47)	0.976	27.12 ± 2.40 (23.09 - 32.55)	27.48 ± 2.59 (21.16 - 31.96)	27.30 ± 2.49 (21.16 - 32.55)	0.310
OCPT-iHC	9.00 ± 1.59 (4.35 - 12.38)	0.138	9.05 ± 1.42 (6.23 - 12.16)	9.27 ± 1.69 (5.52 - 12.01)	9.16 ± 1.56 (5.52 - 12.16)	0.332	8.63 ± 1.67 (4.35 - 12.13)	9.03 ± 1.55 (6.22 - 12.38)	8.83 ± 1.62 (4.35 - 12.38)	0.023*
OCPT-eHC	13.70 ± 2.23 (6.99 - 18.69)	0.011*	14.16 ± 2.03 (9.40 - 18.40)	14.04 ± 1.96 (8.70 - 17.15)	14.10 ± 1.98 (8.70 - 18.40)	0.604	13.13 ± 2.19 (6.99 - 18.69)	13.48 ± 2.59 (8.39 - 17.96)	13.30 ± 2.40 (6.99 - 18.69)	0.189
OCPT-JF	16.15 ± 2.35 (9.31 - 21.55)	0.164	16.67 ± 2.35 (11.95 - 21.55)	16.10 ± 2.20 (10.25 - 20.12)	16.38 ± 2.28 (10.25 - 21.55)	0.091	16.06 ± 1.79 (12.34 - 20.68)	15.78 ± 2.91 (9.31 - 21.48)	15.92 ± 2.41 (9.31 - 21.48)	0.485
Op-JF	43.29 ± 2.93 (36.65 - 50.08)	0.014*	44.08 ± 2.77 (38.94 - 50.08)	43.51 ± 3.09 (36.65 - 49.42)	43.80 ± 2.94 (36.65 - 50.08)	0.068	42.86 ± 2.44 (38.12 - 47.59)	42.70 ± 3.25 (36.94 - 49.40)	42.78 ± 2.86 (36.94 - 49.40)	0.565
Op-DP	54.54 ± 3.50 (42.95 - 64.31)	0.038*	55.33 ± 3.35 (48.42 - 64.31)	54.78 ± 3.73 (48.35 - 61.44)	55.05 ± 3.54 (48.35 - 64.31)	0.191	53.78 ± 2.85 (48.46 - 59.84)	54.27 ± 3.90 (42.95 - 63.45)	54.03 ± 3.41 (42.95 - 63.45)	0.238
OCPT-DP	36.72 ± 4.07 (25.62 - 46.63)	0.062	37.31 ± 3.31 (29.32 - 44.08)	37.21 ± 3.81 (26.99 - 45.66)	37.26 ± 3.55 (26.99 - 45.66)	0.869	36.18 ± 4.07 (27.17 - 45.78)	36.18 ± 4.91 (25.62 - 46.63)	36.18 ± 4.49 (25.62 - 46.63)	0.998
JF-DP	34.18 ± 4.15 (25.72 - 56.63)	0.003*	35.22 ± 3.43 (27.29 - 41.41)	34.88 ± 4.11 (27.21 -47.59)	35.05 ± 3.77 (27.21 - 47.59)	0.565	33.51 ± 3.20 (27.60 - 44.61)	33.13 ± 5.27 (25.72 - 56.63)	33.32 ± 4.34 (25.72 - 56.63)	0.561

JF-DP = distance between the posterior most end of jugular foramen to digastric point, OCAT-Bas = distance from the anterior tip of occipital condyle to basion, OCAT-Op = distance from the anterior tip of occipital condyle to opisthion, OC-H = occipital condyle height, OC-L = occipital condyle length, OCPT-eHC = distances from posterior tip of occipital condyle to extracranial orifice of hypoglossal canal, OCPT-iHC = distances from posterior tip of occipital condyle to intracranial orifice of hypoglossal canal, OCPT-JF = distance from the posterior tip of occipital condyle to the posterior most end of jugular foramen, OCPT-Bas = distance from the posterior tip of occipital condyle to basion, OCPT-DP = distance between the posterior tip of occipital condyle and digastric point, OCPT-Op = distance from the posterior tip of occipital condyle to opisthion, OC-W = occipital condyle width, Op-DP = distance between the end of the posterior border of foramen magnum (opisthion) to digastric point, and Op-JF = distance between the opisthion and posterior most end of jugular foramen. *Statistically significant difference between group.

Table 9. Mean distances of AID, PID, APD, TD, and FMI

Parameters	Total (N =100)		Male (N =50)		Female (N=50)		*p* value
	Mean ± SD (mm)	Min – max (mm)	Mean ± SD (mm)	Min – max (mm)	Mean ± SD (mm)	Min – max (mm)	
AID	21.17 ± 2.55	13.53 - 27.54	21.17 ± 2.61	13.53 - 27.54	21.16 ± 2.52	15.53 - 25.76	0.984
PID	39.55 ± 4.26	28.93 - 51.14	39.83 ± 4.57	31.67 - 51.14	39.26 ± 3.95	28.93 - 47.27	0.507
APD	34.19 ± 2.46	27.87 - 39.81	34.72 ± 2.35	27.87 - 39.81	33.66 ± 2.47	28.50 - 39.67	0.031*
TD	29.17 ± 2.14	24.13 - 35.32	29.11 ± 2.41	24.13 - 35.32	29.23 ± 1.86	25.51 - 33.57	0.777
FMI	1.18 ± 0.10	0.95 - 1.18	1.20 ± 0.11	0.95 - 1.46	1.15 ± 0.08	1.00 - 1.37	0.021*

AID = anterior intercondylar distance of occipital condyle, APD = anteroposterior diameter of foramen magnum, FMI = foramen magnum index, PID = posterior intercondylar distance of occipital condyle, and TD = transverse diameter of foramen magnum. *Statistically significant difference between group.

1. Morphological analysis and morphometry of the occipital condyle

The adult human dry skulls with intact OC from 50 males and 50 females provided by Department of Anatomy, Faculty of Medicine, Chulalongkorn University were used. All skulls had no evidence of OC fracture and broken at the cranial base. The morphological types that were found are represented in **Fig. 30.** The most prevalent shape of OC was S-like condyle (26.0 %) in males and oval-like condyle (41.0 %) in females. Statistically significant difference of OC shape was found between sex ($p = 0.037$), but not found between sides in male ($p = 0.886$) and in female ($p = 0.757$). Prevalence of morphological types of OC is presented in **Table 10.**

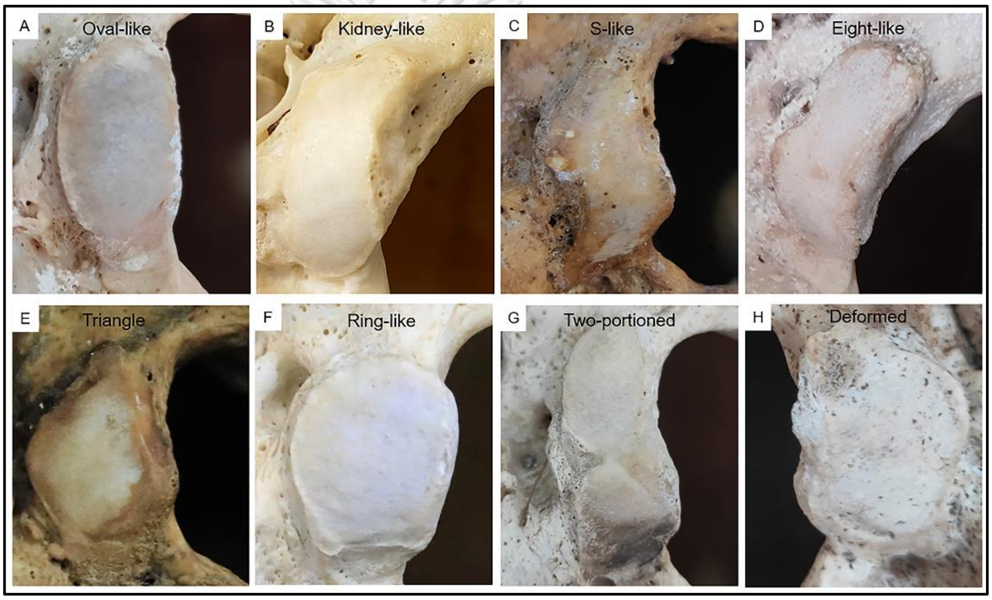

Figure 30. Photographs showing eight shapes of occipital condyle - A: oval-like condyle; B: kidney-like condyle; C: S-like condyle; D: eight-like condyle; E: triangle condyle; F: ring-like condyle; G: two-portioned condyle, and H: deformed condyle, respectively.

Symmetrical and asymmetrical forms were observed in 46.0 % (46/100) and 54.0 % (54/100) of the skulls, respectively. As a result, OC symmetry was found in 20.0 % (20/100) of males and 26.0 % (26/100) of females. Prevalence of symmetrical type of OC is presented in **Table 11.**

Table 10. Prevalence of morphological types of OC

Type	Number of occipital condyles									*p* value
	Male				Female				Total	
	Left	Right	Total	*p* value	Left	Right	Total	*p* value		
I	14 (14.0%)	11 (11.0%)	25 (25.0%)	0.886	23 (23.0%)	18 (18.0%)	41 (41.0%)	0.757	66 (33.0%)	0.037*
II	4 (4.0%)	7 (7.0%)	11 (11.0%)		9 (9.0%)	7 (7.0%)	16 (16.0%)		27 (13.5%)	
III	13 (13.0%)	13 (13.0%)	26 (26.0%)		6 (6.0%)	8 (8.0%)	14 (14.0%)		40 (20.0%)	
IV	6 (6.0%)	4 (4.0%)	10 (10.0%)		1 (1.0%)	3 (3.0%)	4 (4.0%)		14 (7.0%)	
V	7 (7.0%)	8 (8.0%)	15 (15.0%)		9 (9.0%)	10 (10.0%)	19 (19.0%)		34 (17.0%)	
VI	-	1 (1.0%)	1 (1.0%)		-	1 (1.0%)	1 (1.0%)		2 (1.0%)	
VII	3 (3.0%)	2 (2.0%)	5 (5.0%)		-	1 (1.0%)	1 (1.0%)		6 (3.0%)	
VIII	3 (3.0%)	4 (4.0%)	7 (7.0%)		2 (2.0%)	2 (2.0%)	4 (4.0%)		11 (5.5%)	
Total	50 (50.0%)	50 (50.0%)	100 (100.0%)		50 (50.0%)	50 (50.0%)	100 (100.0%)		200 (100.0%)	

Type I: oval-like condyle; type II: kidney-like condyle; type III: S-like condyle; type IV: eight-like condyle; type V: triangle condyle; type VI: ring-like condyle; type VII: two-portioned condyle, and type VIII: deformed condyle. *Statistically significant difference between group.

Table 11. Prevalence of symmetrical type of OC

Type	Number of symmetry (%)		
	Male	Female	Total
I	7 (35.0%)	13 (65.0%)	20 (43.5%)
II	2 (10.0)	4 (20.0%)	6 (13.0%)
III	6 (30.0%)	4 (20.0%)	10 (21.7%)
IV	2 (10.0%)	-	2 (4.3%)
V	1 (5.0%)	4 (20.0%)	5 (10.9%)
VI	-	-	-
VII	1 (5.0%)	-	1 (2.2%)
VIII	1 (5.0%)	1 (5.0%)	2 (4.3%)
Total	20 (100.0%)	26 (100.0%)	46 (100.0%)

Type I: oval-like condyle; type II: kidney-like condyle; type III: S-like condyle; type IV: eight-like condyle; type V: triangle condyle; type VI: ring-like condyle; type VII: two-portioned condyle, and type VIII: deformed condyle.

The OC protruded into FM in 31.5 % (63/200). As a results, 32.0 % (32/100) of males and 31.0 % (31/100) of females. Furthermore, OC protrusion was identified in 29.0 % (29/100) on the left side and 34.0 % (34/100) on the right side (**Table 12**). There was no significant difference in OC protrusion between sex (*p = 0.879*), and sides in male (*p = 0.668*) and in female (*p = 0.517*).

Table 12. Prevalence of OC protrude into FM

Type	Number of OC protrusion								Total	*p* value
	Male			*p* value	Female			*p* value		
	Left	Right	Total		Left	Right	Total			
Presence	15 (15.0%)	17 (17.0%)	32 (32.0%)	0.668	14 (14.0%)	17 (17.0%)	31 (31.0%)	0.517	63 (31.5%)	0.879
Absence	35 (35.0%)	33 (33.0%)	68 (68.0%)		36 (36.0%)	33 (33.0%)	69 (69.0%)		137 (68.5%)	
Total (N = 100)	50 (50.0%)	50 (50.0%)	100 (100.0%)		50 (50.0%)	50 (50.0%)	100 (100.0%)		200 (100.0%)	

OC = occipital condyle

The mean and range of length, width, and height of OC were 22.13 ± 2.51 (18.16 - 28.80), 10.41 ± 1.48 (7.38 - 15.07), and 7.45 ± 1.14 (5.24 - 10.81) mm, respectively in males, and 20.50 ± 2.08 (16.02 - 25.97), 10.62 ± 1.34 (7.43 - 13.70), and 7.34 ± 1.13 (4.54 - 9.71) mm, respectively in females, (**Fig. 31**). The *p* - value for the length of OC between male and female was highly significant (*p = 0.000*), however there was no significant difference in the width (*p = 0.294*) or height (*p = 0.484*) of the OC. Additionally, we noticed a significant difference in OC height between the left and right sides of male (*p = 0.024*) and female (*p = 0.003*) (**Table 8**).

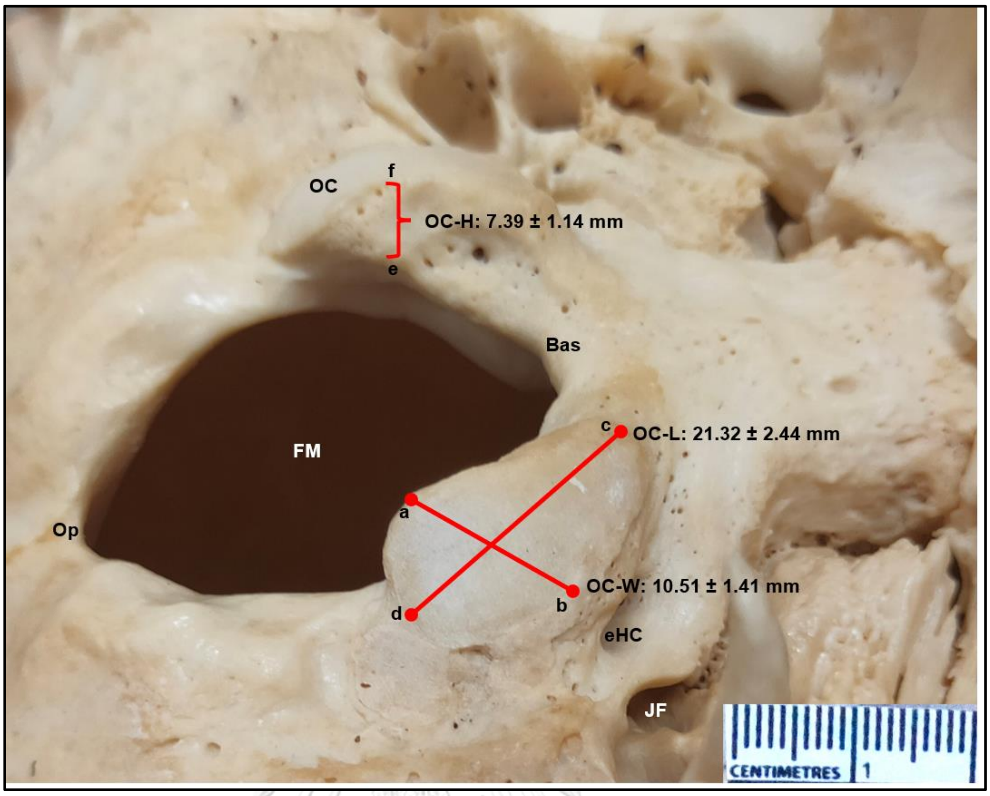

Figure 31. Inferior view of occipital bone showing the mean distances of total OC-L (left side), OC-W (left side), and OC-H (right side), respectively. a = the most medial point on the medial border of occipital condyle, b = the most lateral point on the lateral border of occipital condyle, c = anterior tip of occipital condyle, d = posterior tip of occipital condyle, e = upper boundary of medial margin of occipital condyle, f = lower boundary of medial margin of occipital condyle. Bas = basion, eHC = extracranial orifice of hypoglossal canal, FM = foramen magnum, JF = jugular foramen, OC = occipital condyle, OC-H = occipital condyle height, OC-L = occipital condyle length, and OC-W = occipital condyle width, and Op = opisthion.

OC was classified according to its length (**Table 13**)**.** The most prevalence of OC length of sex was the moderate length (62**.**5%)**.** In comparison, females showed a greater prevalence of short OC types (41**.**0%)**.** There was a significant sex difference in the proportions of OC types (*p = 0.001*)**.**

Table 13. Prevalence of type of OC length

Type	**Classification of occipital condyle according to its length**						**Total**	***p* value**
	Male			**Female**				
	Left	**Right**	**Total**	**Left**	**Right**	**Total**		
Short	12 (12.0%)	13 (13.0%)	25 (25.0 %)	21 (21.0%)	20 (20.0%)	41 (41.00 %)	66 (33.0 %)	0.001*
Moderate	34 (34.0%)	32 (32.0%)	66 (66.0 %)	29 (29.0%)	30 (30.0%)	59 (59.0 %)	125 (62.5 %)	
Long	4 (4.0%)	5 (5.0%)	9 (9.0 %)	-	-	-	9 (4.5%)	
Total	50 (50.0%)	50 (50.0%)	100 (100.0 %)	50 (50.0%)	50 (50.0%)	100 (100.0 %)	200 (100.0 %)	

*Statistically significant difference between group.

The mean AID and PID in male skulls were 21.17 ± 2.61 (13.53 - 27.54) and 39.83 ± 4.57 (31.67 - 51.14) mm, while in female skulls they were 21.16 ± 2.52 (15.53 - 25.76) and 39.26 ± 3.95 (28.93 - 47.27) mm (**Table 9**). There was no significant sex difference in AID ($p = 0.984$) or PID ($p = 0.507$) (**Fig. 32**).

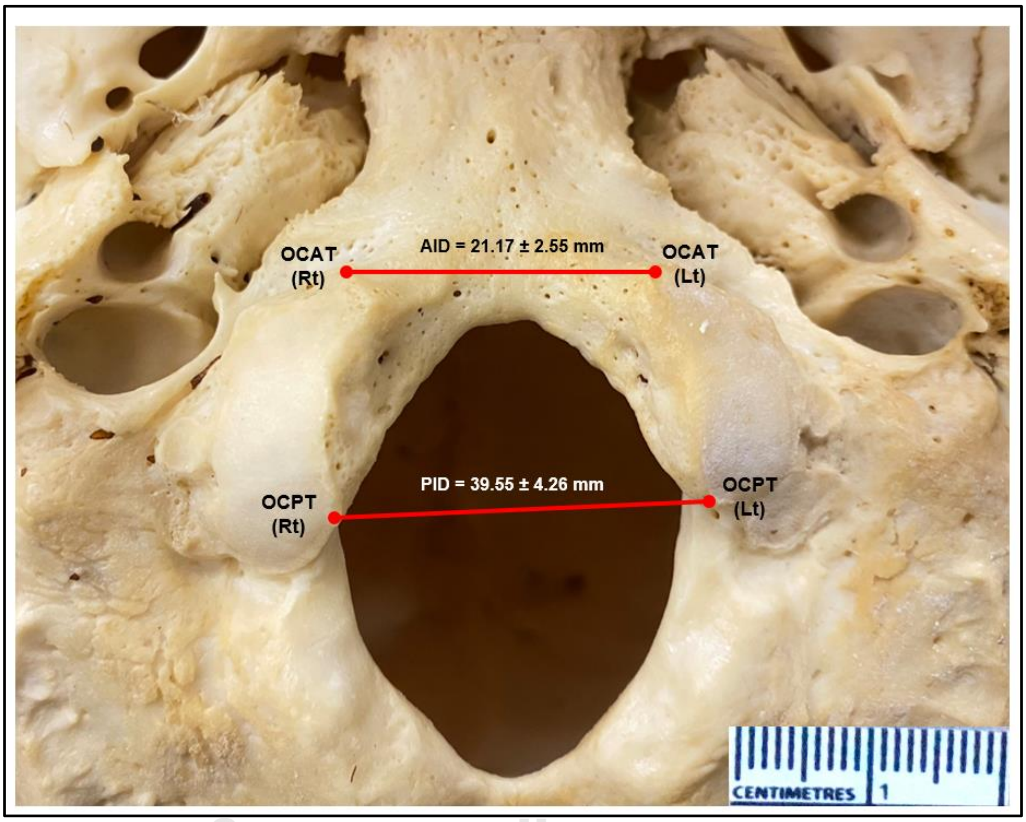

Figure 32. Inferior view of occipital bone showing the mean of total AID and PID. AID = anterior intercondylar distance of occipital condyle, OCAT = anterior tip of occipital condyle, OCPT = posterior tip of occipital condyle, and PID = posterior intercondylar distance of occipital condyle.

2. Morphological analysis and morphometry of the foramen magnum

Morphological types of FM found in the present study are demonstrated in **Fig. 33.** Eight morphological types were identified among 100 FM: Hexagonal 27.0 %, Pentagonal 12.0 %, Biconvex 12.0 %, Heptagonal 11.0 %, Tetragonal 11.0 %, Pear 11.0 %, Oval 9.0 %, and Rounded 7.0 %. The irregular shape was not found in this study. There was no significant difference in FM shapes between sex ($p = 0.876$). The prevalence of each morphological type of FM is presented in **Table 14.**

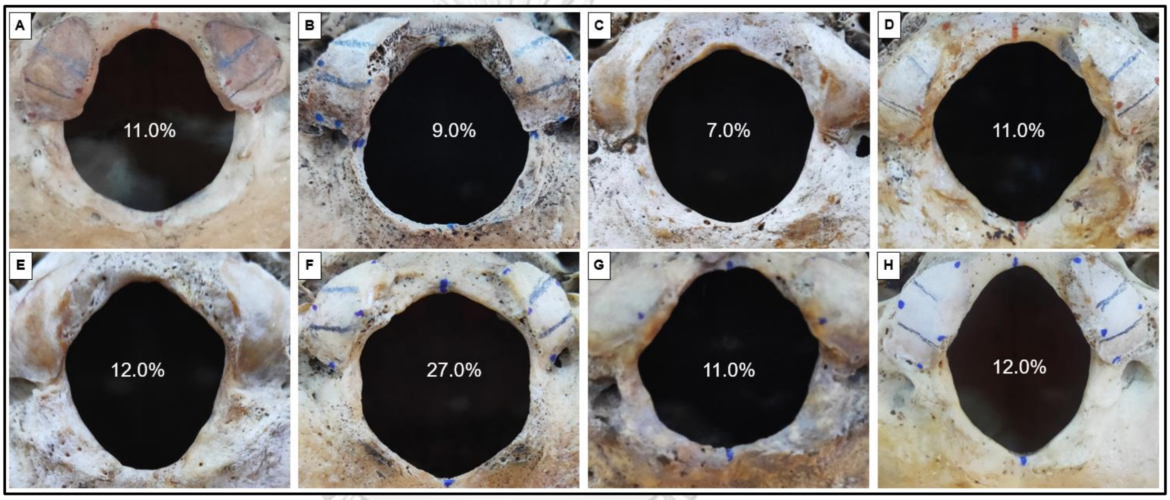

Figure 33. Foramen magnum in different shapes (inferior view). A: Pear; B: Oval; C: Rounded; D: Tetragonal; E: Pentagonal; F: Hexagonal; G: Heptagonal and H: Biconvex, respectively.

Table 14. Prevalence of morphological types of FM

Shapes	Number of FM of different types (%)			*p* value
	Male	Female	Total	
Pear	5 (10.0%)	6 (12.0%)	11 (11.0 %)	0.876
Oval	4 (8.0%)	5 (10.0%)	9 (9.0 %)	
Rounded	5 (10.0%)	2 (4.0%)	7 (7.0 %)	
Tetragonal	6 (12.0%)	5 (10.0%)	11 (11.0 %)	
Pentagonal	5 (10.0%)	7 (14.0%)	12 (12.0 %)	
Hexagonal	14 (28.0%)	13 (26.0%)	27 (27.0 %)	
Heptagonal	4 (8.0%)	7 (14.0%)	11 (11.0 %)	
Biconvex	7 (14.0%)	5 (10.0%)	12 (12.0 %)	
Total (N = 100)	50 (100.0 %)	50 (100.0 %)	100 (100.0 %)	

FM = foramen magnum

The mean APD and TD in male skulls were 34.72 ± 2.35 (27.87 - 39.81) and 29.11 ± 2.41 (24.13 - 35.32) mm, respectively, while in female skulls they were 33.66 ± 2.47 (28.50 - 39.67) and 29.23 ± 1.86 (25.51 - 33.57) mm (**Table 9**). There was a significant sex difference in APD ($p = 0.031$), but no significant sex difference in TD ($p = 0.777$) (**Fig. 34**). Furthermore, the average FMI in males was 1.20 ± 0.11 (0.95 - 1.46) and 1.15 ± 0.08 (1.00 - 1.37) in females (**Table 9**). There was a significant difference in FMI between males and females ($p = 0.021$). Additionally, the oval shape was detected in 39.0 %, while the rounded shape was found in 61.0 %. The prevalence of FM with an oval shape was determined to be 48.0 % (24/50) in males and 30.0 % (15/50) in females.

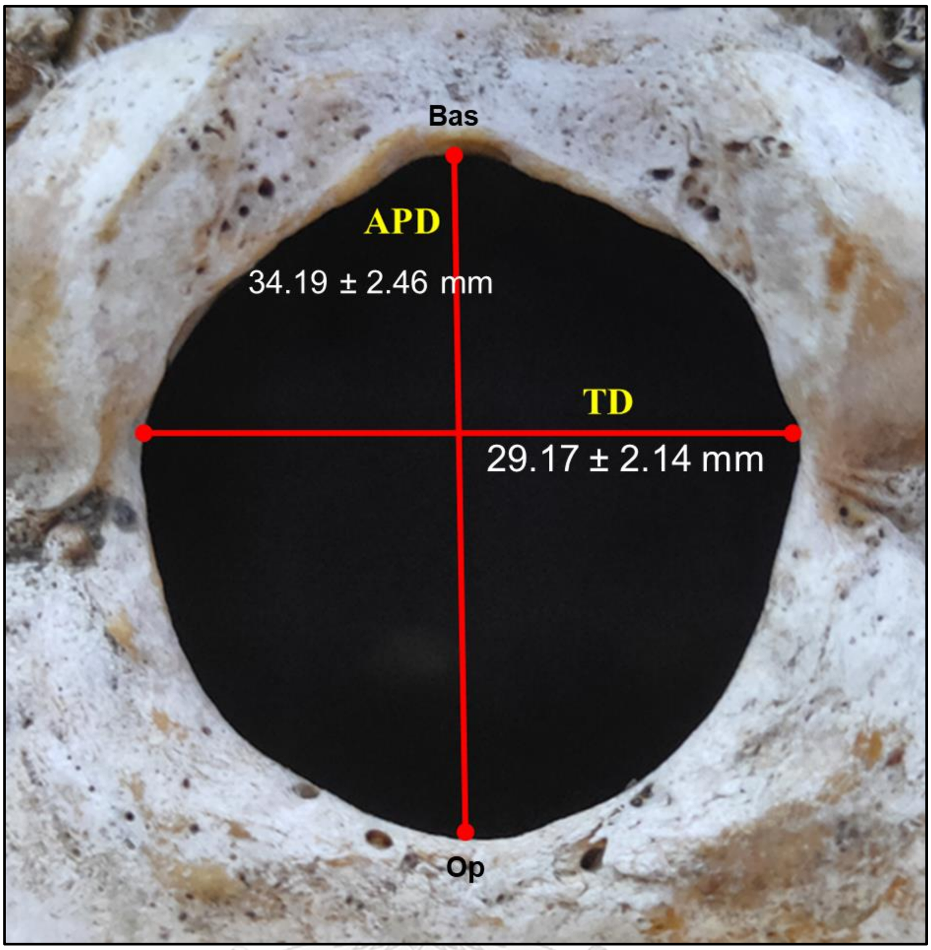

Figure 34. Inferior view of occipital bone showing the mean of total APD and TD. APD = anteroposterior diameter of foramen magnum, Bas = basion, Op = opisthion, and TD = transverse diameter of foramen magnum.

The mean distance of OCAT-Bas and OCAT-Op were 11.49 ± 1.50 (8.27 - 15.85), 40.09 ± 2.84 (33.82 - 47.52) mm in male and 11.48 ± 1.36 (8.57 - 14.34), 38.13 ± 3.35 (24.47 - 44.29) mm in female. The mean distance of OCPT-Bas and OCPT-Op were 25.50 ± 2.25 (20.37 - 31.59), 27.46 ± 2.86 (21.46 - 35.47) mm in male, 24.88 ± 2.08 (19.86 - 32.34), 27.30 ± 2.49 (21.16 - 32.55) mm in female (**Fig. 35**) (**Table 8**). There were significant differences between sex in OCAT- Op (*p = 0.000*) and OCPT- Bas (*p = 0.047*). However, we found a statistically significant difference in OCPT- Bas between sides (*p = 0.005*).

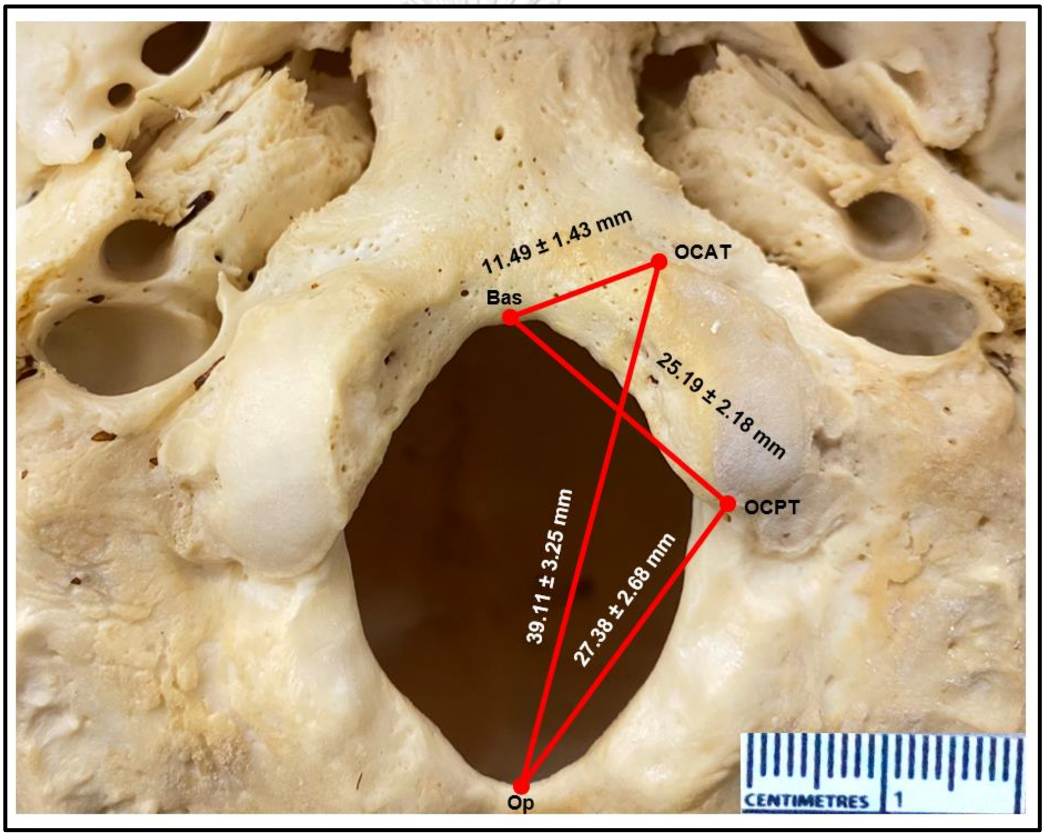

Figure 35. Inferior view of occipital bone showing the mean total OCAT- Bas, OCAT- Op, OCPT- Bas, and OCPT- Op in the left side. Bas = basion, OCAT = anterior tip of occipital condyle, OCPT = posterior tip of occipital condyle, and Op = opisthion.

3. The location of hypoglossal orifice and its relation to occipital condyle

The iHC was commonly found in location 3 in 46.0% (46/100) of male and 44.0% (44/100) of female. In contrast, eHC was found in 76.0 % (76/100) of males and 72.0 % (72/100) of females in location 1. There were no significant different in the location of iHC and eHc between female sides (*p = 0.292* and *0.585*, respectively) and location of eHC between male sides (*p = 0.058*). However, there was a statistically significant difference in iHC location between male sides (*p = 0.000*) (**Table 15**) (**Fig. 36**).

Table 15. Location of the iHC and related to part of OC in male and female skull

Location of HC orifices in relation to OC	Intracranial orifice of hypoglossal canal (iHC)								Extracranial orifice of hypoglossal canal (eHC)							
	Male			*p* value	Female			*p* value	Male			*p* value	Female			*p* value
	Left	Right	Total		Left	Right	Total		Left	Right	Total		Left	Right	Total	
Location 1	3 (3.0%)	4 (4.0%)	7 (7.0%)	0.000*	3 (3.0%)	3 (3.0%)	6 (6.0%)	0.292	43 (43.0%)	33 (33.0%)	76 (76.0%)	0.058	38 (38.0%)	34 (34.0%)	72 (72.0%)	0.585
Location 2	9 (9.0%)	28 (28.0%)	37 (37.0%)		13 (13.0%)	22 (22.0%)	35 (35.0%)		6 (6.0%)	13 (13.0%)	19 (19.0%)		10 (10.0%)	12 (12.0%)	22 (22.0%)	
Location 3	29 (29.0%)	17 (17.0%)	46 (46.0%)		25 (25.0%)	19 (19.0%)	44 (44.0%)		1 (1.0%)	4 (4.0%)	5 (5.0%)		2 (2.0%)	4 (4.0%)	6 (6.0%)	
Location 4	9 (9.0%)	1 (1.0%)	10 (10.0%)		9 (9.0%)	6 (6.0%)	15 (15.0%)		-	-	-		-	-	-	
Location 5	-	-	-		-	-	-		-	-	-		-	-	-	
Total	50 (50.0%)	50 (50.0%)	100 (100.0%)		50 (50.0%)	50 (50.0%)	100 (100.0%)		50 (50.0%)	50 (50.0%)	100 (100.0%)		50 (50.0%)	50 (50.0%)	100 (100.0%)	

Location 1: anterior 1/3 of OC; Location 2: Junction between anterior and middle 1/3 of OC; Location 3: middle 1/3 of OC; Location 4: Junction between middle and posterior 1/3 of OC and location 5: Posterior 1/3 of OC. HC = hypoglossal canal and OC = occipital condyle. *Statistically significant difference between group.

The symmetry of eHC and iHC location in relation to OC was found in 64.0 % (males = 35.0 %, females = 29.0 %) and 36.0 % (males = 18.0 %, females = 18.0 %), respectively. As a result, the most common symmetry of eHC location was found in location 1 (89.06%), while the most common symmetry of iHC location was found in location 3 (61.11%). Prevalence of symmetrical type of HC location is presented in **Table 16.**

Table 16. Prevalence of symmetrical type of HC location

Location of HC related to OC	Intracranial orifice of hypoglossal canal (iHC)			Extracranial orifice of hypoglossal canal (eHC)		
	Male	Female	Total	Male	Female	Total
Location 1	-	1 (5.56%)	1 (2.78%)	31 (88.57%)	26 (89.65%)	57 (89.06%)
Location 2	5 (27.78%)	5 (27.78%)	10 (27.78%)	3 (8.57%)	2 (6.90%)	5 (7.81%)
Location 3	13 (72.22%)	9 (50.00%)	22 (61.11%)	1 (2.86%)	1 (3.45%)	2 (3.13%)
Location 4	-	3 (16.67%)	3 (8.33%)	-	-	-
Location 5	-	-	-	-	-	-
Total	18 (100.0%)	18 (100.0%)	36 (100.0%)	35 (100.0%)	29 (100.0%)	64 (100.0%)

Location 1: anterior 1/3 of OC; Location 2: Junction between anterior and middle 1/3 of OC; Location 3: middle 1/3 of OC; Location 4: Junction between middle and posterior 1/3 of OC and location 5: Posterior 1/3 of OC. HC = hypoglossal canal and OC = occipital condyle.

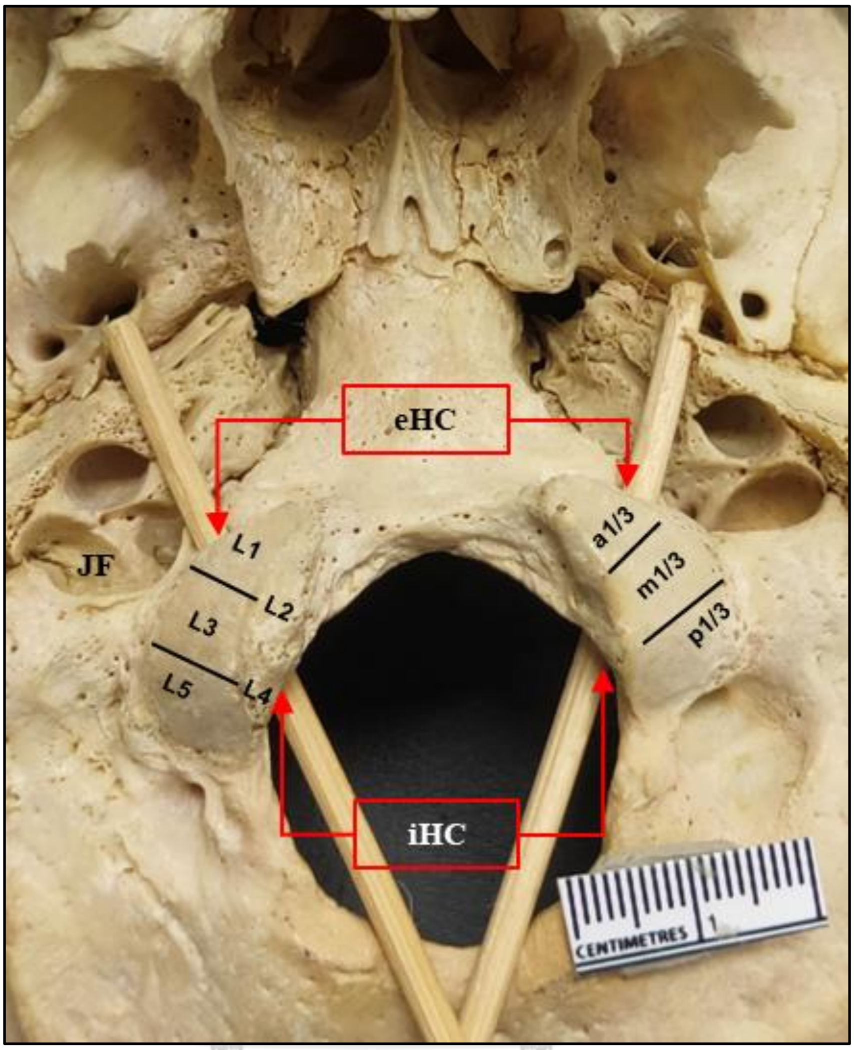

Figure 36. Inferior view of occipital bone showing relation between hypoglossal canal and occipital condyle. a1/3 = anterior one third of occipital condyle, eHC = extracranial orifice of hypoglossal canal, iHC = intracranial orifice of hypoglossal canal, JF = jugular canal, L1 = anterior 1/3 of occipital condyle, L2 = junction between anterior and middle 1/3 of occipital condyle, L3 = middle one third of occipital condyle, L4 = junction between middle and posterior 1/3 of occipital condyle, L5 = posterior one third of occipital condyle, m1/3 = middle one third of occipital condyle, OC = occipital condyle, and p1/3 = posterior one third of occipital condyle.

The mean OCPT-iHC was 9.16 ± 1.56 (5.52 - 12.16) mm in males and 8.83 ± 1.62 (4.35 - 12.38) mm in females. There was no statistically significant difference between sex (*p = 0.138*), but there was a difference between sides (*p = 0.030*). Males had a mean OCPT-eHC of 14.10 ± 1.98 (8.70 - 18.40) mm while females had a mean OCPT-eHC of 13.30 ± 2.40 (6.99 - 18.69) mm. There was a difference in OCPT-eHC between the sex (*p = 0.011*), but not between sides (*p = 0.519*) (**Fig. 37**) (**Table 8**).

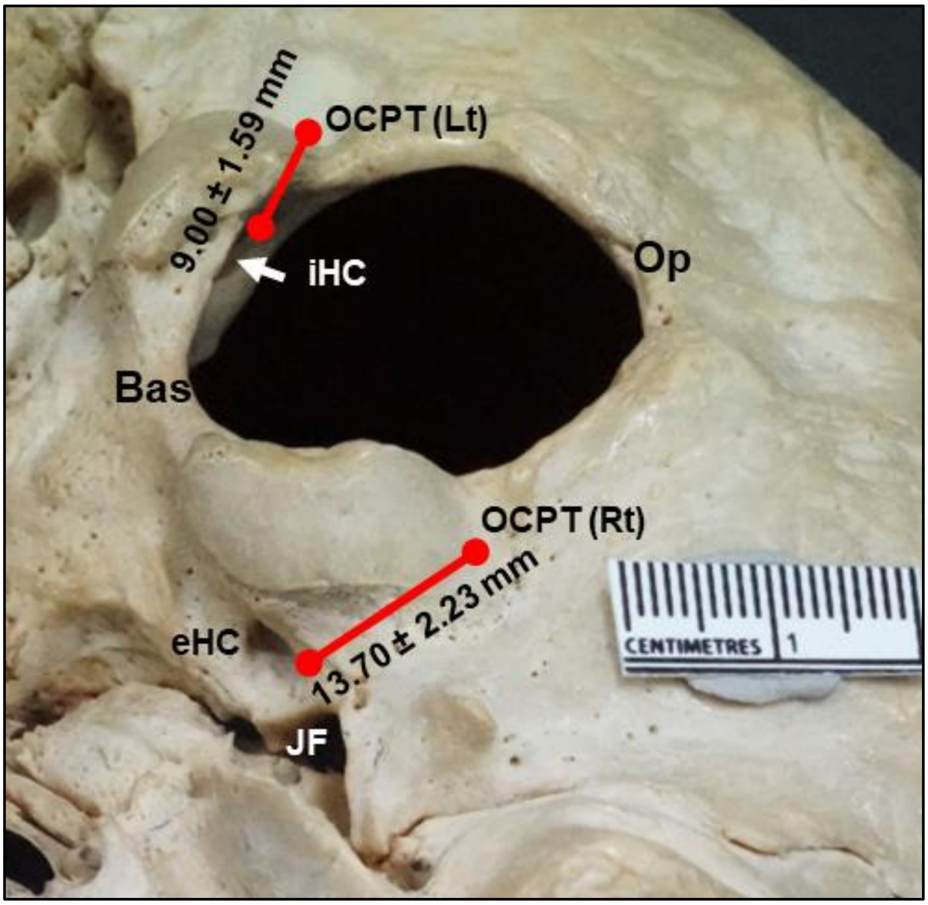

Figure 37. The right inferolateral view of occipital bone showing total mean distances of OCPT-eHC (right side) and OCPT-iHC (left side). Bas = basion, eHC = extracranial orifice of hypoglossal canal, iHC = intracranial orifice of hypoglossal canal, JF = jugular foramen, OCPT = posterior tip of the occipital condyle, and Op = opisthion.

4. The relation between jugular foramen and occipital condyle

The JF was related to the anterior 2/3 of the OC in 81.0% (162/200), the anterior 1/3 of the OC in 12.5% (25/200), and the entire OC length in 6.5% (13/200) (**Table 17**) (**Fig. 38**). Additionally, JF was related to anterior 1/3 of OC length in 17.0% of male (left = 15.0%, right = 2.0%), and 8.0% of female (left = 6.0%, right = 2.0%), anterior 2/3 of OC length in 80.0% of male (left = 35.0%, right = 45.0%), and 82.0% of female (left = 41.0%, right = 41.0%), and entire OC length in 3.0% of male (left = 0.0%, right = 3.0%), and 10.0% of female (left = 3.0%, right = 7.0%). There was a statistically significant difference in JF related to OC between sides of male ($p = 0.001$), but no statistically significant difference in JF related to OC between sides of female ($p = 0.165$).

Table 17. Extent of JF in relation to OC

JF in relation to OC	Male			*p* value	Female			*p* value	Total
	Left	Right	Total		Left	Right	Total		
Anterior 1/3 of OC length	15 (15.0%)	2 (2.0%)	17 (17.0%)	0.001*	6 (6.0%)	2 (2.0%)	8 (8.0%)	0.165	25 (12.5 %)
Anterior 2/3 of OC length	35 (35.0%)	45 (45.0%)	80 (80.0%)		41 (41.0%)	41 (41.0%)	82 (82.0%)		162 (81.0 %)
Entire OC length	-	3 (3.0%)	3 (3.0%)		3 (3.0%)	7 (7.0%)	10 (10.0%)		13 (6.5 %)
Total	50 (50.0%)	50 (50.0%)	100 (100.0%)		50 (50.0%)	50 (50.0%)	100 (100.0%)		200 (100.0 %)

JF = jugular foramen, and OC = occipital condyle. *Statistically significant difference between group.

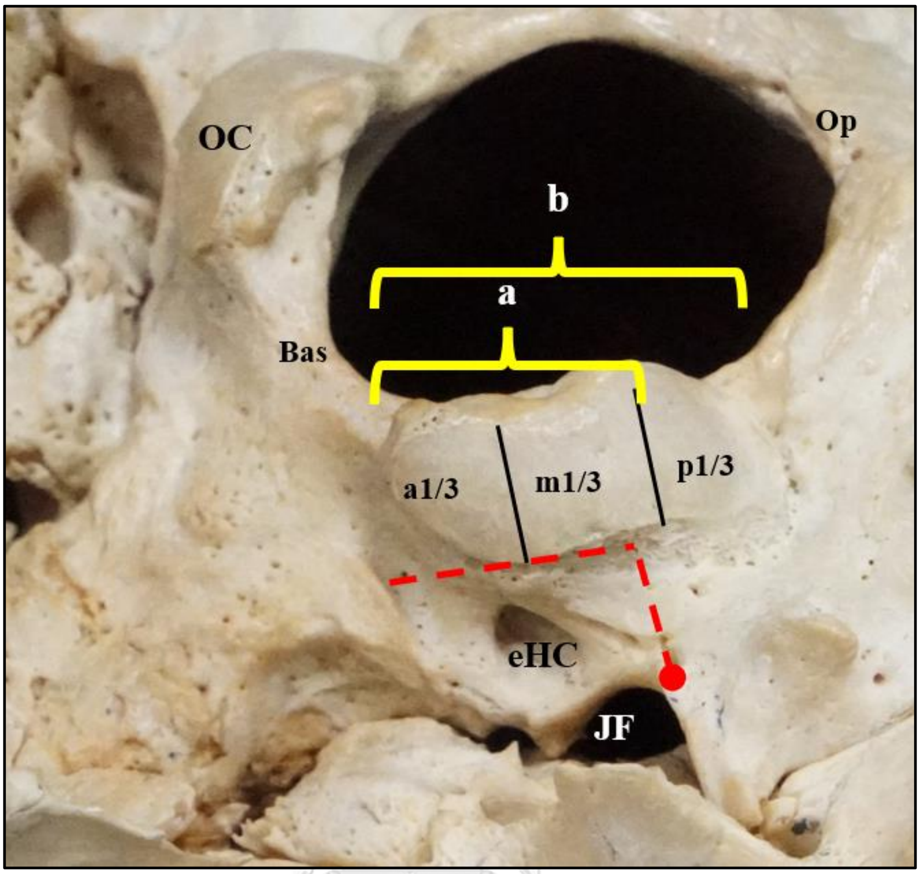

Figure 38. The right inferolateral view of occipital bone showing jugular foramen related to anterior two third of occipital condyle length (red line). a = anterior two third of occipital condyle, a1/3 = anterior one third of occipital condyle, b = entire occipital condyle length, Bas = basion, eHC = extracranial orifice of hypoglossal canal, JF = jugular foramen, m1/3 = middle one third of occipital condyle, OC = occipital condyle, Op = opisthion, and p1/3 = posterior one third of occipital condyle.

Males had an OCPT-JF of 16.38 ± 2.28 (10.25 - 21.55) mm while females had an OCPT-JF of 15.92 ± 2.41 (9.31 - 21.48) mm **(Fig. 39).** The mean Op-JF were 43.80 ± 2.94 (36.65 - 50.08) mm in males and 42.78 ± 2.86 (36.94 - 49.40) mm in females **(Fig. 40).** There was no significant difference of the OCPT-JF between sex ($p = 0.164$) or sides ($p = 0.102$), however there was a significant difference of the Op-JF between sex ($p = 0.014$) and no significant difference was found in sides ($p = 0.080$) **(Table 8).**

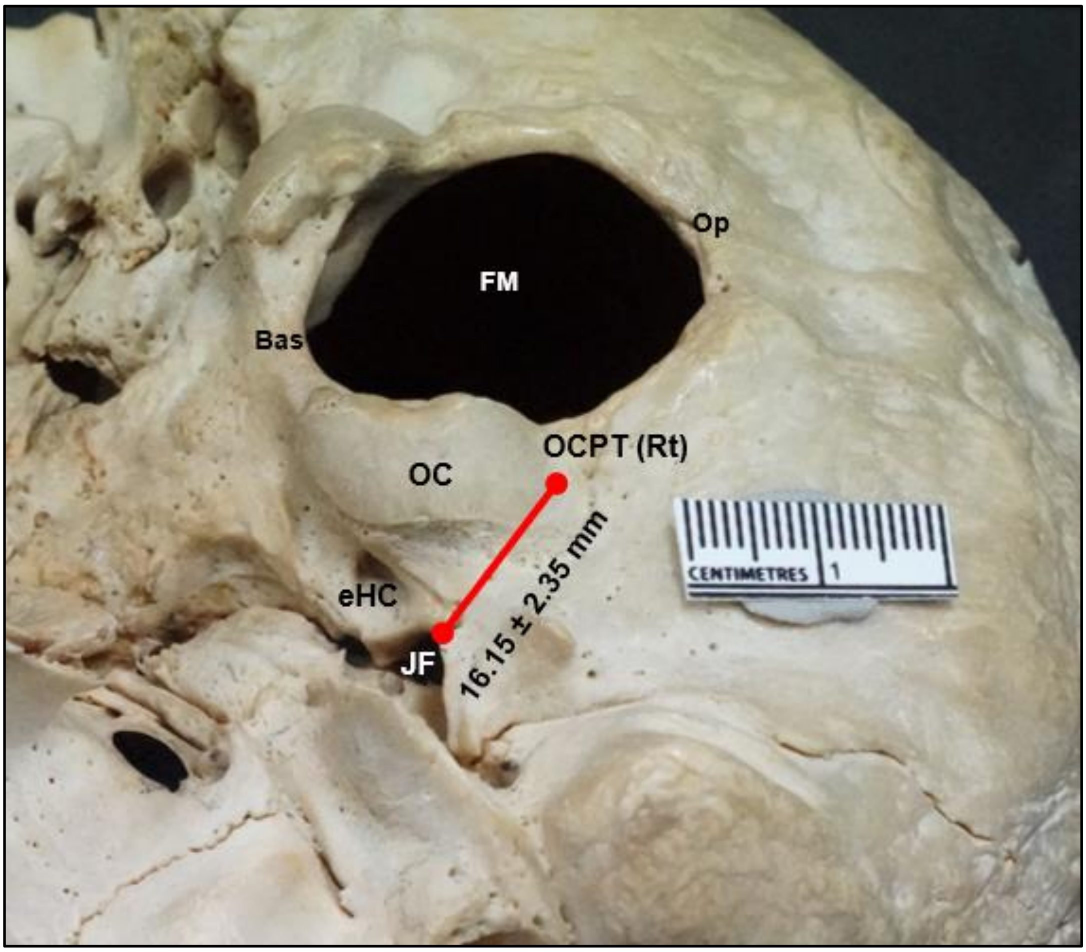

Figure 39. The right inferolateral view of occipital bone showing the total mean distance of OCPT-JF (right side). Bas = basion, extracranial orifice of hypoglossal canal, FM = foramen magnum, JF = jugular foramen, OC = occipital condyle, OCPT = posterior tip of occipital condyle, and Op = opisthion.

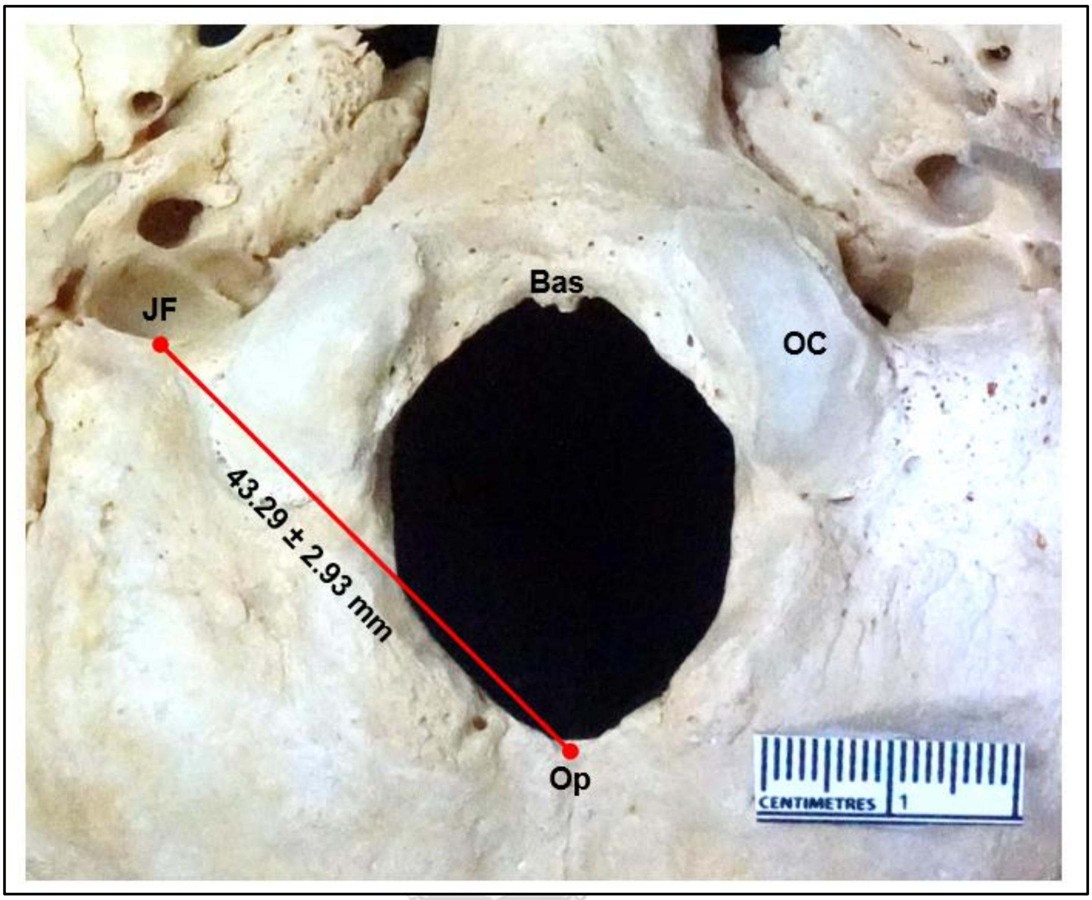

Figure 40. Inferior view of occipital bone showing the total mean distance of Op-JF (right side). Bas = basion, JF = jugular foramen, OC = occipital condyle, and Op = opisthion.

5. The prevalence of posterior condylar canal (PCC)

The PCC was found in 74.0 % (148/200 sides) of the sides of skulls, with 75 sides of males and 73 sides of females. More frequency was found on the right side (78.0 %) than on the left side (70.0 %). Bilateral PCC was found in 57.0 % (57/100) and unilateral PCC was 34.0 % (left = 13.0 %, right = 21.0 %) (**Fig. 28**) (**Table 18**). There was no statistically significant difference in the presence of PCC in sex (*p = 0.747*).

Table 18. Prevalence of PCC

Types of PCC	Number of PCC		Total	*p* value
	Male	Female		
Present bilaterally	29 (29.0%)	28 (28.0%)	57 (57.0 %)	0.747
Absent	4 (4.0%)	5 (5.0%)	9 (9.0 %)	
Present in left side	6 (6.0%)	7 (7.0%)	13 (13.0 %)	
Present in right side	11 (11.0%)	10 (10.0%)	21 (21.0 %)	
Total	50 (50.0%)	50 (50.0%)	100 (100.0 %)	

PCC = posterior condylar canal

6. The distance between digastric point and surrounding structures

The mean Op-DP, OCPT-DP, JF-DP were 55.05 ± 3.54 (48.35 - 64.31), 37.26 ± 3.55 (26.99 - 45.66), and 35.05 ± 3.77 (27.21 - 47.59) mm in males, and 54.03 ± 3.41 (42.95 - 63.45), 36.18 ± 4.49 (25.62 - 46.63), and 33.32 ± 4.34 (25.72 - 56.63) in females, respectively. There was a significant difference of the Op-DP (*p = 0.038*) and JF-DP (*p = 0.003*) between sex (**Fig. 41A**) (**Table 8**). The triangle consists of Op-DP, JF-DP and Op-JF is presented in **Fig. 41B.**

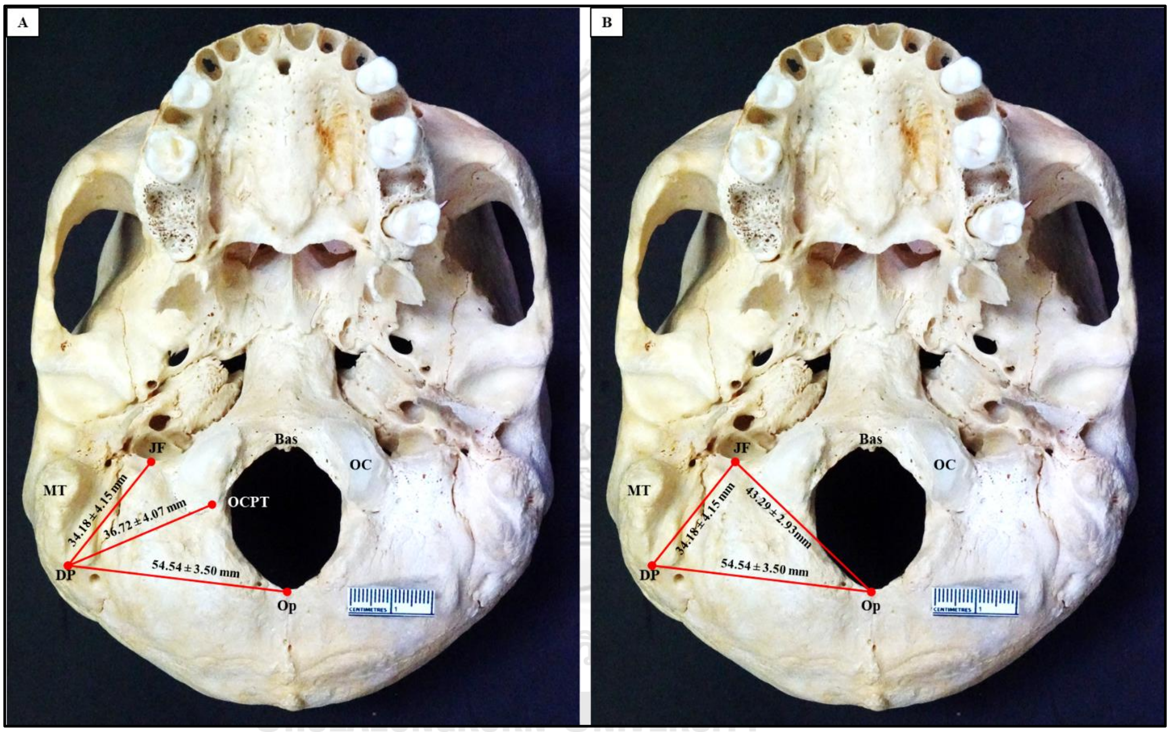

Figure 41. inferior view of occipital bone showing A: The mean distances of total Op-DP, OCPT-DP, and JF-DP. B: The triangle consists of Op-DP, JF-DP and Op-JF. Bas = basion, DP = digastric point, JF = jugular foramen, MT = mastoid process, OC = occipital condyle, OCPT = posterior tip of occipital condyle, and Op =opisthion.

Chapter V Discussion

The OCs are two bony structures found on both side of FM on the inferior surface of the occipital bone. It is commonly characterized as an ovoid structure with a convex downward and lateral projection and a long axis that runs anteriorly and medially. The morphological or morphometric analysis of OC has been used in the majority of CVJ anatomical and biomechanical studies (1, 20-22) . Verma et al. (2016) (18) concluded that the shape of OC was also important during condylectomy. The kidney-like, triangles, and deformed types required wider condylectomy to reach the ventral lesions. The nail insertion was easier and more convenient to fix in an oval-like because of its large surface area, while it is difficult in a triangle, ring-like, and two-portioned type of OC. Naderi et al. (2005) (19) suggested that the shape of OC may affect the amount of condylectomy. In this study, the most prevalent shape of OC was oval-like condyle or type I (33.0 %), which was comparable with previous research (18, 19, 21, 27, 35). In contrast to our findings, Arago et al. (2017) (20) , found that S-like condyle or type III was the most common shape, while Bayat et al. (2014) (36), found that kidney-like condyle or type II was the most common shape. In this study, 46.0 % of OC had a symmetrical shape. However, symmetrical shape was identified in 51.0% (19) and 62.0% (27) of the cases in previous studies. OC protrusion into FM with a prevalence of 20.7% (37) and 20.0% (38) of the skulls. In the case of OC protrusion, more bone resection was required during the transcondylar approach (32) . In this study, we revealed that OC protruded into FM in 31.5 % of the skulls.

In the current study, the mean length of OC was 21.32 ± 2.44 mm, which was shorter than OC length reported by Di et al. (2019), (23.58 ± 1.96) (1) and Saluja et al. (2016) (22.75 ± 2.90) (23) . Females had a significantly shorter OC than males similar to previous reports (24) (26) (**Table 1**). Moreover, OC was classified into three types based on its length. In our analysis, the most common was moderate type (range; 20 – 26 mm) (62.5 %) similar to previous research (19, 28) (**Table 2**). Removing the same amount of bone stock leads in increased O-C1 joint instability in shorter condyles compared to longer ones (28). However, a longer condyle may require more extensive resection for optimal visualization (23, 27). Bejjani et al. (2000) (15)

claimed that resection of less than 70% of the length of OC would not reveal evidence of CVJ instability, although other previous studies suggested that resection of less than 50% of the length of OC would not show evidence of CVJ instability (1, 5, 17, 30, 31, 33) (**Table 3**). As a result, we proposed in this work that the appropriated resection should be less than 11.07 mm in male and 10.25 mm in female from the posterior tip of OC. The average width of OC was 10.51 ± 1.41 mm, and the average height of OC was 7.39 ± 1.14 mm. The dimension of OC was smaller than the results reported by Di et al. (2019) (1) and Saluja et al. (2016) (23) (**Table 1**). The width of OC is important in surgery because it determines how much medially the condyle can be resected (27). A patient with a large OC has limited exposure to the ventral aspect of the CVJ (40). The height of the OC is also important during condylectomy because it is necessary to determine how deep the OC must be drilled (21). Furthermore, the higher thickness of OC may improve in the successful insertion of screws during occipitocervical fixation (23).

Table 19. Comparison of AID and PID with previous studies

Parameters	Sex	Naderi et al. (2005) (19)	Saluja et al. (2016) (23)	Cheruiyot et al. (2018) (28)	Farid et al. (2018) (34)	Current study
		(N = 202) Turkey	(N = 114) India	(N = 52) Kenya	(N = 75) Egypt	(N = 100) Thailand
AID (mm)	Male	-	-	19.71 ± 2.47	-	21.17 ± 2.61 (13.53 - 27.54)
	Female	-	-	19.62 ± 2.96	-	21.16 ± 2.52 (15.53 - 25.76)
	Total	21.0 ± 2.8 (13.8 – 32.5)	17.81 ± 2.93 (12.68-26.82)	19.66 ± 2.70	18.97 ± 2.03	21.17 ± 2.55 (13.53 - 27.54)
PID (mm)	Male	-	-	39.41 ± 2.73	-	39.83 ± 4.57 (31.67 - 51.14)
	Female	-	-	37.56 ± 3.21	-	39.26 ± 3.95 (28.93 - 47.27)
	Total	41.6 ± 2.9 (35.1 – 48.3)	38.91 ± 4.16 (27.62-49.58)	38.52 ± 3.09	38.39 ± 4.4	39.55 ± 4.26 (28.93 - 51.14)

AID = anterior intercondylar distance of occipital condyle

PID = posterior intercondylar distance of occipital condyle

The anterior and posterior intercondylar distances demonstrate how the OC is oriented and converging, which is necessary for screw insertion during occipitocervical fixation. The tip of the OC is close to the median plane, which should be noted while applying screws to the OC. This understanding is important for avoiding damage to nearby neurovascular structures (23) . As a result, shorter AID and PID may offer challenges during condylectomy by lateral approach (23). In our study, the mean AID and PID were 21.17 ± 2.55 (13.53 - 27.54) and 39.55 ± 4.26 (28.93 - 51.14) mm, respectively. Our AID and PID values were longer than those of Farid and Fattah (2018) (34) but shorter than those of Naderi et al. (2005) (19) (**Table 19**). However, we found no difference in AID or PID between sex. In contrast, Cheruiyot et al. (2018) (28) revealed that PID was significantly longer in males than females (*p = 0.002*), this suggests that females have narrow sagittal intercondylar angles compared to males (**Fig. 5**). As a result, a wider sagittal condylar angle appears to be more advantageous for accessing the ventral FM (35).

Table 20. Comparison of OCAT-Bas, OCAT-Op, OCPT-Bas, and OCPT-Op with previous studies

Parameters	**Sides**	**Sex**	**Naderi et al. (2005) (19)**	**Kalthur et al. (2014) (27)**	**Saluja et al. (2016) (23)**	**Ilhan et al. (2017) (4)**	**Current study**
			(N = 202) Turkey	**(N = 71) India**	**(N = 114) India**	**(N = 100) Turkey**	**(N = 100) Thailand**
OCAT-Bas	**Left**	**Male**	-	11.6 ± 2.1	-	-	11.69 ± 1.60 (8.27 - 15.85)
		Female	-	13.0 ± 2.7	-	-	11.60 ± 1.28 (8.83 - 14.34)
		Total	11.1 ± 1.5 (7.1 – 18.0)	-	9.56 ± 1.33 (6.55 - 12.9)	12.2 ± 186 (8.04 – 15.96)	-
	Right	**Male**	-	11.0 ± 1.8	-	-	11.29 ± 1.39 (8.58 - 14.75)
		Female	-	11.3 ± 1.3	-	-	11.36 ± 1.44 (8.57 - 14.33)
		Total	10.5 ± 1.5 (6.4 – 15.8)	-	9.74 ± 1.78 (6.37 - 15.39)	11.99 ± 2.2 (7.68 – 17.81)	-
	Total		10.8 ± 1.5 (6.4 - 18.0)	12.0 ± 2.0	9.65 ± 1.56 (6.37 - 15.39)	12.09 ± 1.76 (6.43 – 16.67)	11.49 ± 1.43 (8.27 - 15.85)
OCAT-Op	**Left**	**Male**	-	40.0 ± 3.2	-	-	40.27 ± 2.92 (34.68 - 47.52)
		Female	-	39.0 ± 3.6	-	-	38.18 ± 3.47

							(24.47 - 44.07)
		Total	39.1 ± 3.0 (27.2 - 47.1)	-	37.88 ± 2.5 (33.32 - 43)	39.21 ± 3.72 (25.21 – 48.67)	-
	Right	**Male**	-	40.0 ± 3.0	-	-	39.91 ± 2.77 (33.82 - 46.27)
		Female	-	39.1 ± 3.1	-	-	38.08 ± 3.26 (28.11 - 44.29)
		Total	38.9 ± 2.9 (26.5 - 47.1)	-	37.53 ± 2.26 (33.72 - 43.92)	39.62 ± 3.19 (32.09 – 48.22)	-
	Total		39.0 ± 2.9 (26.5 - 47.1)	39.0 ± 3.0	37.70 ± 2.37 (33.32 - 43.92)	39.43 ± 3.34 (29.6 – 47.4)	39.11 ± 3.25 (24.47 - 47.52)
OCPT-Bas	**Left**	**Male**	-	27.6 ± 2.5	-	-	25.28 ± 2.32 (20.37 - 31.17)
		Female	-	27.7 ± 2.6	-	-	24.55 ± 2.06 (19.86 - 29.46)
		Total	28.1 ± 2.0 (22.0 - 34.2)	-	26.93 ± 2.16 (23.32 - 32.16)	27.96 ± 2.48 (22.6 – 35.67)	-
	Right	**Male**	-	27.3 ± 2.3	-	-	25.71 ± 2.17 (21.72 - 31.59)
		Female	-	26.9 ± 2.0	-	-	25.22 ± 2.06 (20.23 - 32.34)
		Total	27.5 ± 2.0 (21.8 - 32.6)	-	28.16 ± 3.26 (22.08 - 39.35)	27.91 ± 3.48 (21.44 – 47.64)	-
	Total		27.8 ± 2.9 (21.8 - 34.2)	27.0 ± 2.0	27.54 ± 2.8 (22.08 - 39.35)	27.93 ± 2.67 (22.06 – 39.49)	25.19 ± 2.18 (19.86 - 32.34)
OCPT-Op	**Left**	**Male**	-	28.0 ± 2.6	-	-	27.45 ± 2.98 (21.46 - 35.47)
		Female	-	29.3 ± 3.3	-	-	27.12 ± 2.40 (23.09 - 32.55)
		Total	26.2 ± 2.2 (18.9 - 34.2)	-	26.17 ± 2.51 (21.42 - 33.64)	27.5 ± 2.56 (21.57 – 36.41)	-
	Right	**Male**	-	27.8 ± 2.6	-	-	27.46 ± 2.76 (21.53 - 34.37)
		Female	-	28.2 ± 2.5	-	-	27.48 ± 2.59 (21.16 - 31.96)
		Total	26.7 ± 2.4 (21.2 - 34.5)	-	26.78 ± 1.92 (22.26 - 31.14)	27.54 ± 3.13 (19.67 – 39.68)	-
	Total		26.4 ± 2.3 (18.9 - 34.5)	28.0 ± 2.0	26.48 ± 2.24 (21.42 - 33.64)	27.52 ± 2.59 (21.15 – 35.26)	27.38 ± 2.68 (21.16 - 35.47)

OCAT- Bas = distance between the anterior tip of occipital condyle and basion, OCAT-Op = distance between the anterior tip of occipital condyle and opisthion, OCPT-Bas = distance between the posterior tip of occipital condyle and basion, and OCPT-Op = distance between the posterior tip of occipital condyle and opisthion

For surgical approaches, the distance between the posterior tip of the OC and the opisthion is also important. The total mean of OCAT- Bas, OCAT- Op, OCPT- Bas, and OCPT-Op in our study was 11.49 ± 1.43, 39.11 ± 3.25, 25.19 ± 2.18, and 27.38 ± 2.68 mm, respectively. This is shorter than the results reported by Ilhan et al. (2017) (4). Moreover, the mean distance of OCPT – Op in this study was longer than that of Naderi et al. (2005) (19) and Saluja et al. (2016) (23), but less than that of Kalthur et al (2014) (27) (**Table 20**). The longer OCPT- Op distance is essential because it represents the width of surgical exposure in suboccipital craniotomy and gives a free corridor for posterolateral approach, and a longer corridor provides a larger space for a FLA (4, 27).

Table 21. Comparison of APD, TD, and FMI with previous studies

Parameters	Sex	Muthukumar et al. (2005) (38)	Kizilkanat et al. (2006) (43)	Chethan et al. (2012) (37)	Kanodia et al. (2012) (61)	Bello et al. (2013) (62)	Singh et al. (2019) (42)	Current study
		(N = 50) India	(N = 59) Turkey	(N = 53) India	(N = 100) India	(N = 240) * Nigeria	(N = 120) India	(N = 100) Thailand
APD (mm)	Male	-	-	-	-	34.5 ± 3.9	-	34.72 ± 2.35 (27.87 - 39.81)
	Female	-	-	-	-	33.5 ± 4.5	-	33.66 ± 2.47 (28.50 - 39.67)
	Total	33.3 (27 - 39)	34.8 ± 2.2 (29.7 - 39.7)	31 ± 2.4	34.1 ± 2.9	34.3 ± 4.1 (22.3-45.9)	33.79 ± 2.60 (30.05 - 40.07)	34.19 ± 2.46 (27.87 - 39.81)
TD (mm)	Male	-	-	-	-	30.6 ± 2.8	-	29.11 ± 2.41 (24.13 - 35.32)
	Female	-	-	-	-	28.9 ± 3.5	-	29.23 ± 1.86 (25.51 - 33.57)
	Total	27.9 (23 - 32)	29.6 ± 2.4 (24.4 - 38.6)	25.2 ± 2.4	27.5 ± 2.5	30.1 ± 3.1 (19.9-38.3)	28.25 ± 1.83 (24.25 – 32.32)	29.17 ± 2.14 (24.13 - 35.32)
FMI	Male	-	-	-	-	-	-	1.20 ± 0.11 (0.95 - 1.46)
	Female	-	-	-	-	-	-	1.15 ± 0.08 (1.00 - 1.37)
	Total	-	1.2 ± 0.1 (1 – 1.3)	1.2 ± 0.1	-	-	-	1.18 ± 0.10 (0.95 - 1.18)

APD = anteroposterior diameter of foramen magnum, FMI = foramen magnum index, and TD = transverse diameter of foramen magnum. * Computerized tomography (CT) scans.

FM located in the center of the skull base and provides access to essential structures such as the medulla oblongata, meninges, and vertebral arteries (34). In this investigation, the most common shape of FM was hexagonal (27.0 %), but round shape was uncommon (7.0 %), which differed from prior studies (37, 39, 41, 42) . The shape of FM is necessary for determining the amount of bone to be removed. A patient with a small FM, a short distance between the FM and the brainstem, and a large OC has limited exposure to the ventral aspect of the CVJ. Transcondylar approaches would be beneficial in these patients (4, 40). In the present study APD of FM was 34.19 ± 2.46 (27.87 - 39.81) mm which were consistent with the findings of Kizilkanat et al. (2006) (43) , Kanodia et al. (2012) (61), and Bello et al. (2013) (62), while Chethan et al. (2012) (37) and Singh et al. (2019) (42) reported lower values than the present study. We discovered that the TD value was 29.17 ± 2.14 (24.13 - 35.32) mm, which was slightly higher than previous studies (37, 42, 61, 62), but shorter than Kizilkanat et al. (2006) (43)

investigation (**Table 21**). FMI can also determine the shape of FM, which can be oval or round (38). In the case of a lesion located anterior to the brainstem, if the FM was oval in shape, a wider resection would be required than a rounded one (32) . A round shape provides a wider operative angle than an oval shape (41). In this study, we noticed that 39.0 % of the shapes in our FMI computation were oval, whereas Muthukumar et al. (2005) (38) reported 46.0 % and Sahoo et al. (2015) (63) reported 47.8%. In this study, males showed a higher prevalence of oval shape than females by using FMI, suggesting that a wider resection of FM would be needed in males.

Table 22. Comparison of location of eHC and iHC with previous studies

Locations	Hypoglossal canals	Sides	Sex	Anterior 1/4 of OC	Junction of 1/4 and 2/4 of OC	2/4 of OC	Junction of 2/4 and 3/4 of OC	3/4 of OC	Junction of 3/4 and 4/4 of OC	4/4 of OC
Naderi et al. (2005) (19) (N = 202) Turkey	eHC	Left	Male							
			Female							
			Total	100 (50.7%)	79 (40.1%)	17 (8.5%)	1 (0.5%)	-	-	-
		Right	Male							
			Female							
			Total	152 (77.1%)	40 (20.3%)	5 (2.5%)	-	-	-	-
	iHC	Left	Male							
			Female							
			Total	-	18 (9.1%)	38 (19.2%)	110 (55.8%)	31(15.7%)	-	-
		Right	Male							
			Female							
			Total	-	8 (4.1%)	24 (12.8%)	112 (56.8%)	51 (25.8%)	2 (1.1%)	-
Parvindokht et al. (2015) (64) (N = 46) Iran	eHC	Left	Male							
			Female							
			Total							
		Right	Male							
			Female							
			Total							
	iHC	Left	Male							
			Female							
			Total	-	7 (30.43%)	13 (56.52%)	3 (13.04%)	-	-	-

		Right	Male							
			Female							
			Total	1 (4.35%)	2 (8.70%)	15 (65.22%)	5 (21.74%)	-	-	-
Kalthur et al. (2014) (27) (N = 71) India				**Anterior 1/3 of OC**	**Middle 1/3 of OC**	**Posterior 1/3 of OC**				
	eHC	Left	Male	100.0%	-	-				
			Female	87.5%	12.5%	-				
			Total	-	-	-				
		Right	Male	98.1%	1.8%	-				
			Female	100.0%	-	-				
			Total	-	-	-				
	iHC	Left	Male	-	100.0%	-				
			Female	-	100.0%	-				
			Total	-	-	-				
		Right	Male	-	100.0%	-				
			Female	-	100.0%	-				
			Total	-	-	-				
Current study (N = 100) Thailand				**Anterior 1/3 of OC**	**Junction between anterior and middle 1/3 of OC**	**Middle 1/3 of OC**	**Junction between middle and posterior 1/3 of OC**	**Posterior 1/3 of OC**		
	eHC	Left	Male	43 (43.0%)	6 (6.0%)	1 (1.0%)	-	-		
			Female	38 (38.0%)	10 (10.0%)	2 (2.0%)	-	-		
			Total							
		Right	Male	33 (33.0%)	13 (13.0%)	4 (4.0%)	-	-		
			Female	34 (34.0%)	12 (12.0%)	4 (4.0%)	-	-		
			Total							
	iHC	Left	Male	3 (3.0%)	9 (9.0%)	29 (29.0%)	9 (9.0%)	-		
			Female	3 (3.0%)	13 (13.0%)	25 (25.0%)	9 (9.0%)	-		
			Total	-	-	-	-	-		
		Right	Male	4 (4.0%)	28 (28.0%)	17 (17.0%)	1 (1.0%)	-		

			Female	3 (3.0%)	22 (22.0%)	19 (19.0%)	6 (6.0%)	-		
			Total	-	-	-	-	-		

eHC = extracranial orifice of hypoglossal canal, iHC = intracranial orifice of hypoglossal canal, and OC = occipital condyle.

In this study, the majority of iHC was located at the middle 1/3 of OC (45.0%), while the majority of eHC was found at the anterior 1/3 of OC (74.0%). There was no HC orifice in the posterior 1/3 of OC (location 5). However, we noticed that the location of eHC had a higher symmetry in relation to OC than iHC, while the iHC location was more variable than eHC. Therefore, iHC was more likely to be injured during OC resection than eHC. Moreover, the location of eHC and iHC has been reported in other studies (19, 27, 64) (**Table 22**). As a result of this study, which used 50.0 % or less posterior OC resection, the HC was not reached. During OC resection, it was recommended not to drill beyond HC to prevent the complications of CN XII nerve injuries and O-C1 joint instabilities. OCPT-iHC and OCPT-eHC are extremely important during transcondylar approach in determining the maximal amount of OC resection without reaching and injuring structures in HC (17, 18).

Table 23. Comparison of OCPT-eHC and OCPT-iHC with previous studies

Parameters	Sides	Sex	Kizilkanat et al. (2006) (43)	Karasu et al. (2009) (33)	Parvindokht et al. (2015) (64)	Lyrtzis et al. (2017) (17)	Di et al. (2019) (1)	Current study
			(N = 59) Turkey	**(N = 20) Turkey**	**(N = 23) Iran**	**(N = 141) Greece**	**(N = 50) China**	**(N = 100) Thailand**
OCPT-eHC (mm)	Left	Male	-	-	-	-	-	14.16 ± 2.03 (9.40 - 18.40)
		Female	-	-	-	-	-	13.13 ± 2.19 (6.99 - 18.69)
		Total	-	-	-	-	14.54 ± 1.55	-
	Right	Male	-	-	-	-	-	14.04 ± 1.96 (8.70 - 17.15)
		Female	-	-	-	-	-	13.48 ± 2.59 (8.39 - 17.96)
		Total	-	-	-	-	14.68 ± 1.69	-
	Total		-	13.22 ± 2.24	-	-	14.61 ± 1.61	13.70 ± 2.23 (6.99 - 18.69)
OCPT-iHC (mm)	Left	Male	-	-	-	8.38 ± 1.12 (5.48–12.04)	-	9.05 ± 1.42 (6.23 - 12.16)
		Female	-	-	-	7.97 ± 1.30 (4.38–11.12)	-	8.63 ± 1.67 (4.35 - 12.13)
		Total	12.4 ± 2.3 (8.4 - 17.6)	-	11.69 ± 2.68	-	10.23 ± 1.14	-
	Right	Male	-	-	-	8.30 ± 1.30 (5.98–12.79)	-	9.27 ± 1.69 (5.52 - 12.01)
		Female	-	-	-	8.02 ± 1.24 (4.71–11.41)	-	9.03 ± 1.55 (6.22 - 12.38)
		Total	12.2 ± 2.2 (8.2 - 17.4)	-	11.17 ± 2.34	-	10.18 ± 1.44	-
	Total		-	8.4 ± 1.15	11.43 ± 2.51 (7.0 – 20.0)	-	10.21 ± 1.29	9.00 ± 1.59 (4.35 - 12.38)

OCPT-eHC = distances from posterior tip of occipital condyle to extracranial orifice of hypoglossal canal, OCPT-iHC = distances from posterior tip of occipital condyle to intracranial orifice of hypoglossal canal.

The distance between OCPT and iHC is highly important because iHC is located closer to the posterior tip of the OC than eHC. The mean OCPT-iHC in our study was 9.00 ± 1.59 mm, which is shorter than Di et al. (2019), (10.21 ± 1.29) (1) , Kizilkanat et al. (2006) (12.3 ± 2.4) (43) , and Parvindokht et al. (11.43 ± 2.51) (64) , while longer than in previous studies (17, 33) (**Table 23**).

In agreement with Verma et al. (2016) (18), we found that the majority of JFs were related to the anterior 2/3 of the OC in 81.0% of cases and the anterior 1/3 of the OC in 12.5% of cases. Therefore, neurovascular structures injury should be aware when performing OC resection. Verma et al. (2016) (18) revealed that the OCPT-JF was 15.73 ± 3 mm on the right side and 16.77 ± 2.9 mm on the left side. In our study, we found that the mean distance of OCPT - JF was 16.15 ± 2.35 mm. Our findings were higher than those reported by Kalthur et al. (2014) (15.0 ± 2) (27) , therefore It's important to avoid approaching JF during condylectomy because important cranial nerves run parallel to the vascular structures.

The posterior condylar emissary vein, which connects the JF with CF, often passes via PCC (32, 36). It should be identified on preoperative CT and MR images before surgery because it can be large, and its perforation can cause massive venous bleeding (9). PCC was identified in 74.0 % in this study, which was similar to Barut et al. (2009) (32), who reported that PCC was present in 71.0 % and was mainly bilateral (62.0%). Moreover, Bayat et al. (2014) (36) and Muthukumar et al. (2005) (38) report that PCC was found in 60.0% of cases, while Vanitha et al. (2015) (49) found that the PCC presented in 88.1%, in which 49.0% were bilateral and 37.0% were unilateral. Additionally, PCC was present in 60% of skulls and was more frequently found on the right side (92.0%) and less frequently found on the left side (68.0%) (38).

The extracranial estimation of intracranial venous sinuses is essential for the neurosurgeons to minimize the venous sinus damage, which can result in blood loss or sinus obstruction, lead to venous infarction (52) . Raso et al. (2011) (53) examined the DP in 127 skulls (254 sides), showing that DP projected over SS in 49.6 % on the right and 29.9% of cases on the left. When the DP did not project over the SS, the mean distance between this point and SS was

3.10 mm. Therefore, surface landmarks are often used in surgical planning. The DP is a visible landmark in lateral approaching to the posterior cranial fossa (54). Many studies have been conducted to assess SS by using surface landmarks such as asterion, zygomatic root, inion, mastoid process, and the top of the mastoid notch (TMN) on the skull (65-68**).** In this study, we measured the distance between DP and other structures including Op, OCPT, and JF because DP was easily identified on skull surface and was related to SS. The mean distance of Op-DP, OCPT-DP, and JF-DP values were 54.54 ± 3.50, 36.72 ± 4.07, and 34.18 ± 4.15 mm, respectively. We proposed that during craniotomy, the posterolateral limit from the posterior tips of OC to DP be less than 36.0 mm and Op to DP be less than 54.0 mm to avoid SS injury. Furthermore, the safe triangular area for craniotomy includes Op-DP, JF-DP, and Op-JF is shown in **Fig. 41B.**

Chapter VI Conclusion

In conclusion, the morphological analysis and morphometry of OC and its relation to surrounding structures were described in our study. CVJ is a common site for various lesions. The lesions at CVJ are difficult to manage because of their location and complex anatomic relations. In the current study, the S-like condyle was the most common shape of OC in males, whereas the oval-like condyle was the most prevalent in females. The appropriate resection should be less than 50%. As a result, OC resection from the posterior tip of the OC should be less than 11.07 mm in males and 10.25 mm in females to prevent CVJ instability. Additionally, the condyle resection on the medial border from the posterior tip of the OC should be less than 9.0 mm in males and 8.5 mm in females to prevent CN XII passing through iHC. Furthermore, females had smaller OC-L, OCAT- Op, OCPT- Bas, OCPT-eHC, Op-JF, Op-DP, and JF-DP values than males. The morphological analysis and morphometric data of the OC and its relationship to the DP, FM, JF, HC, and PCC provide a benefit for the surgeon to avoid neurovascular injury and CVJ instability. However, preoperative radiological evaluations including plain radiography, CT, and MRI are essential for surgical success.

The major limitation of our study is a lack of knowledge about the age and history of underlying diseases that may affect the measurements. Further cadaveric and radiological evaluations will provide a better understanding of the relationship between the anatomy and radiological measurements.

REFERENCES

1. Di G, Fang X, Hu Q, Zhou W, Jiang X. A Microanatomical Study of the Far Lateral Approach. World neurosurgery. 2019;127:932-42.

2. Tümörlere KBAYİ. The Far Lateral approach for ıntra-Dural anteriorly situated tumours at the Craniovertebral Junction. Turkish neurosurgery. 2011;21(4):494-8.

3. Rosa S, Baird JW, Harshfield D, Chehrenama M. Craniocervical junction syndrome: anatomy of the craniocervical and atlantoaxial junctions and the effect of misalignment on cerebrospinal fluid flow. Hydrocephalus-Water on the Brain: IntechOpen; 2018. p. 27-39.

4. Pelin I, Kayhar B, Erturk M, Sengul G. Morphological analysis of occipital condyles and foramen magnum as a guide for lateral surgical approaches. MOJ Anat Physiol. 2017;3(6):188-94.

5. MEHDI W, NIAZ A, IRFAN M, TASDIQUE S, MAJEED S. Far Lateral Transcondylar Approach for Anterior Foramen Magnum Lesions. Pakistan Journal Of Neurological Surgery. 2020;24(2):149-55.

6. Wu A, Zabramski JM, Jittapiromsak P, Wallace RC, Spetzler RF, Preul MC. Quantitative analysis of variants of the far-lateral approach: condylar fossa and transcondylar exposures. Operative Neurosurgery. 2010;66(suppl_2):ons191-ons8.

7. George JR, Francis T, Francis J, Samuel JE. Morphometric study of dry human occipital bone and its clinical relevance. Int J Anat Res. 2019;7:6230 - 3.

8. Scoville JP, Mazur MD, Couldwell WT. Unique Far-Lateral Closure Technique: Technical Note. Operative Neurosurgery. 2019;18(4):384-90.

9. Moscovici S, Umansky F, Spektor S. “Lazy” far-lateral approach to the anterior foramen magnum and lower clivus. Neurosurg Focus. 2015;38(4):1 - 9.

10. Au K, Richardson AM, Morcos J. Far Lateral Approach and Its Variants. Skull Base Surgery of the Posterior Fossa. 1 ed: Springer; 2018. p. 65-73.

11. Karam YR, Menezes AH, Traynelis VC. Posterolateral approaches to the craniovertebral junction. Neurosurgery. 2010;66(suppl_3):A135-A40.

12. Chaddad Neto F, Doria-Netto HL, Campos Filho JMd, Reghin Neto M, Rothon Jr AL, Oliveira Ed. The far-lateral craniotomy: tips and tricks. Arq Neuropsiquiatr. 2014;72(9):699-705.

13. Lanzino G, Paolini S, Spetzler RF. Far-lateral approach to the craniocervical junction.

Operative Neurosurgery. 2005;57(suppl_4):367-71.

14. Cardoso AC, Fontes RB, Tan LA, Rhoton Jr AL, Roh SW, Fessler RG. Biomechanical effects of the transcondylar approach on the craniovertebral junction. Clin Anat. 2015;28(5):683-9.

15. Bejjani GK, Sekhar LN, Riedel CJ. Occipitocervical fusion following the extreme lateral transcondylar approach. Surg Neurol. 2000;54(2):109-16.

16. Mazur MD, Couldwell WT, Cutler A, Shah LM, Brodke DS, Bachus K, et al. Occipitocervical instability after far-lateral transcondylar surgery: a biomechanical analysis. Neurosurgery. 2017;80(1):140-5.

17. Lyrtzis C, Piagkou M, Gkioka A, Anastasopoulos N, Apostolidis S, Natsis K. Foramen magnum, occipital condyles and hypoglossal canals morphometry: anatomical study with clinical implications. Folia Morphol (Warsz). 2017;76(3):446-57.

18. Verma R, Kumar S, Rai AM, Mansoor I, Mehra RD. The anatomical perspective of human occipital condyle in relation to the hypoglossal canal, condylar canal, and jugular foramen and its surgical significance. J Craniovertebr Junction Spine. 2016;7(4):243 - 9.

19. Naderi S, Korman E, Cıtak G, Güvençer M, Arman C, Şenoğlu M, et al. Morphometric analysis of human occipital condyle. Clin Neurol Neurosurg. 2005;107(3):191-9.

20. Aragao JA, De Santana GM, Da Cruz de Moraes RZ, Aragão I, Aragão F, Reis FP. Morphological analysis on the occipital condyles and review of the literature. Int J Morphol. 2017;3(35):1129-32.

21. Anjum A, Pandurangam G, Garapati S, Bandarupalli N, Rabbani H, Divya P. Morphology and morphometric study of occipital condyles. Int J Anat Res. 2021;9(1.3):7905-11.

22. Karam YR, Traynelis VC. Occipital condyle fractures. Neurosurgery. 2010;66(suppl_3):56-9.

23. Saluja S, Das SS, Vasudeva N. Morphometric analysis of the occipital condyle and its surgical importance. Journal of clinical and diagnostic research: JCDR. 2016;10(11):AC01.

24. Rai H, Keluskar V, Patil S, Bagewadi A. Accuracy of measurements of foramen magnum and occipital condyle as an indicator for sex determination using computed tomography. Indian J Health Sci Biomed Res. 2017;10(1):80 - 3.

25. Oliviera OFd, Tinoco R, Júnior ED, Araujo LGd, Silva R, Paranhos LR. Sex determination from occipital condylar measurements by baudoin index in forensic purposes. Int J Morphol.

2013;31:1297-300.

26. Kumar A, Nagar M. Human adult occipital condyles: A morphometric analysis. Res Rev J Med Health Sci. 2014;3(4):112-6.

27. Kalthur SG, Padmashali S, Gupta C, Dsouza AS. Anatomic study of the occipital condyle and its surgical implications in transcondylar approach. J Craniovertebr Junction Spine. 2014;5(2):71 - 7.

28. Cheruiyot I, Mwachaka P, Saidi H. Morphometry of Occipital condyles: Implications for transcondylar approach to craniovertebral junction lesions. Anatomy Journal of Africa. 2018;7(2):1224-31.

29. Gilroy AM, MacPherson BR, Ross LM, Broman J, Josephson A. Atlas of anatomy. 3 ed: Thieme Stuttgart; 2008. 742 p.

30. Vishteh AG, Crawford NR, Melton MS, Spetzler RF, Sonntag VK, Dickman CA. Stability of the craniovertebral junction after unilateral occipital condyle resection: a biomechanical study. J Neurosurg. 1999;90(1):91-8.

31. Shin H, Barrenechea IJ, Lesser J, Sen C, Perin NI. Occipitocervical fusion after resection of craniovertebral junction tumors. J Neurosurg Spine. 2006;4(2):137-44.

32. Barut NR, Kale AN, Turan Suslu Hk, Ozturk A, Bozbuga M, Sahinoglu K. Evaluation of the bony landmarks in transcondylar approach. Br J Neurosurg. 2009;23(3):276-81.

33. Karasu A, Cansever T, Batay F, Sabanci PA, Al-Mefty O. The microsurgical anatomy of the hypoglossal canal. Surg Radiol Anat. 2009;31(5):363 - 7.

34. Farid SA, Fattah IOA. Morphometric Study of Human Adult Occipital Condyle, Hypoglossal Canal and Foramen Magnum in Dry Skull of Modern Egyptians. Int J Clin Dev Anat. 2018;4(1):19 - 26.

35. Ozer MA, Celik S, Govsa F, Ulusoy MO. Anatomical determination of a safe entry point for occipital condyle screw using three-dimensional landmarks. Eur Spine J. 2011;20(9):1510-7.

36. Bayat P, Bagheri M, Ghanbari A, Raoofi A, Bayat P, Bagheri M. Characterization of occipital condyle and comparison of its dimensions with head and foramen magnum circumferences in dry skulls of Iran. Int j morphol. 2014;32(2):444-8.

37. Chethan P, Murlimanju BV, Prashanth KU, Prabhu LV, Krishnamurthy A, Somesh MS, et al. Morphological analysis and morphometry of the foramen magnum: an anatomical investigation.

Turk Neurosurg. 2012;22(4):416-9.

38. Muthukumar N, Swaminathan R, Venkatesh G, Bhanumathy S. A morphometric analysis of the foramen magnum region as it relates to the transcondylar approach. Acta Neurochir (Wien). 2005;147(8):889-95.

39. Aragão JA, de Oliveira Pereira R, de Moraes RZdC, Reis FP. Morphological types of foramen magnum. Annual Research & Review in Biology. 2014;4(9):1372-8.

40. Wanebo JE, Chicoine MR. Quantitative analysis of the transcondylar approach to the foramen magnum. Neurosurgery. 2001;49(4):934-43.

41. Natsis K, Piagkou M, Skotsimara G, Piagkos G, Skandalakis P. A morphometric anatomical and comparative study of the foramen magnum region in a Greek population. Surg Radiol Anat. 2013;35(10):925-34.

42. Singh A, AgArwAl P, Singh A. Morphological and morphometric study of foramen magnum in dry human skull and its clinical significance. Int J Anat Radiol Surg. 2019;8(3):10 - 2.

43. Kizilkanat ED, Boyan N, Soames R, Oguz O. Morphometry of the hypoglossal canal, occipital condyle, and foramen magnum. Neurosurgery quarterly. 2006;16(3):121-5.

44. Hauser G, De Stefano G. Variations in form of the hypoglossal canal. Am J Phys Anthropol. 1985;67(1):7-11.

45. Nikumbh RD, Nikumbh DB, Karambelkar RR, Shewale AD. Morphological study of hypoglossal canal and its anatomical variation. Int J Health Sci Res. 2013;3(6):54-8.

46. Idowu O. The jugular foramen-a morphometric study. Folia Morphol (Warsz). 2004;63(4):419-22.

47. Rhoton Jr AL. Jugular foramen. Neurosurgery. 2000;47(suppl_3):267-85.

48. Hatiboğlu M, Anil A. Structural variations in the jugular foramen of the human skull. J Anat. 1992;180(Pt 1):191 - 6.

49. Vanitha CT, Kadlimatti H. Study on incidence of posterior condylar canal in North Karnataka: clinical significance. Int J Clin Surg. 2015;3(1):50 - 4.

50. Hellstern V, Aguilar-Pérez M, Schob S, Bhogal P, AlMatter M, Kurucz P, et al. Endovascular treatment of dural arteriovenous fistulas of the anterior or posterior condylar vein. Clin Neuroradiol. 2019;29(2):341-9.

51. Aly I, Tubbs RS. The Sigmoid Sinus. Anatomy, Imaging and Surgery of the Intracranial

Dural Venous Sinuses: Elsevier; 2020. p. 47-58.

52. Tubbs RS, Loukas M, Shoja MM, Bellew MP, Cohen-Gadol AA. Surface landmarks for the junction between the transverse and sigmoid sinuses: application of the "strategic" burr hole for suboccipital craniotomy. Oper Neurosurg. 2009;65(suppl_6):37-41.

53. Raso JL, Silva Gusmão SN. A new landmark for finding the sigmoid sinus in suboccipital craniotomies. Oper Neurosurg. 2011;68(suppl_1):1-6.

54. Kizilkanat E, Boyan N, Ozsahin E, Soames R, Oguz O. Surface landmarks for suboccipital craniotomy. Neurosurgery Quarterly. 2013;23(2):133-6.

55. Offiah CE, Day E. The craniocervical junction: embryology, anatomy, biomechanics and imaging in blunt trauma. Insights into imaging. 2017;8(1):29-47.

56. Lopez AJ, Scheer JK, Leibl KE, Smith ZA, Dlouhy BJ, Dahdaleh NS. Anatomy and biomechanics of the craniovertebral junction. Neurosurg Focus. 2015;38(4):1-8.

57. Rhoton Jr AL. The far-lateral approach and its transcondylar, supracondylar, and paracondylar extensions. Neurosurgery. 2000;47(suppl_3):195-209.

58. Mazur MD, Dailey AT, Shah L, Scoville JP, Couldwell WT. Delayed occipitocervical instability with cranial settling after far-lateral transcondylar surgery for invasive skull base tumor. Oper Neurosurg (Hagerstown). 2019;16(2):250-5.

59. Nagare SP, Chaudhari RS, Birangane RS, Parkarwar PC. Sex determination in forensic identification, a review. J Forensic Dent Sci. 2018;10(2):61-6.

60. Sangvichien S, Boonkaew K, Chuncharunee A, Komoltri C, Udom C, Chandee T. Accuracy of cranial and mandible morphological traits for sex determination in Thais. Siriraj Med J. 2008;60(5):240-3.

61. Kanodia G, Parihar V, Yadav YR, Bhatele PR, Sharma D. Morphometric analysis of posterior fossa and foramen magnum. Journal of neurosciences in rural practice. 2012;3(03):261-6.

62. Bello S, Zagga A, Kalale S, Usman J, Bello A, Abdulhameed A, et al. Measurements of Foramen Magnum using Computerised Tomography in Sokoto State, Nigeria. Int J Health and Medical Information. 2013;2:29-35.

63. Sahoo S, Giri S, Panda S, Panda P, Sahu MC, Mohapatra C. Morphometric analysis of the foramen magnum and the occipital condyles. Int J Pharm Sci Rev Res. 2015;33(2):198-204.

64. Parvindokht B, Reza DM, Saeid B. Morphometric analysis of hypoglossal canal of the

occipital bone in Iranian dry skulls. Journal of craniovertebral junction & spine. 2015;6(3):111.

65. Ucerler H, Govsa F. Asterion as a surgical landmark for lateral cranial base approaches. Journal of Cranio-Maxillofacial Surgery. 2006;34(7):415-20.

66. Ugur HC, Dogan I, Kahilogullari G, Al-Beyati ES, Ozdemir M, Kayaci S, et al. New practical landmarks to determine sigmoid sinus free zones for suboccipital approaches: an anatomical study. Journal of Craniofacial Surgery. 2013;24(5):1815-8.

67. Li R, Qi L, Yu X, Li K, Bao G. Mastoid notch as a landmark for localization of the transverse-sigmoid sinus junction. BMC neurology. 2020;20(1):1-7.

68. Kubo M, Mizutani T, Shimizu K, Matsumoto M, Iizuka K. New methods for determination of the keyhole position in the lateral suboccipital approach to avoid transverse-sigmoid sinus injury: Proposition of the groove line as a new surgical landmark. Neurochirurgie. 2021;67(4):325-9.

Appendix

A: Box plots of the independent t-test analysis findings

1) Dimensions of occipital condyle

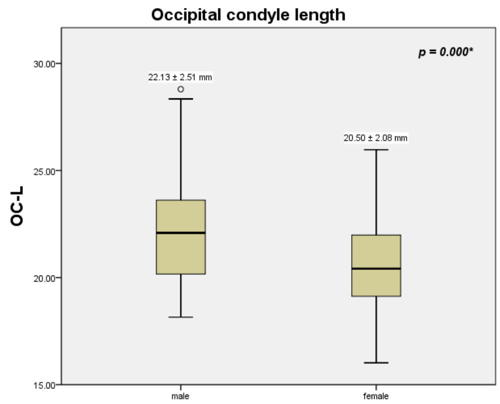

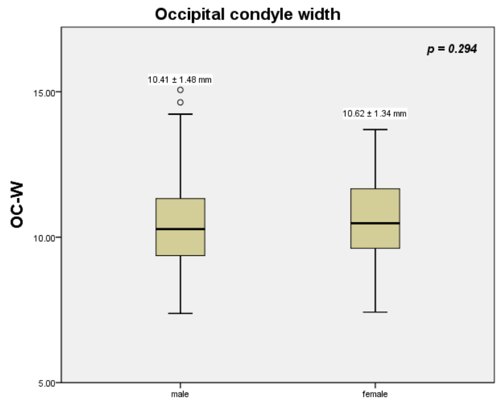

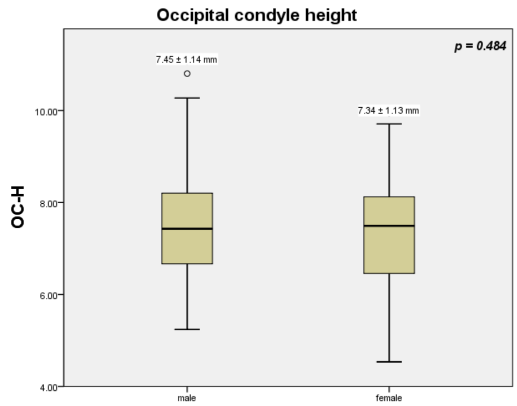

2) The tips of occipital condyle to basion and opisthion

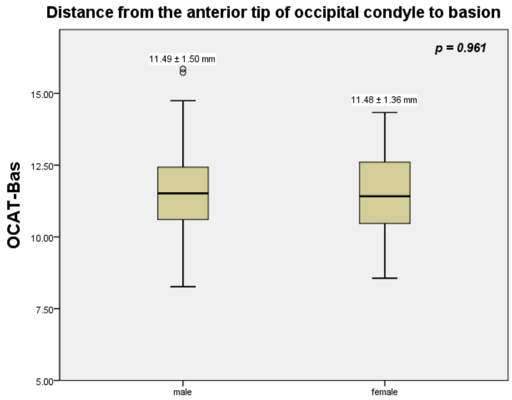

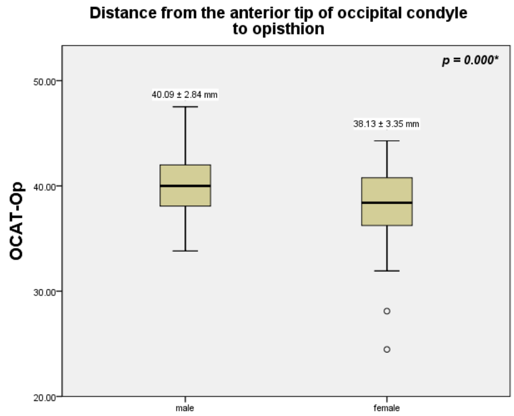

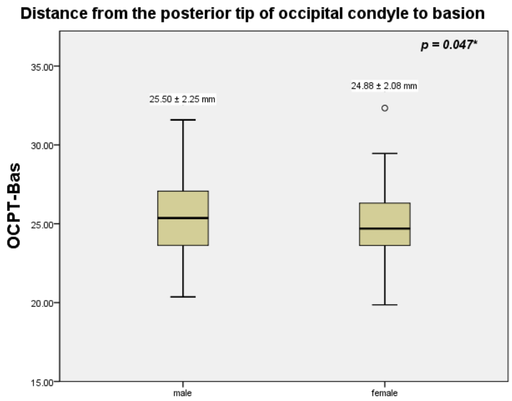

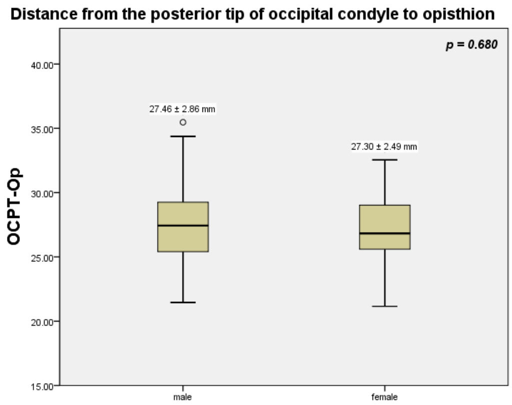

3) Distances between occipital condyle and hypoglossal orifices

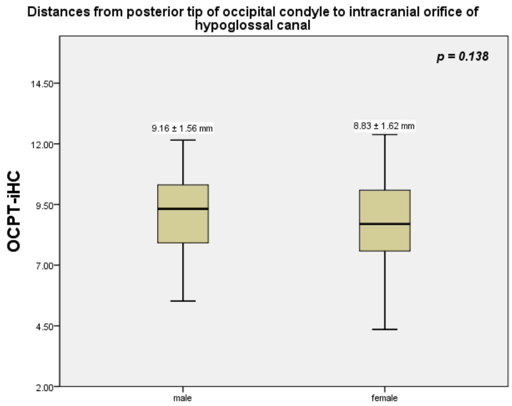

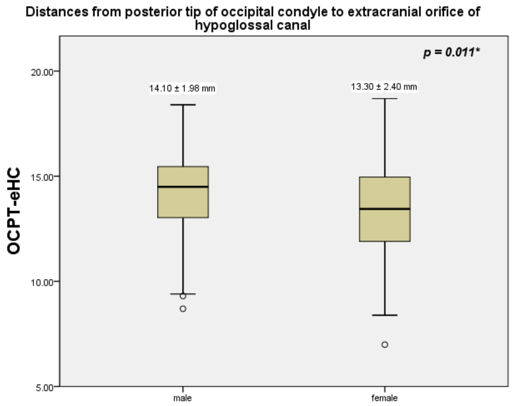

4) Distance between jugular foramen and occipital condyle

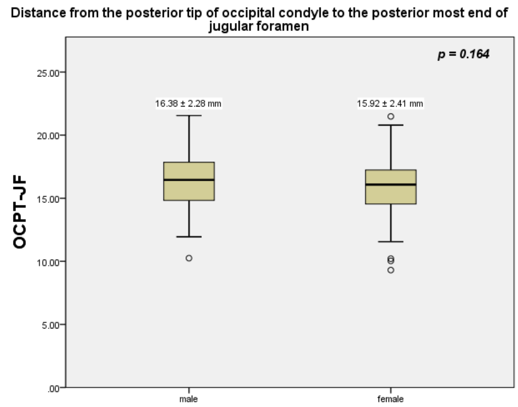

5) Distance between jugular foramen and opisthion

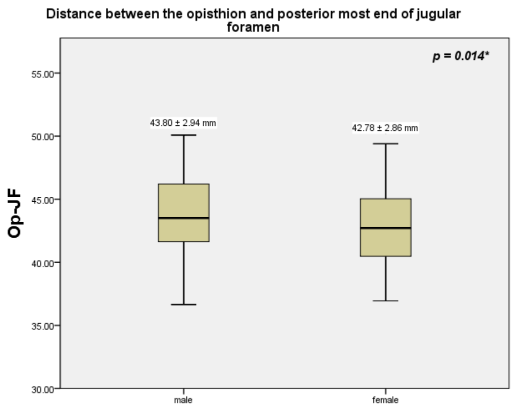

6) Distance between digastric point and surrounding structures

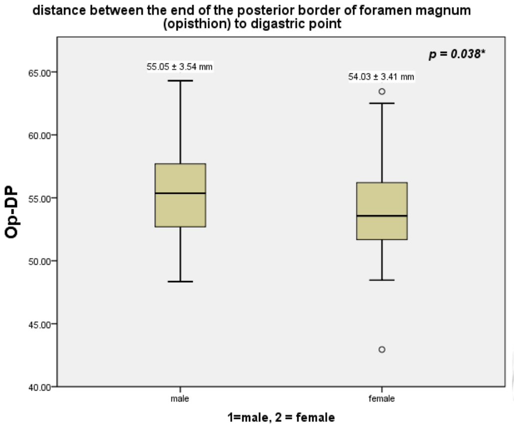

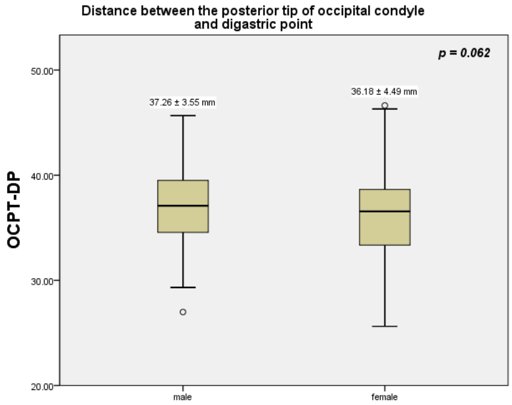

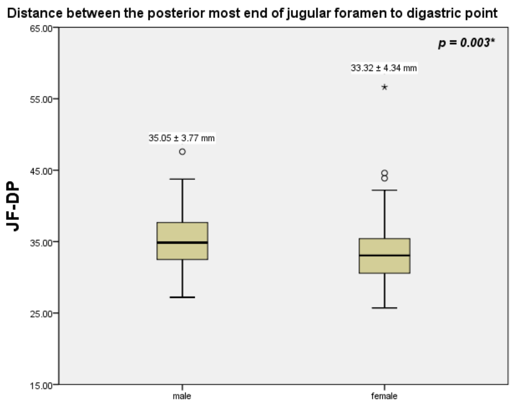

7) The intercondylar distance of occipital condyle

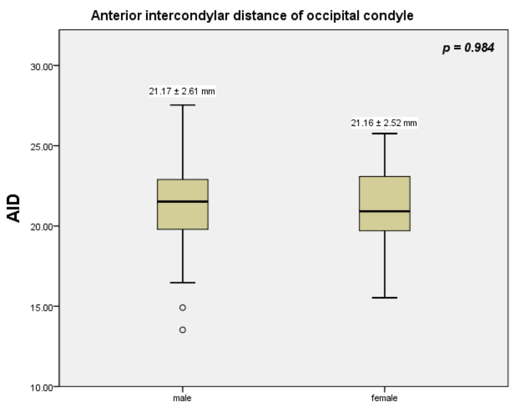

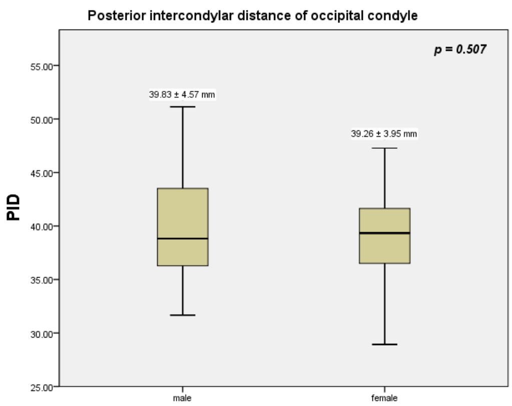

8) Diameter of foramen magnum

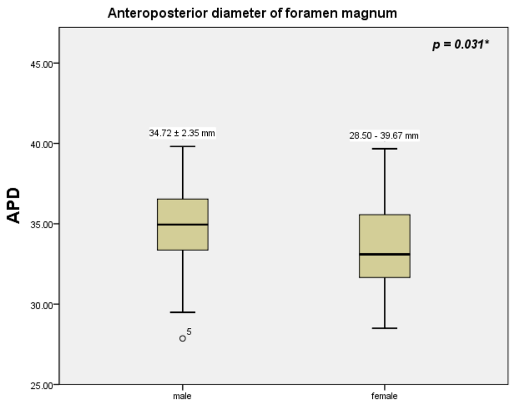

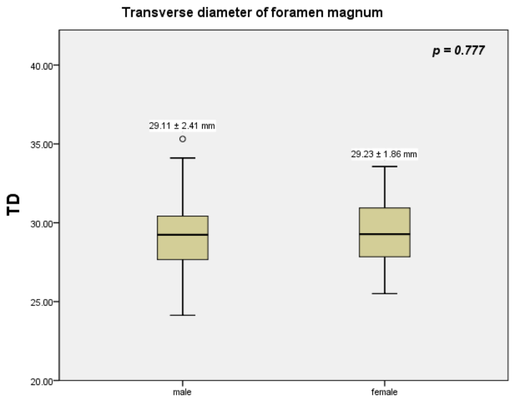

B: Scatter plot

1) Diameter of foramen magnum

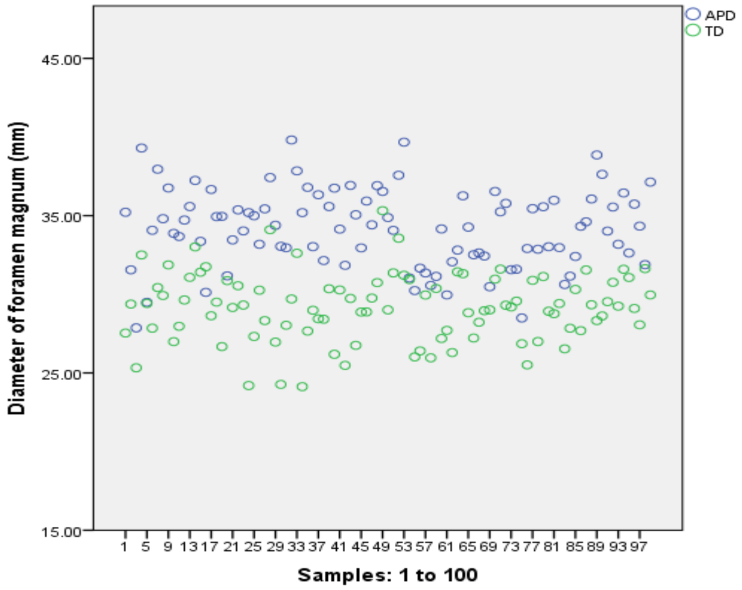

2) Foramen magnum index (FMI)

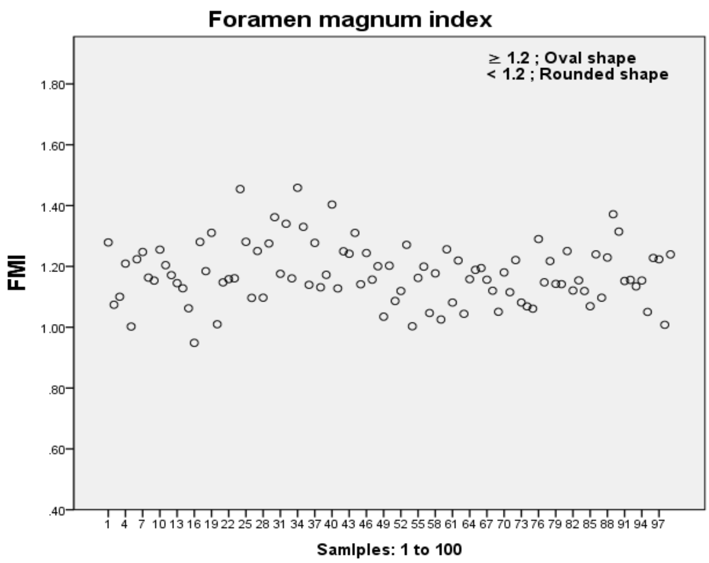

3) The intercondylar distance of occipital condyle

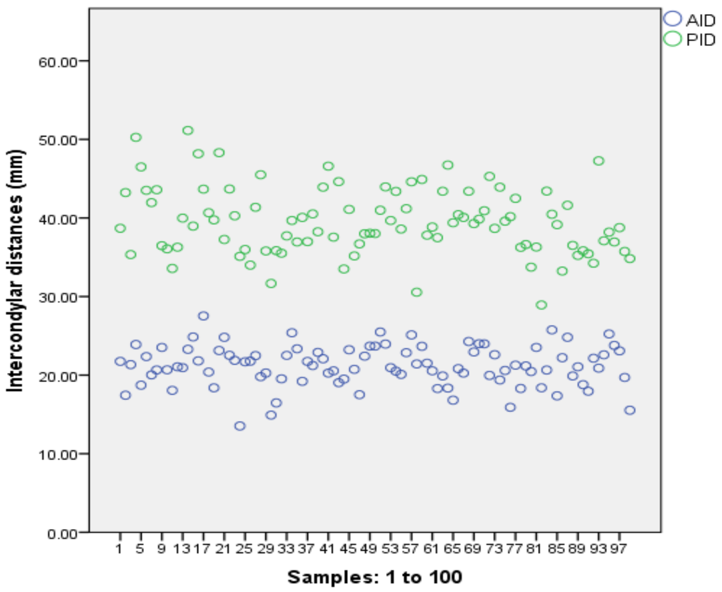

4) Dimensions of occipital condyle

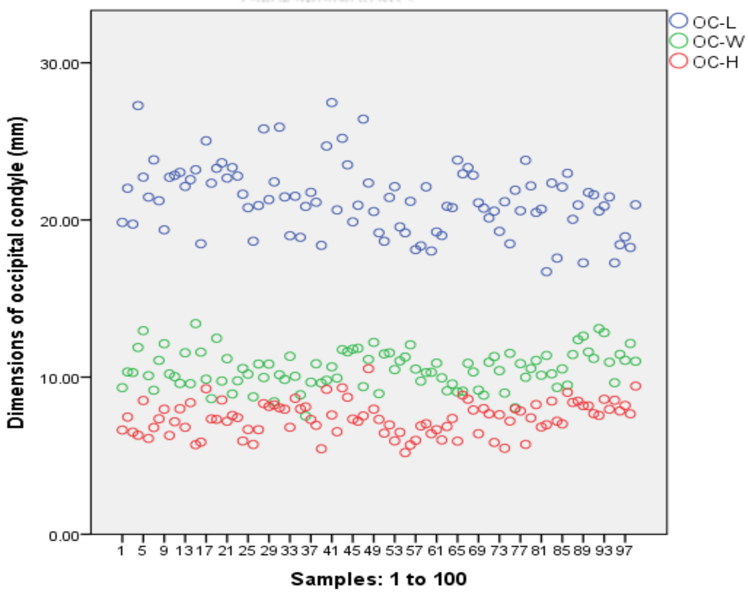

5) The tips of occipital condyle to basion and opisthion

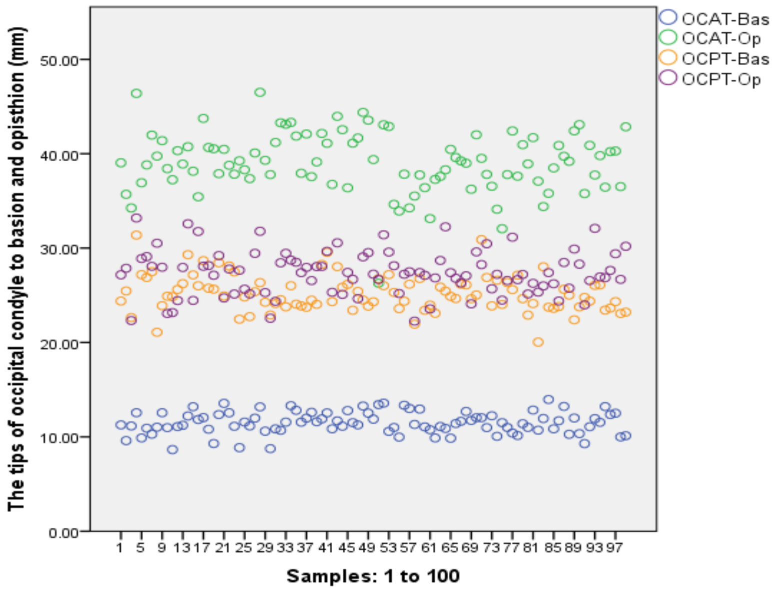

6) Distances between occipital condyle and hypoglossal orifices

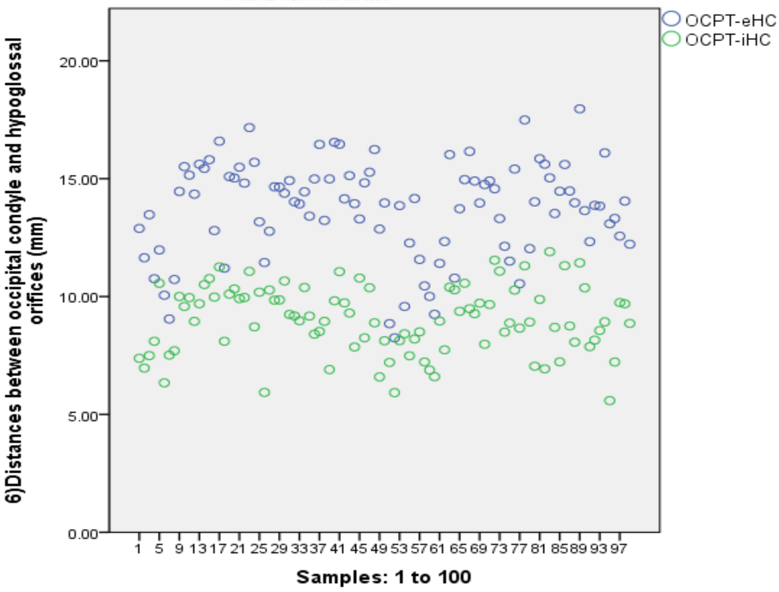

7) Distance between jugular foramen and opisthion and posterior tip of occipital condyle

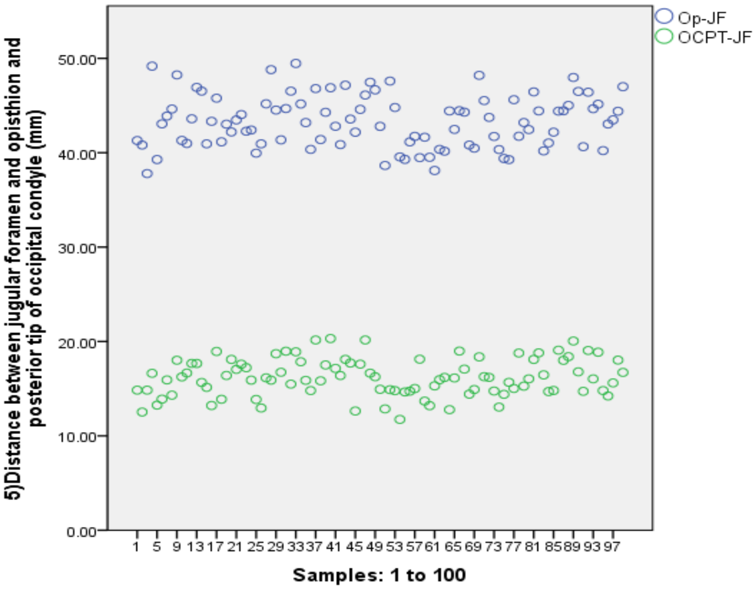

8) Distance between digastric point and surrounding structures

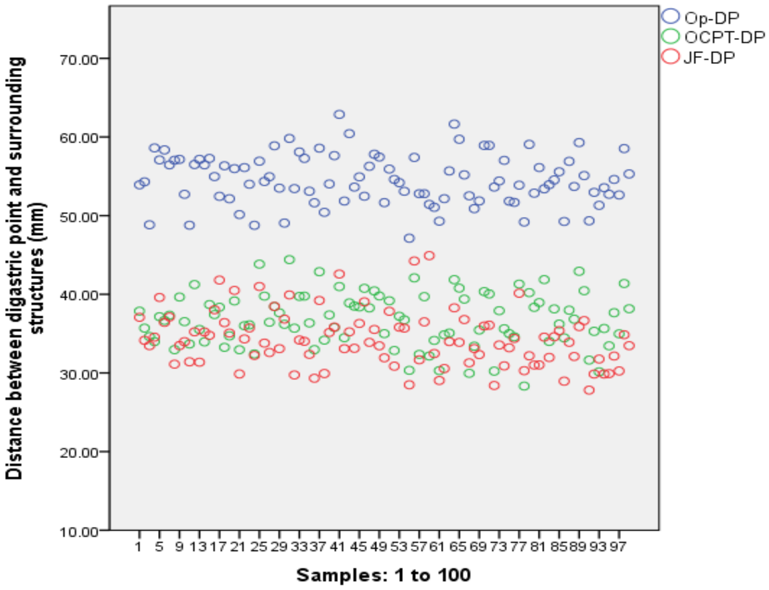

VITA

NAME Pakpoom Thintharua

DATE OF BIRTH 27 June 1990

PLACE OF BIRTH Suratthani

INSTITUTIONS ATTENDED B.S. (Medical Sciences), Naresuan University, March 4, 2013.

HOME ADDRESS 339/92 Condo Meesuk, Prachasan Rd, Na Mueang , Mueang Chachoengsao , Chachoengsao, 24000

PUBLICATION

1. Thintharua P, Larbcharoensub N, Suriyonplengsaeng C, Wongprasert K, Tissue Microarray Analysis of Vascular Endothelial Growth Factor-A Protein in Cholangiocarcinoma. The 40th Annual Conference of the Anatomy Association of Thailand. 2017 May; poster presentation.
2. Chandee N, Kleuwphunga N, Thintharua P, Somrit M, Sridurongrit S, Suriyonplengseang C, Weerachatyanukul W, Asuvapongpatana S. 3D Reconstruction of developing hearts in chick embryos. Chula Med J 2018 May – Jun; 62(3): 319 - 21
3. Kruangkum T, Saetan J, Chotwiwatthanakun C, Vanichviriyakit R, Thongrod S, Thintharua P, Tulyananda T, Sobhon P. Co-culture of males with late premolt to early postmolt female giant freshwater prawns, Macrobrachium rosenbergii resulted in greater abundances of insulin-like androgenic gland hormone and gonad maturation in male prawns as a result of olfactory receptors. Animal reproduction science. 2019 Nov 1;210:106198.
4. Chandee N, Kruepunga N, Leckchaoum T, Thintharua P, Weerachatyanukul W, Asuvapongpatana S. Late administration of caffeine affects cardiac maturation in chick embryos: a combined two and threedimensional morphogenetic and gene analyses. Eur. j. anat. 2020:211-20.
5. Thintharua P, Dharmasaroja P. Histology Study in Undergraduate

Medical Education. Ramathibodi Medical Journal. 2020 Sep 30;43(3):34-40.

6. Boonsri B, Yacqub-Usman K, Thintharua P, Myint KZ, Sae-Lao T, Collier P, Suriyonplengsaeng C, Larbcharoensub N, Balasubramanian B, Venkatraman S, Egbuniwe IU. Effect of Combining EGFR Tyrosine Kinase Inhibitors and Cytotoxic Agents on Cholangiocarcinoma Cells. Cancer Research and Treatment: Official Journal of Korean Cancer Association. 2021 Apr;53(2):457.

7. Thintharua P, Dharmasaroja P. Technologies-enhanced Anatomical Study in Undergraduate Medical Students. Ramathibodi Medical Journal 2021;44. doi:10.33165/rmj.2021.44.4.250876.

8. Thintharua P and Chentanez V. Morphological and Morphometric Analysis of the Foramen Magnum: Pertinent data for surgical procedure at craniovertebral junction.The 44th Annual Conference of the Anatomy Association of Thailand. 2022 May; poster presentation.

9. Chentanez V, Thintharua P. Surgical Anatomy of the occipital condyle and its relation to hypoglossal canal. The FASEB Journal. 2022 May;36.